

Search for long-lived, massive particles in events with displaced vertices and missing transverse momentum in $\sqrt{s} = 13$ TeV pp collisions with the ATLAS detector

M. Aaboud *et al.*^{*}
(ATLAS Collaboration)

(Received 13 October 2017; published 28 March 2018)

A search for long-lived, massive particles predicted by many theories beyond the Standard Model is presented. The search targets final states with large missing transverse momentum and at least one high-mass displaced vertex with five or more tracks, and uses 32.8 fb^{-1} of $\sqrt{s} = 13$ TeV pp collision data collected by the ATLAS detector at the LHC. The observed yield is consistent with the expected background. The results are used to extract 95% C.L. exclusion limits on the production of long-lived gluinos with masses up to 2.37 TeV and lifetimes of $\mathcal{O}(10^{-2}) - \mathcal{O}(10)$ ns in a simplified model inspired by split supersymmetry.

DOI: 10.1103/PhysRevD.97.052012

I. INTRODUCTION

The lack of explanation for the dark matter observed in the universe [1], the gauge hierarchy problem [2,3], and the lack of exact gauge coupling unification at high energies [4] all indicate that the Standard Model (SM) is incomplete and needs to be extended. Many attractive extensions of the SM have been proposed, but decades of searches have set severe constraints on the masses of promptly decaying particles predicted by these models. Searches targeting the more challenging experimental signatures of new long-lived particles (LLPs) have therefore become increasingly important and must be pursued at the Large Hadron Collider (LHC).

A number of beyond-SM (BSM) models predict the existence of massive particles with lifetimes in the picoseconds to nanoseconds range. Many of these particles would decay in the inner tracker volume of the experiments at the LHC. The decay products of such particles often contain several electrically charged particles, which can be reconstructed as tracks. If the LLP decays within the tracking volume but at a discernible distance from the interaction point (IP) of the incoming beams, a displaced vertex can be reconstructed by using dedicated tracking and vertexing techniques.

There are various mechanisms by which particles obtain significant lifetimes in BSM theories. The decays of such

particles can be suppressed in so-called hidden valley models [5] where large barrier potentials reduce the rate of kinematically allowed decays. Long-lived particles also appear in models with small couplings, such as those often found in R -parity-violating supersymmetry (SUSY) [6,7]. Finally, decays via a highly virtual intermediate state also result in long lifetimes, as is the case for a simplified model inspired by split SUSY [8,9] used as a benchmark model for the search presented here. In this model, the supersymmetric partner of the gluon, the gluino (\tilde{g}), is kinematically accessible at LHC energies while the SUSY partner particles of the quarks, the squarks (\tilde{q}), have masses that are several orders of magnitude larger. Figure 1 shows pair production of gluinos decaying to two quarks and the lightest supersymmetric particle (LSP), assumed to be the lightest neutralino ($\tilde{\chi}_1^0$). The $\tilde{g} \rightarrow q\bar{q}\tilde{\chi}_1^0$ decay is suppressed as it proceeds via a highly virtual squark. Depending on the scale of the squark mass, the gluino lifetime can be picoseconds or longer, which is above the hadronization

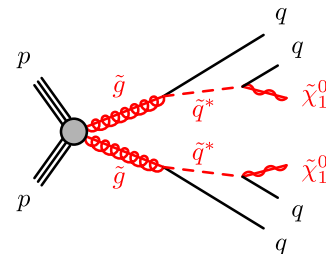


FIG. 1. Diagram showing pair production of gluinos decaying through $\tilde{g} \rightarrow q\bar{q}\tilde{\chi}_1^0$ via a virtual squark \tilde{q}^* . In split SUSY scenarios, because of the very large squark mass, the gluinos are long-lived enough to hadronize into R -hadrons that can give rise to displaced vertices when they decay.

*Full author list given at the end of the article.

time scale. Therefore, the long-lived gluino, which transforms as a color octet, is expected to hadronize with SM particles and form a bound color-singlet state known as an R -hadron [10].

This search utilizes the ATLAS detector and attempts to reconstruct the decays of massive R -hadrons as displaced vertices (DVs). The analysis searches for LLP decays occurring $\mathcal{O}(1\text{--}100)$ mm from the reconstructed primary vertex (PV) and is sensitive to decays of both electrically charged and neutral states emerging from the PV. The analysis targets final states with at least one DV with a high reconstructed mass and a large track multiplicity in events with large missing transverse momentum E_T^{miss} . This analysis builds on that of Ref. [11] where the ATLAS Collaboration set limits on such processes using 8 TeV pp collisions from the LHC. In Run 2 of the LHC starting in 2015, the increased center-of-mass energy of $\sqrt{s} = 13$ TeV gives significant increases in the production cross sections of heavy particles, providing extended mass sensitivity compared to previous searches. Decays of new, long-lived particles have been searched for in a variety of experimental settings. These include studies by ATLAS [12–21], CMS [22–29], LHCb [30–33], CDF [34], D0 [35,36], BABAR [37], Belle [38], and ALEPH [39]. The searches involve a range of experimental signatures, including final states with leptons, jets, and combinations thereof. Dedicated techniques make use of nonpointing or delayed photons, as well as tracking, energy, and timing measurements of the long-lived particle itself until it decays.

The experimental apparatus is described in Secs. II, and III discusses the data set and simulations used for this analysis. The special reconstruction algorithms and event selection criteria are presented in Sec. IV. Section V discusses the sources of backgrounds relevant to this search and the methods employed to estimate the expected yields. The sensitivity to experimental and theoretical uncertainties of the analysis is described in Sec. VI. Section VII presents the results and their interpretations.

II. ATLAS DETECTOR

The ATLAS experiment [40,41] at the LHC is a multipurpose particle detector with a forward-backward-symmetric cylindrical geometry and a near 4π coverage in solid angle.¹ The detector consists of several layers of subdetectors. From the IP outwards there is an inner tracking detector (ID), electromagnetic and hadronic calorimeters, and a muon spectrometer (MS).

¹ATLAS uses a right-handed coordinate system with its origin at the nominal IP in the center of the detector and the z axis along the beam pipe. The x axis points from the IP to the center of the LHC ring, and the y axis points upward. Cylindrical coordinates (R, ϕ) are used in the transverse plane, ϕ being the azimuthal angle around the beam pipe. The pseudorapidity is defined in terms of the polar angle θ as $\eta = -\ln \tan(\theta/2)$.

The ID extends from a cylindrical radius of about 33 mm to 1100 mm and to $|z|$ of about 3100 mm, and is immersed in a 2 T axial magnetic field. It provides tracking for charged particles within the pseudorapidity region $|\eta| < 2.5$. At small radii, silicon pixel layers and stereo pairs of silicon microstrip detectors provide high-resolution position measurements. The pixel system consists of four barrel layers and three forward disks on either side of the IP. The barrel pixel layers, which are positioned at radii of 33.3 mm, 50.5 mm, 88.5 mm, and 122.5 mm are of particular relevance to this work. The silicon microstrip tracker (SCT) comprises four double layers in the barrel and nine forward disks on either side. The radial position of the innermost (outermost) SCT barrel layer is 299 mm (514 mm). The final component of the ID, the transition-radiation tracker (TRT), is positioned at larger radii, with coverage up to $|\eta| = 2.0$.

The calorimeter provides coverage over the range $|\eta| < 4.9$. It consists of an electromagnetic calorimeter based on lead and liquid argon with coverage for $|\eta| < 3.2$ and a hadronic calorimeter. Hadronic calorimetry in the region $|\eta| < 1.7$ uses steel absorbers and scintillator tiles as the active medium. Liquid-argon calorimetry with copper absorbers is used in the hadronic end-cap calorimeters, which cover the region $1.5 < |\eta| < 3.2$. A forward calorimeter using copper and tungsten absorbers with liquid argon completes the calorimeter coverage up to $|\eta| = 4.9$.

The MS consists of three large superconducting toroid systems each containing eight coils and a system of trigger and precision tracking chambers, which provide trigger and tracking capabilities in the range $|\eta| < 2.4$ and $|\eta| < 2.7$, respectively.

A two-level trigger system is used to select events [42]. The first-level trigger is implemented in custom electronics and uses information from the MS trigger chambers and the calorimeters. This is followed by a software-based high-level trigger system, which runs reconstruction algorithms similar to those used in off-line reconstruction. Combined, the two levels reduce the 40 MHz bunch-crossing rate to approximately 1 kHz of events saved for further analysis.

III. DATA SET AND SIMULATED EVENTS

The experimental data used in this paper are from proton-proton (pp) collisions at $\sqrt{s} = 13$ TeV collected in 2016 at the LHC. After applying requirements on detector status and data quality, the integrated luminosity of the sample corresponds to 32.8 fb^{-1} . The uncertainty in the 2016 integrated luminosity is 2.2%. It is derived, following a methodology similar to that detailed in Ref. [43], from a calibration of the luminosity scale using x - y beam-separation scans performed in May 2016. The events in this data set have an average of 25 simultaneous pp interactions in the same bunch crossing.

This search makes use of a number of signal Monte Carlo (MC) samples to determine the efficiency

for selecting signal events and the associated uncertainty. In each sample, gluinos were pair produced in pp collisions and then hadronized, forming metastable R -hadrons. The gluino contained in each R -hadron later decays to SM quarks and a neutralino as shown in Fig. 1. The mass of the gluino ($m_{\tilde{g}}$) in the simulated samples is between 400 and 2000 GeV, its lifetime τ varies from 0.01 to 50 ns, and the neutralino mass $m_{\tilde{\chi}_1^0}$ ranges from 100 GeV to $m_{\tilde{g}} - 30$ GeV. To evaluate signal efficiencies for lifetimes not simulated, events in the produced samples are reweighted to different lifetimes. The samples were simulated with PYTHIA 6.428 [44]. The AUET2B [45] set of tuned parameters for the underlying event and the CTEQ6L1 [46] parton distribution function (PDF) set are used. Dedicated routines [10,47,48] for hadronization of heavy colored particles were used to simulate the production of R -hadrons. The hadronization process primarily yields mesonlike states ($\tilde{g}q\bar{q}$), but baryon-like states ($\tilde{g}qqq$) and glueball-like states ($\tilde{g}g$) are predicted as well. Following the hadronization, approximately half of the \tilde{g} -based R -hadrons have electric charge $Q \neq 0$, and the charges of the two R -hadrons produced in the event are uncorrelated. The electric charge of the R -hadron is determined by its SM parton content, and while $Q = -1, 0$, and 1 dominate, a few percent have double charge. It is worth noting that the vertexing algorithms used in this search (see Sec. IV A) are agnostic to the electric charge of the LLP as only the decay products are reconstructed.

The cross sections are calculated at next-to-leading order (NLO) assuming a squark mass large enough to completely decouple squark contributions. The most significant contributions to the NLO QCD corrections come from soft-gluon emission of the colored particles in the initial and final states [49–51]. The resummation of soft-gluon emission is taken into account at next-to-leading-logarithm accuracy (NLO + NLL) [49,51,52]. The uncertainty in the cross-section predictions is defined as an envelope of the predictions resulting from different choices of PDF sets (CTEQ6.6 [53] and MSTW2008 [54]) and the factorization and renormalization scales, as described in Ref. [50]. The nominal cross section is obtained using the midpoint of the envelope.

The ATLAS detector simulation [55] is based on GEANT4 [56], and dedicated routines are employed to simulate interactions of R -hadrons with matter [48,57,58]. The model used assumes an R -hadron–nucleon cross section on the order of 10 mb per nucleon for each light valence quark of the R -hadron, varying slightly with the boost of the bound system [58]. For glueball-like states ($\tilde{g}g$), the interaction cross section is assumed to be the same as for the mesonlike states ($\tilde{g}q\bar{q}$). The per-parton interaction probability is roughly inversely proportional to the squared parton mass, rendering the interactions of the gluinos themselves negligible. For the glueball-like states, $g \rightarrow q\bar{q}$ transitions create an effective mass for the gluon similar to that of the mesonlike states [48].

The decay of the R -hadron is simulated by a modified version of PYTHIA 6.428 and includes the three-body decay of the gluino, fragmentation of the remnants of the light-quark system, and hadronization of the decay products. In all signals considered, the kinematics of the decay products are determined primarily by the mass of the gluino and the kinematics of the R -hadron it is contained in.

R -hadron production was simulated using PYTHIA 6.428; however, it is not expected to accurately model the initial-state radiation (ISR) or final-state radiation (FSR). To obtain a more accurate description of these effects, MADGRAPH5_aMC@NLO 2.2.3 [59] was used to generate additional samples of $\tilde{g}\tilde{g}$ production at leading order with up to two additional partons in the matrix element, and interfaced to the PYTHIA 8.186 parton shower model, with the A14 [60] set of tuned parameters together with the NNPDF2.3LO [61] PDF set. The distribution of the transverse momentum p_T of the $\tilde{g}\tilde{g}$ system simulated with PYTHIA 6 is reweighted to match the distribution obtained for corresponding MADGRAPH5_aMC@NLO samples.

All MC samples include simulation of additional pp interactions in the detector from the same or nearby bunch crossings, referred to as pileup. These additional inelastic pp interactions that occur in the detector were generated using PYTHIA 8.186 [62] tuned with the A2 parameter set [63] and overlaid with the hard-scattering event. Simulated events are reconstructed using the same algorithms used for the collision data.

IV. RECONSTRUCTION AND EVENT SELECTION

While the reconstruction of DV candidates makes use of the ID, the entirety of the ATLAS detector is used to reconstruct the jets and E_T^{miss} in each event, thereby providing additional discrimination between signal and background. Hadronic jets are reconstructed from calibrated three-dimensional topo clusters [64] using the anti- k_t jet clustering algorithm [65,66] with a radius parameter of 0.4. Jet candidates are initially calibrated assuming their energy depositions originate from electromagnetic showers, and then corrected by scaling their four-momenta to the energies of their constituent particles [67–70]. Electrons, photons, and muons are also reconstructed and calibrated, although no explicit requirements are placed on them in this search. The E_T^{miss} is calculated using all calibrated objects as well as those reconstructed tracks not associated with these objects. The latter contribution accounts for potential diffuse, low- p_T imbalances [71,72].

A. Reconstruction of displaced tracks and vertices

In the standard ATLAS tracking algorithm [73], triplets of hits in the pixel and/or the SCT detectors are used to seed the track finding. By adding further hits along the seed trajectories, track candidates are fitted and subsequently extrapolated into the TRT. This algorithm places constraints

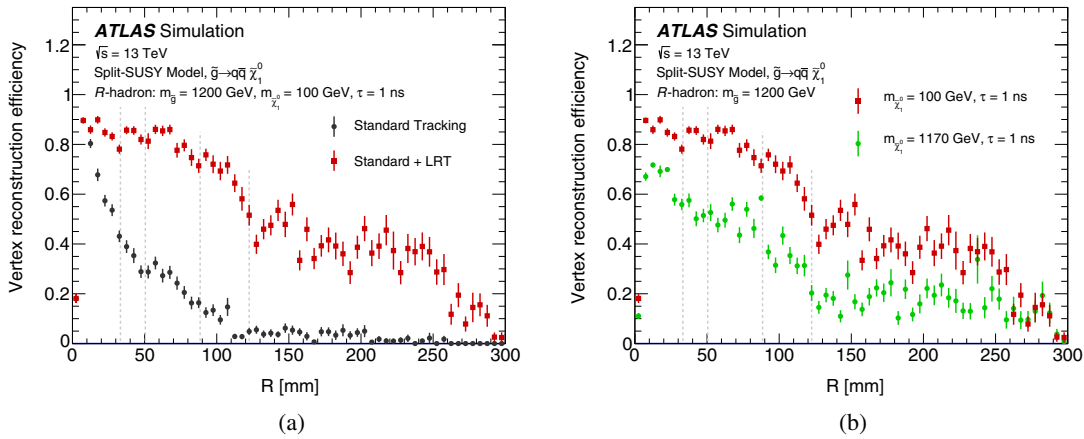


FIG. 2. Vertex reconstruction efficiency as a function of radial position R . The efficiency is defined as the probability for a true LLP decay to be matched with a reconstructed DV fulfilling the vertex preselection criteria. In (a) the efficiencies with and without the special LRT processing are shown for one benchmark signal, while (b) shows two R -hadron signal samples with different gluino-neutralino mass differences when using LRT processing.

on the transverse and longitudinal impact parameters of track candidates with respect to the PV² ($|d_0| < 10$ mm and $|z_0| < 250$ mm, respectively). These constraints result in low efficiency for reconstructing tracks originating from a DV, as such tracks typically have a larger transverse impact parameter than those emerging from the interaction point.

In order to recover tracks from DVs, an additional *large-radius tracking* (LRT) algorithm pass [74] is performed, using only hits not already associated with tracks reconstructed by the standard tracking algorithm. Requirements on the impact parameters are relaxed, allowing tracks to have $|d_0| < 300$ mm and $|z_0| < 1500$ mm. Furthermore, requirements on the number of hits shared by several tracks are slightly relaxed. The tracks from the standard processing and the LRT processing are treated as a single collection in the subsequent reconstruction steps.

Tracks satisfying $p_T > 1$ GeV are selected for the DV reconstruction. In order to remove fake tracks, a track is discarded if it simultaneously has no TRT hits and fewer than two pixel hits. Tracks with fewer than two pixel hits are therefore required to fall within the TRT acceptance of $|\eta| < 2$. Tracks are also required to have $|d_0| > 2$ mm in order to reject tracks that originate from the PV and from most short-lived particles, such as b -hadrons. This last requirement also ensures that the track from an electrically charged LLP will not be associated with the DV.

The DV reconstruction algorithm starts by finding two-track seed vertices from pairs of selected tracks. Seed vertices with a high quality of fit are retained. Both tracks of a seed vertex are required to not have hits in pixel layers at smaller radii than the seed vertex, and to have a hit in the nearest pixel or SCT layer at larger radius. If the seed vertex

²The PV is required to have at least two associated tracks and satisfy $|z| < 200$ mm. If several exist, the vertex with the largest $\sum(p_T^{\text{track}})^2$ is selected.

position is inside or within several millimeters of a tracker layer, hits of that particular layer are neither forbidden nor required. Kinematic requirements on the direction of the vector sum of the momenta of the tracks associated with the seed vertex are applied to make sure it is consistent with the decay of a particle originating from the PV.

At this stage, a track can be associated with multiple two-track seed vertices. In order to resolve such ambiguities, an iterative process based on the incompatibility graph approach [75] is applied. After this procedure, each track is associated with at most one seed vertex.

Multitrack DVs are then formed iteratively using the collection of seed vertices. For a given seed vertex V_1 , the algorithm finds the seed vertex V_2 that has the smallest value of d/σ_d , where d is the three-dimensional distance between V_1 and V_2 , and σ_d is the estimated uncertainty in d . If $d/\sigma_d < 3$, a single DV is formed from all the tracks of both seed vertices and the merged vertex is refitted. The merging is repeated until no other compatible seed vertices are found. Simultaneously, the significance of each track's association with its vertex is evaluated upon merging, and poorly associated tracks not satisfying additional criteria are removed before the vertex is refitted. This procedure is repeated until no other tracks fail to meet these criteria. Finally, DVs separated by less than 1 mm are combined and refitted. DV candidates are only considered in this search if they fall in the fiducial volume $R = \sqrt{x^2 + y^2} < 300$ mm and $|z| < 300$ mm.

Figure 2 shows the DV reconstruction efficiency, defined as the probability for a true LLP decay to be matched with a reconstructed DV fulfilling the vertex preselection criteria (described in Sec. IV C) as a function of R . The improvement with respect to standard tracking at large radii is shown in Fig. 2(a), while Fig. 2(b) shows how the efficiency of the LRT-based DV reconstruction depends on the mass difference $\Delta m = m_{\tilde{g}} - m_{\tilde{\chi}_1^0}$. With larger mass

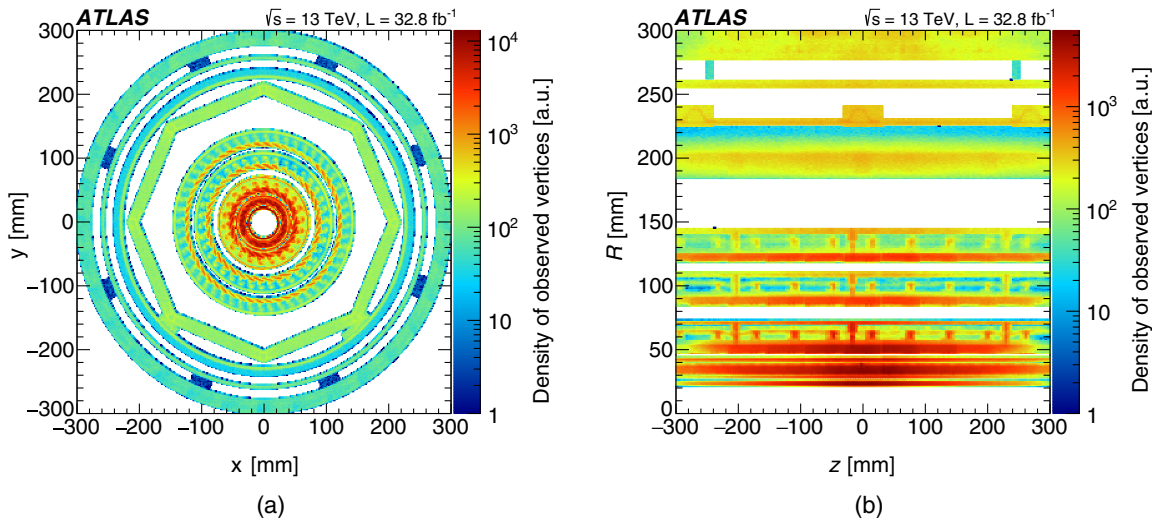


FIG. 3. Two-dimensional maps of the observed vertex density in regions vetoed by the material map, projected in the (a) x - y plane and (b) z - R plane. The color scale is in arbitrary units (a.u.).

difference, more and higher p_T particles are produced in the gluino decay, which increases the reconstruction efficiency of the DV.

B. Material-dominated regions and the effect of disabled detector modules

An important background in any search for displaced vertices comes from hadronic interactions in material-rich regions of the detector [76,77]. In order to suppress this background, a map defining regions with known material is constructed by studying the positions of DVs in $\sqrt{s} = 13$ TeV minimum-bias data. The map is used to reject vertices within the material regions. In these studies, the vertices from the long-lived SM hadrons K_S^0 and Λ^0 are vetoed by discarding vertices that match their expected track multiplicities and reconstructed masses. The application of the map-based veto significantly reduces the contribution from hadronic interactions at the cost of discarding approximately 42% of the fiducial volume. The material map is visualized in Fig. 3, in which the locations of the observed vertices failing this veto are projected onto the x - y and R - z planes.

In addition to the material veto map, a veto is applied to reject vertices in regions sensitive to the effect of disabled pixel modules. This requirement discards 2.3% of the total fiducial volume.

C. Event and vertex selections

All events used in this analysis must satisfy the following selection requirements. First, the data were passed through a filter during prompt reconstruction and were made available in a raw data format in order to facilitate the special processing with dedicated track and DV reconstruction required by this analysis. This initial filtering, used as a common preselection for several searches

that require special reconstruction, includes requirements on an E_T^{miss} , multijet, or single-lepton trigger. For the E_T^{miss} -triggered events used in the signal region (SR) of this search, an additional requirement is imposed on *hadronic* E_T^{miss} , a quantity similar to E_T^{miss} but with all clusters of energy deposited in the calorimeter calibrated as if they come from hadrons. The filtering of the first 75% of the data set also required the presence of one trackless³ jet with $p_T > 70$ GeV or two trackless jets with $p_T > 25$ GeV, and hadronic $E_T^{\text{miss}} > 130$ GeV. For the last 25% of the data set, the trackless jet requirement was removed and hadronic $E_T^{\text{miss}} > 180$ GeV was required instead. This change was made in order to improve sensitivity for low- Δm signal scenarios [78–80], which are unlikely to give rise to jets with high p_T from the displaced decays. The MC events used in this analysis were processed separately in two subsamples with sizes proportional to the integrated luminosities of the two subsamples.

Additional detector-level quality requirements are applied, vetoing events that are affected by calorimeter noise, data corruption, or other effects occurring at the time the data were recorded. Events are required to have at least one PV. To mitigate the contamination of high- E_T^{miss} events from noncollision background (NCB) processes such as beam halo, additional quality requirements are placed on the leading jet in each event. These requirements use the longitudinal calorimeter-sampling profile of these jets to select for high- p_T hadronic activity originating within the detector volume and reduce NCB contributions to at most 10% early in the event selection. Together with the requirement that such events contain a DV candidate, these criteria

³A jet is considered trackless if $\sum p_T^{\text{track}} < 5$ GeV, where the sum is taken over all tracks reconstructed in the first reconstruction pass matched to both the PV and the jet.

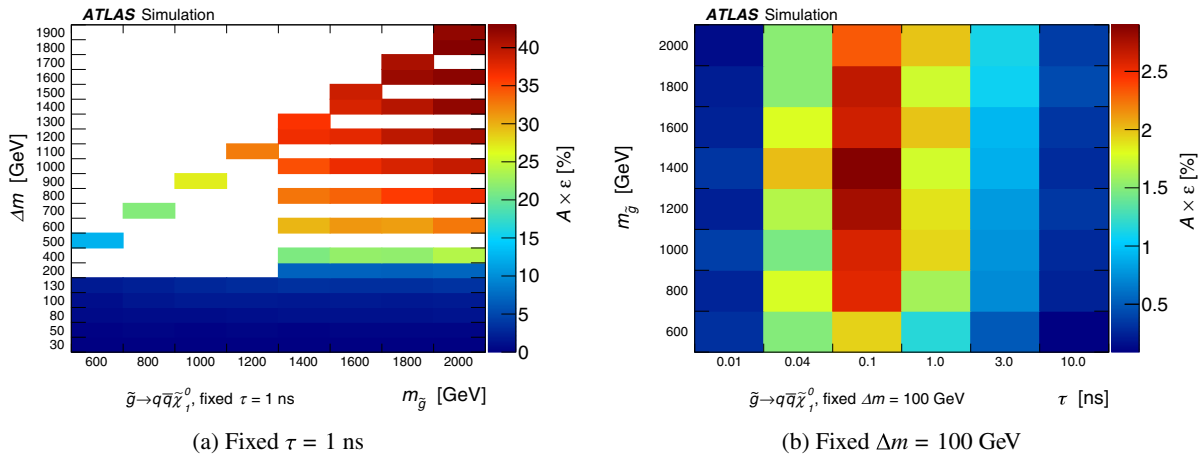


FIG. 4. Fractions of selected events for several signal MC samples, illustrating how $\mathcal{A} \times \epsilon$ varies with the model parameters. In (a) the gluino lifetime τ is fixed to 1 ns, and in (b) the mass difference Δm is fixed at 100 GeV.

are called the *event preselection* and, along with additional DV requirements, are used in the construction of the control region (CR).

To further improve signal sensitivity, the *full event selection* criteria that are used in the construction of the SR require that the event be recorded by an E_T^{miss} trigger and satisfy $E_T^{\text{miss}} > 250$ GeV. This last requirement ensures that the events are in the plateau of the efficiency turn-on curve for both the E_T^{miss} trigger and the requirement on the hadronic E_T^{miss} described above.

The DV candidates are required to satisfy the following conditions, referred to as the *vertex preselection*:

- (1) The vertex position must be within the fiducial volume $R < 300$ mm and $|z| < 300$ mm.
- (2) The vertex must be separated by at least 4 mm in the transverse plane from all reconstructed PVs.
- (3) The vertex must not be in a region that is material rich or affected by disabled detector modules, as described in Sec. IV B.
- (4) The vertex fit must have $\chi^2/N_{\text{DOF}} < 5$.

These vertex preselection criteria ensure high-quality measurements of the DV properties and reduce the number of vertices from instrumental effects. Vertices satisfying these criteria are used in the background estimation. For the *final vertex selection* used in the SR of this search, vertices are required to have at least five associated tracks and a reconstructed invariant mass $m_{\text{DV}} > 10$ GeV. These stricter requirements allow the use of vertices with lower mass and 3–4 tracks for building and validating background estimates, and give a low-background search with good signal sensitivities for a large part of the parameter space for the models of interest.

Figure 4 shows the acceptance times efficiency ($\mathcal{A} \times \epsilon$) of the SR, for several benchmark signal models. In Fig. 4(a), the $\mathcal{A} \times \epsilon$ is shown for models with different gluino and neutralino masses but fixed lifetime of 1 ns. The $\mathcal{A} \times \epsilon$ depends strongly on the gluino-neutralino mass

difference, which is directly proportional to the visible DV mass. For models with $m_{\tilde{g}} > 1.5$ TeV and $\Delta m > 1$ TeV, the search presented here attains an acceptance times efficiency of as much as 40%. For models with $\Delta m \lesssim 100$ GeV the $\mathcal{A} \times \epsilon$ is 5% or lower. In Fig. 4(b), Δm is fixed at 100 GeV while the lifetime τ is varied within $0.01 \text{ ns} < \tau < 10 \text{ ns}$. The $\mathcal{A} \times \epsilon$ is highest for lifetimes around 0.1 ns [corresponding to decay lengths of $\mathcal{O}(10)$ mm]. Signal models with low Δm are less likely to pass both the event- and vertex-level requirements, due to lower intrinsic E_T^{miss} and smaller visible DV mass.

V. BACKGROUND PROCESSES AND THEIR ESTIMATED YIELDS

Given the requirements on the mass ($m_{\text{DV}} > 10$ GeV) and track multiplicity ($n_{\text{tracks}} \geq 5$) placed on the DV candidates in the SR, there is no irreducible background from SM processes. The entirety of the background expected for this search is instrumental in origin. Three sources of such backgrounds are considered in the analysis. Hadronic interactions can give rise to DVs far from the interaction point, especially where there is material in the detector, support structures, and services. Decays of short-lived SM particles can occur close to each other and be combined into high-mass vertices with large track multiplicities, in particular in the regions closest to the beams. Finally, low-mass vertices from decays of SM particles or hadronic interactions can be promoted to higher mass if accidentally crossed by an unrelated track at a large angle. Each source of background is estimated with a dedicated method, and is separately evaluated in 12 radial detector regions⁴ divided approximately by material structures in the ID volume within the fiducial region.

⁴The boundaries for these regions are at $R = 22, 25, 29, 38, 46, 73, 84, 111, 120, 145, 180$, and 300 mm.

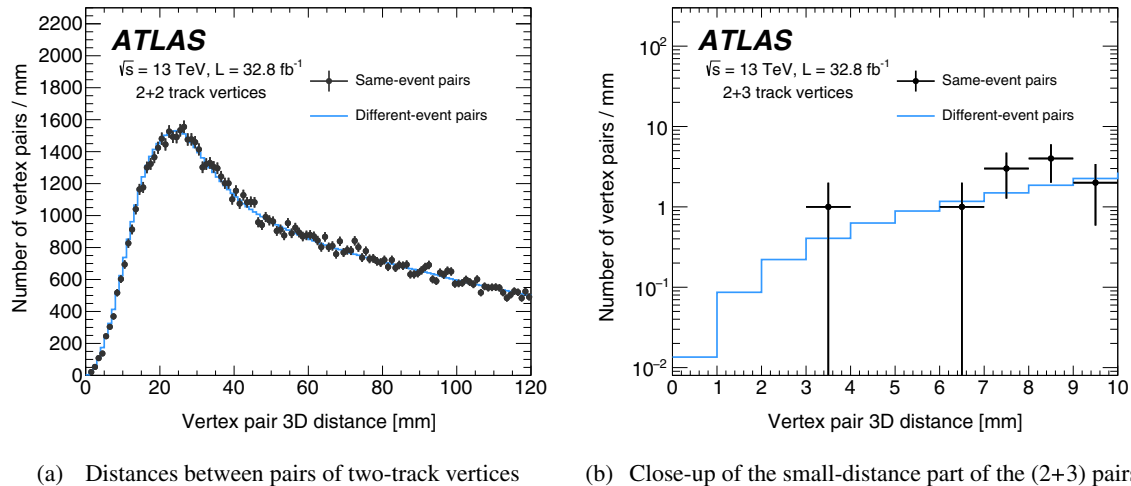


FIG. 5. Distributions of intervertex distances in reweighted pairs of vertices passing the vertex preselection in events passing the event preselection. The same-event (black markers) and different-event (blue histogram) samples are shown for (a) pairs of two-track vertices, and (b) the small-distance part of the (2 + 3)-pair combinations. The model yield for intervertex distance lower than 1 mm gives the prediction for the vertices in the high-mass region resulting from merging during DV reconstruction.

To retain a large number of DVs, the estimates below are performed on events satisfying the event preselection criteria. To obtain a final estimate for the SR, an additional *event selection transfer factor* $\epsilon_{\text{SR}} = (5.1 \pm 2.5) \times 10^{-3}$ is applied. This factor is determined by measuring the efficiency of the full event selection with respect to the preselection. The events used for calculating ϵ_{SR} are required to have a DV candidate satisfying the vertex preselection. This method relies on the assumption that the mass and track multiplicity distributions of the DVs do not depend on the quantities used in the event selection, which was demonstrated in data to hold within uncertainties. An additional factor κ is applied to account for the potential effect of obtaining multiple DVs per event but is found to be consistent with 1.0 for the region of DV properties probed in this search.

A. Hadronic interactions

As discussed in Sec. IV, the bulk of the hadronic interactions occur in detector regions with dense material, and these are rejected using the material map. However, residual hadronic interactions may survive the selections, either due to imperfections in the material map or from interactions with gas molecules in regions without solid material. The low-mass region of the m_{DV} distribution is dominated by hadronic interactions. Therefore, to estimate this background in the SR, the m_{DV} distribution in the region $m_{\text{DV}} < 10$ GeV is fit to an exponential distribution and extrapolated to the SR with $m_{\text{DV}} > 10$ GeV. The assumptions made by this method and the related uncertainties are discussed in Sec. VI.

B. Merged vertices

The high density of vertices at small radii and the last step of the DV reconstruction, where vertices are combined

if they are separated by less than 1 mm, could result in the merging of two DVs with low masses and track multiplicities into a single DV with significantly higher mass and track multiplicity. To quantify this contribution, vertices from distinct events are randomly merged. The distribution of the distance $d(V_1, V_2)$ between two 2-track or 3-track vertices V_1 and V_2 is studied. To obtain a large sample of reference DV pairs, $d(V_1, V_2)$ is measured in a sample in which V_1 and V_2 are taken from different events. This sample is then compared to the sample constructed only from pairs of vertices appearing in the same event. Each of the vertices in these pairs is required to satisfy the DV preselection criteria, and their combined mass is required to be greater than 10 GeV. The resulting distributions are shown in Fig. 5(a) for pairs of 2-track vertices (2 + 2) and 5(b) for the case of a 2-track vertex paired with a 3-track vertex (2 + 3). To extract an estimate of the number of SR vertices merged during DV reconstruction, the different-event distribution is normalized to the same-event distribution in the region $d(V_1, V_2) > 1$ mm, and the estimated contribution from merged vertices is given by the scaled template's integral for $d(V_1, V_2) < 1$ mm.

It is found that the z positions of V_1 and V_2 in the same-event sample are correlated, since they are likely to originate from the same hard-scatter primary vertex. Naturally, this effect is absent in the different-event sample. As a result, the distributions of the longitudinal distance between the vertices in the different-event and same-event samples differ by up to 30% at low values of $d(V_1, V_2)$. To correct for this difference between the two samples, the DV pairs in the different-event sample are reweighted to match the distribution of distances in z in the same-event sample before the yield for $d(V_1, V_2) < 1$ mm is extracted. After applying the weights, the model distribution of the three-dimensional distance $d(V_1, V_2)$ agrees well with that of the

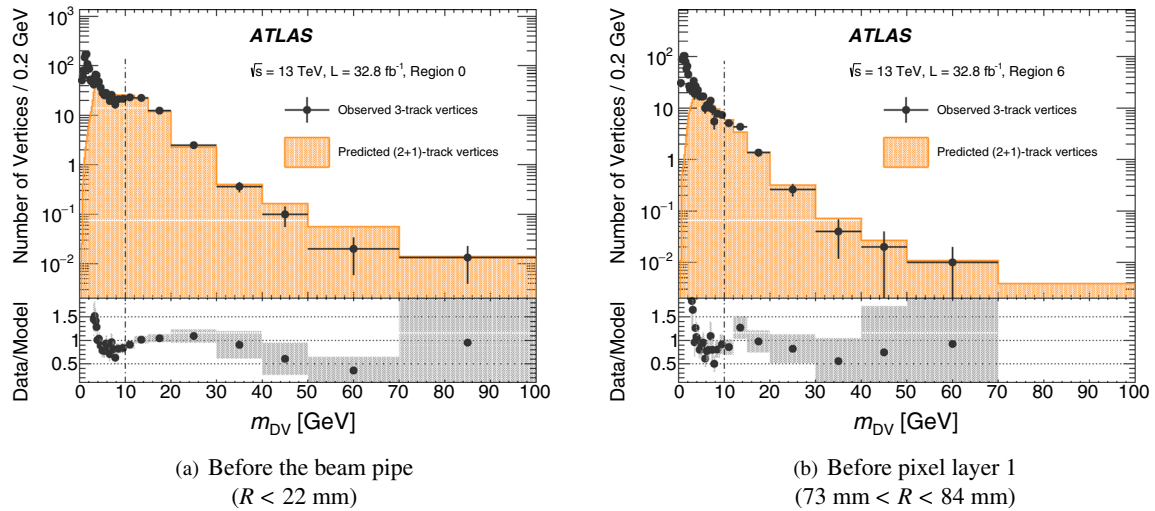


FIG. 6. Distributions of m_{DV} for 3-track vertices in the CR data for two radial regions, along with the normalized predictions from the track-association method. The spectra from the model are normalized to the data in the $m_{\text{DV}} > 10 \text{ GeV}$ region, and the scaling needed is extracted and used as the crossing factors used to calculate the predictions for higher track multiplicities. The error bars and the gray bands in the bottom ratio distributions represent the statistical uncertainties. The region below 10 GeV is not expected to be described by the accidental-crossing model.

same-event sample in the studied range of $d(V_1, V_2) < 120 \text{ mm}$. This reweighting procedure is applied in the distributions shown in Figure 5.

The background from merged DV pairs with $d(V_1, V_2) < 1 \text{ mm}$ and $n_{\text{tracks}} \geq 5$ tracks is estimated from DV pairs where one DV has two tracks and the other has three tracks. This background is found to be orders of magnitude smaller than the accidental-crossing background discussed below. The background from the merging of two 3-track vertices or a 2-track and a 4-track DV is determined to be negligible compared to other sources for higher track multiplicities.

C. Accidental crossing of vertices and tracks

The final and dominant source of background in the SR for this search is low-mass vertices crossed by an unrelated track in the event. It is common for such crossings to occur at large angles with respect to the *distance vector* that points from the PV to the DV. This significantly increases the mass of the DV. In order to estimate the contribution from this effect, $(n + 1)$ -track vertices are constructed by adding a *pseudotrack* to n -track vertices from the data. The pseudotrack is given track parameters drawn randomly from track templates, extracted separately for each radial detector region. These templates are constructed using all tracks associated with DV candidates satisfying $n_{\text{tracks}} \geq 3$ and $m_{\text{DV}} > 3 \text{ GeV}$ found in events passing the event preselection. The templates contain the track p_T , η , and relative azimuthal angle $\Delta\phi$ with respect to the distance vector. In order to model the effect of high-angle crossings, pseudotacks drawn from the templates are required to be at an angle larger than $\sqrt{(\Delta\eta)^2 + (\Delta\phi)^2} = 1$ with respect to the distance vector.

To normalize the prediction from the model constructed by this method, the probability of an accidentally crossing track to become associated with the DV is extracted by comparing the sample of 3-track vertices seen in the data to the $(2 + 1)$ -track vertices from the model in the $m_{\text{DV}} > 10 \text{ GeV}$ region. This probability is referred to as the *crossing factor* and is extracted separately for each radial detector region. Figure 6 shows the resulting $(2 + 1)$ -track predictions from the model along with the 3-track vertices for two selected radial regions. The observed differences in shape between the model and the data are used in Sec. VI to assess an uncertainty in the background estimates from the model. These crossing factors are used to project from an n -track CR to an $(n + 1)$ -track region for events passing the event preselection.

D. Validation of background estimation techniques

To ensure that the methods described above reliably model the backgrounds, two validation regions are constructed and used to test their predictions. The two regions are designed to be free of significant contamination from any signal considered in this analysis. In a low- E_T^{miss} validation region, denoted **VRLM**, the performance of these methods for vertices with exactly four tracks is studied as an intermediate point between the 3-track CR and the ≥ 5 -track SR. The **VRLM** event selection requires $E_T^{\text{miss}} < 150 \text{ GeV}$ and that the minimum azimuthal angle between the E_T^{miss} vector and all reconstructed jets, $\Delta\phi_{\min}(E_T^{\text{miss}}, \text{jets})$, is less than 0.75. These requirements sufficiently reduce the contribution from the considered signal processes that are not excluded by previous searches [11]. The background estimate extracted from the CR is scaled to account for the efficiency ϵ_{VRLM} of the E_T^{miss} and

TABLE I. The number of estimated background vertices with mass $m_{\text{DV}} > 10$ GeV for the DV selections used in the control and validation regions are shown. The $(n+1)$ -track contributions are estimated using the accidental-crossing factor method (Sec. V C), the $(2+2)$ -track and $(2+3)$ -track contributions are obtained from merged vertices (Sec. V B), and the pure n -track contribution is evaluated using the hadronic interactions (Sec. V A). Also shown are the estimated background event yields in the preselection region with at least five tracks. The predicted background event yield in the signal region appears in the bottom row and includes the transfer factors shown. When two uncertainties are shown, the first is statistical while the second is systematic. When one number is given, it represents the combined uncertainty.

Selection	Subregion	Category	Yield
<i>Event preselection $n_{\text{trk}} = 3$, $m_{\text{DV}} > 10$ GeV</i>		Measured total	3093
<i>Event preselection $n_{\text{trk}} = 4$, $m_{\text{DV}} > 10$ GeV</i>	VRLM	$(3+1)$ -track	$12.6 \pm 0.3 \pm 1.1$
		$(2+2)$ -track	3.6 ± 3.6
		Pure 4-track	$0.3^{+0.9}_{-0.3}$
		Subtotal	16 ± 4
		Total (after scaling by ϵ_{VRLM})	9 ± 2
	VRM	$(3+1)$ -track	$137 \pm 3 \pm 30$
		Pure 4-track	16^{+47}_{-16}
		Total	150^{+60}_{-30}
<i>Event preselection $n_{\text{trk}} \geq 5$, $m_{\text{DV}} > 10$ GeV</i>	5-tracks	$(4+1)$ -track	$1.30 \pm 0.07 \pm 0.12$
		$(2+3)$ -track	0.01 ± 0.01
		Pure 5-track	$0.9^{+2.8}_{-0.9}$
		Total	$2.2^{+2.8}_{-0.9}$
	6-tracks	$(5+1)$ -track	$0.37 \pm 0.03 \pm 0.04$
		Pure 6-track	$0.2^{+0.6}_{-0.2}$
		Total	$0.6^{+0.6}_{-0.2}$
	≥ 7 -tracks	$(n+1)$ -track	$0.37 \pm 0.03 \pm 0.04$
		Pure ≥ 7 -track	1^{+3}_{-1}
		Total	1^{+3}_{-1}
Full SR selection	Total		$4.2^{+4.1}_{-1.4}$
	Total (after scaling by $\epsilon_{\text{SR}} \times \kappa$)		$0.02^{+0.02}_{-0.01}$

$\Delta\phi_{\min}(E_{\text{T}}^{\text{miss}}, \text{jets})$ requirements to predict the background in VRLM. Since studies in data show that the m_{DV} and n_{tracks} distributions are independent of these event-level quantities, ϵ_{VRLM} is extracted in a sample with 3-track vertices and applied to the 4-track prediction. It is found to be $\epsilon_{\text{VRLM}} = (56 \pm 6)\%$.

Additional validation of the background estimation methods is done in a material-enriched validation region, VRM. Here, the material veto is inverted and vertices satisfying the other vertex preselection criteria are studied. Due to the abundance of hadronic interactions in this region, it contains many more vertices than VRLM. Since accidental track crossings also happen to vertices from hadronic interactions, this region can be used to validate the accidental-crossing background estimation method. An independent set of crossing factors is derived and applied in this validation region, and their values are found to be similar to those extracted in the samples where the material-rich regions are vetoed.

In both VRLM and VRM, the yields predicted by the background estimation methods are shown in Table I.

E. Final expected yields

The predicted background yields in the various selections are listed in Table I. The yields are shown separately for each of the estimation methods along with the total for each region. Also shown is the final expected yield in the SR after the application of the scaling factors described above. The total SR prediction from the sum of all background sources is $0.02^{+0.02}_{-0.01}$ events, where the total uncertainty includes both the statistical and systematic uncertainties.

VI. UNCERTAINTIES

The estimation of the hadronic interaction background described in Sec. V A relies on the assumption that the mass spectra of such contributions follow an exponential shape. This assumption is tested using interaction vertices in the GEANT4-based simulations described in Sec. III. Based on studies of the deviations from an exponential shape seen in the simulation, an uncertainty of -100% and $+300\%$ is applied to the component of the total background from hadronic interactions. The size of this uncertainty is taken

as the largest deviation observed in all track multiplicities for vertices with $m_{\text{DV}} > 10$ GeV in simulation.

The background in the SR due to merged vertices (Sec. V B) is estimated to be very small with respect to the total background. By comparing the same-event data and different-event model for (2 + 3)-track DV pairs, the largest statistically significant discrepancy in any bin in the studied range is observed to be 60%. To be conservative, the systematic uncertainty for this subdominant background is taken to be 100%.

Uncertainties associated with the contribution from low-mass vertices crossed accidentally by an unrelated track (Sec. V C) are dominated by the uncertainty of the extracted crossing factors. By varying the choice of m_{DV} threshold used for the normalization of the spectra from the background model by ± 5 GeV (with respect to the nominal 10 GeV), an uncertainty is extracted. Since the crossing factors are derived and applied separately for each radial detector region, their uncertainties are as well. The size of the resulting uncertainty for the accidentally crossing track contributions is 10%–20% depending on the radial detector region.

Finally, the event selection transfer factor ϵ_{SR} and the correction κ from event level to vertex level, described in Sec. V, also have associated uncertainties. Both of these uncertainties are derived by varying the kinematic requirements for the vertices. Varying the vertex-level requirements used in these calculations results in uncertainties of 50% in ϵ_{SR} and 16% in κ . Since these factors are applied to all background contributions to obtain a final SR estimate, these uncertainties propagate directly to the final estimate.

While the background uncertainties and expectations are derived from data, additional modeling uncertainties that only affect the signal efficiencies are considered and derived by varying parameters used in the simulation and reconstruction. The effect of varying the amount of simulated pileup within its modeling uncertainty is a few percent for high- Δm samples, and up to 10% for small- Δm samples. To estimate the size of the uncertainty due to ISR modeling, the size of the reweighting of PYTHIA 6 to

MADGRAPH5_aMC@NLO as described in Sec. III is taken as an additional systematic uncertainty. This effect corresponds to an uncertainty of a few percent in the signal efficiency for high- Δm models. However, for low- Δm samples, where the intrinsic $E_{\text{T}}^{\text{miss}}$ is smaller, the signal acceptance depends heavily on radiation effects. For these models, the uncertainty in the ISR modeling yields an uncertainty of as much as 25% in the acceptance.

The uncertainty in the signal efficiency due to variations in the track and DV reconstruction efficiency is determined to be 5%–10% by randomly removing tracks at a rate given by the expected tracking inefficiency. Additional uncertainties related to the trigger efficiency, the jet energy scale and resolution, as well as the reconstruction of the $E_{\text{T}}^{\text{miss}}$, are evaluated and found to be negligible with respect to the leading uncertainties. No additional uncertainty is considered for the modeling of the production of R -hadrons and their interactions with matter. Decays of electrically charged and neutral LLPs are reconstructed as displaced vertices in the ID with similar efficiencies, so this search is less sensitive to the fraction of charged states after hadronization compared to those based on direct-detection signatures. Since the amount of material traversed before a decay in the ID is small, the sensitivity to uncertainties in the per-parton cross section for hadronic interactions is negligible.

VII. RESULTS

The final yields for all regions used in this analysis are shown in Table II. The observed yields are consistent with the expected background in the validation regions, where VRLM contains 9 vertices (9 ± 2 expected) and VRM contains 177 vertices (150 ± 60 expected). The two-dimensional distribution of m_{DV} and track multiplicity is shown in Fig. 7 for events that satisfy the full event-level selection. The final SR yields are highlighted, with 0 events observed ($0.02^{+0.02}_{-0.01}$ expected).

In the absence of a statistically significant excess in the data, exclusion limits are placed on R -hadron models.

TABLE II. The observed number of vertices for the control and validation regions are shown along with the background expectations. The last row shows the expected and observed signal region event yields.

Selection	Subregion	Estimated	Observed
<i>Event preselection $n_{\text{trk}} = 3$, $m_{\text{DV}} > 10$ GeV</i>			3093
<i>Event preselection $n_{\text{trk}} = 4$, $m_{\text{DV}} > 10$ GeV</i>	VRLM	9 ± 2	9
	VRM	150^{+60}_{-30}	177
<i>Event preselection $n_{\text{trk}} \geq 5$, $m_{\text{DV}} > 10$ GeV</i>	5-tracks	$2.2^{+2.8}_{-0.9}$	1
	6-tracks	$0.6^{+0.6}_{-0.2}$	1
	≥ 7 -tracks	1^{+3}_{-1}	3
	Total	$4.2^{+4.1}_{-1.4}$	5
<i>Full SR selection</i>	Total	$0.02^{+0.02}_{-0.01}$	0

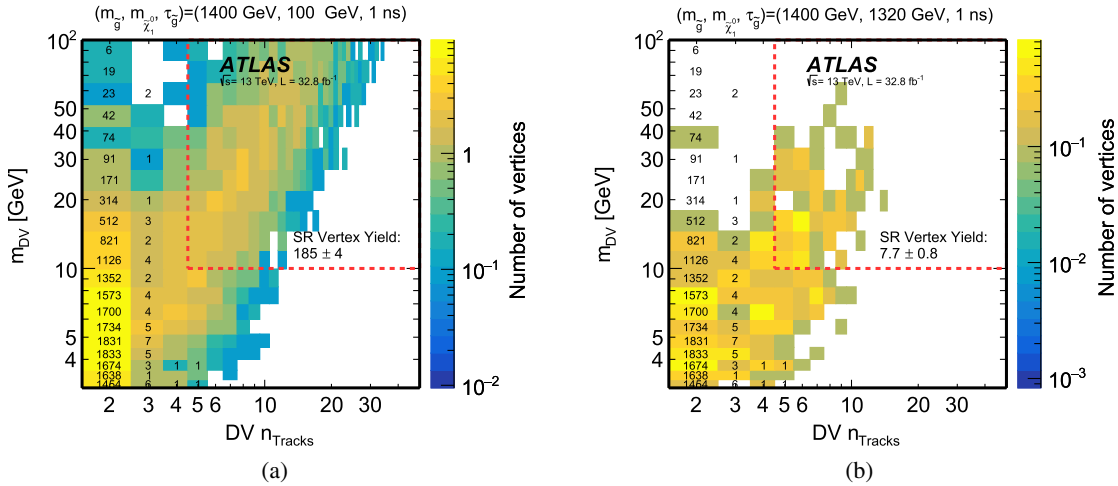


FIG. 7. Two-dimensional distributions of m_{DV} and track multiplicity are shown for DVs in events that satisfy all signal region event selection criteria. Bin numbers correspond to the observations in data, while the color representation shows example distributions for two R -hadron signals used as benchmark models in this search. The dashed line represents the boundary of the signal region requirements, and the expected signal yield in this region is shown.

These 95% confidence-level (C.L.) upper limits are calculated following the CL_s prescription [81] with the profile likelihood used as the test statistic, using the HISTFITTER [82] framework with pseudoexperiments. Upper limits on the cross section for gluino pair production as a function of gluino lifetime are shown in Fig. 8 for example values of $m_{\tilde{g}}$ and $m_{\tilde{\chi}_1^0} = 100$ GeV. Also shown are the signal production cross sections for these gluino masses. Reduced signal

selection efficiencies for low- Δm samples result in less stringent cross-section limits. For $\Delta m = 100$ GeV, the limits are shown in Fig. 9. Lower limits on the gluino mass are also shown as a function of gluino lifetime in Figs. 8 and 9. DV-level fiducial volume and PV-distance requirements reduce the exclusion power in the high and low extremes of gluino lifetime. Similarly, for a fixed gluino lifetime of $\tau = 1$ ns, 95% C.L. exclusion curves are

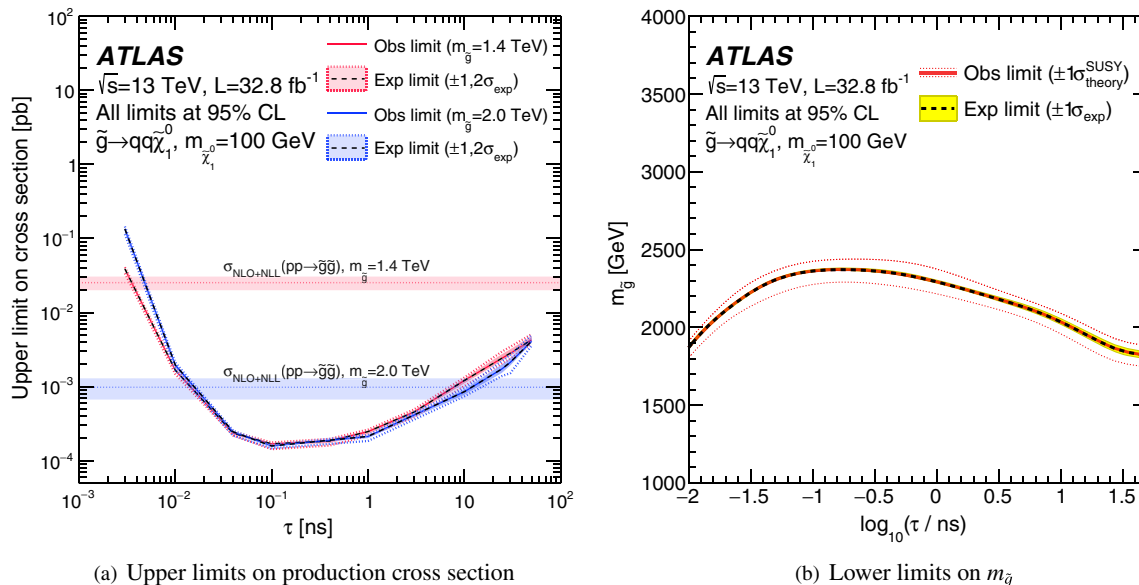


FIG. 8. Upper 95% C.L. limits on the signal cross section are shown in (a) for $m_{\tilde{g}} = 1400$ GeV and $m_{\tilde{g}} = 2000$ GeV as a function of lifetime τ , for fixed $m_{\tilde{\chi}_1^0} = 100$ GeV. Horizontal lines denote the $\tilde{g}\tilde{g}$ production cross section for the same values of $m_{\tilde{g}}$, shown with uncertainties on $\sigma_{\text{theory}}^{\text{SUSY}}$ given by variations of the renormalization and factorization scales, and PDF uncertainties. The lower limit on $m_{\tilde{g}}$ for fixed $m_{\tilde{\chi}_1^0} = 100$ GeV as a function of lifetime τ is shown in (b). The nominal expected and observed limit contours coincide due to the signal region yield's high level of agreement with expectation.

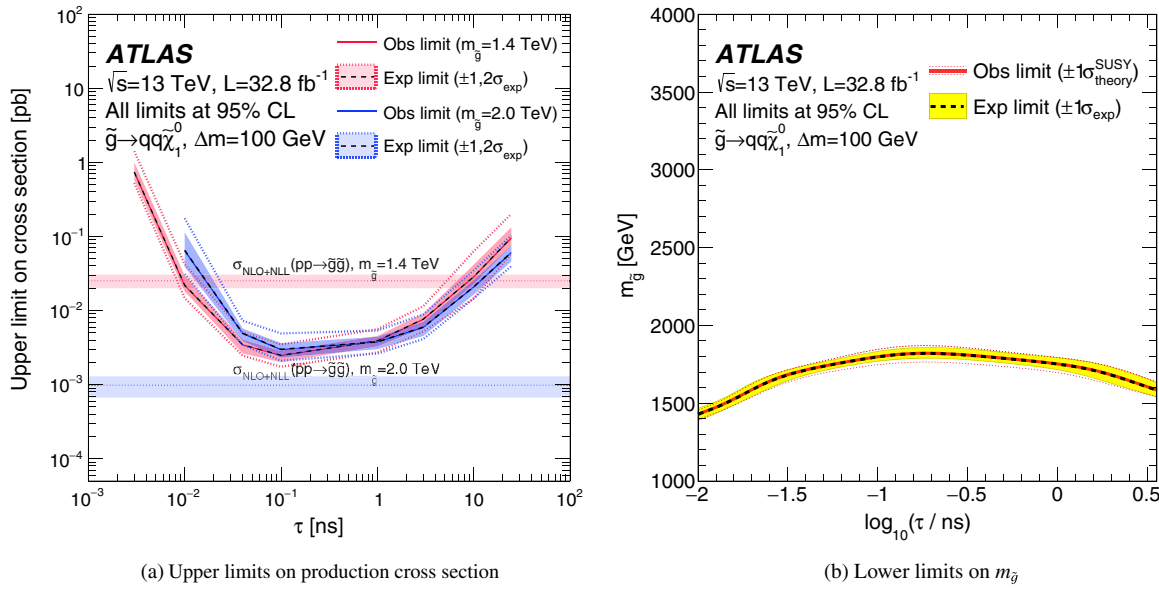


FIG. 9. Upper 95% C.L. limits on the signal cross section are shown in (a) for $m_{\tilde{g}} = 1400$ GeV and $m_{\tilde{g}} = 2000$ GeV as a function of lifetime τ , for fixed $\Delta m = 100$ GeV. Horizontal lines denote the $\tilde{g}\tilde{g}$ production cross section for the same values of $m_{\tilde{g}}$, shown with uncertainties on $\sigma_{\text{theory}}^{\text{SUSY}}$ given by variations of the renormalization and factorization scales, and PDF uncertainties. The lower limit on $m_{\tilde{g}}$ for fixed $\Delta m = 100$ GeV as a function of lifetime τ is shown in (b). The nominal expected and observed limit contours coincide due to the signal region yield's high level of agreement with expectation.

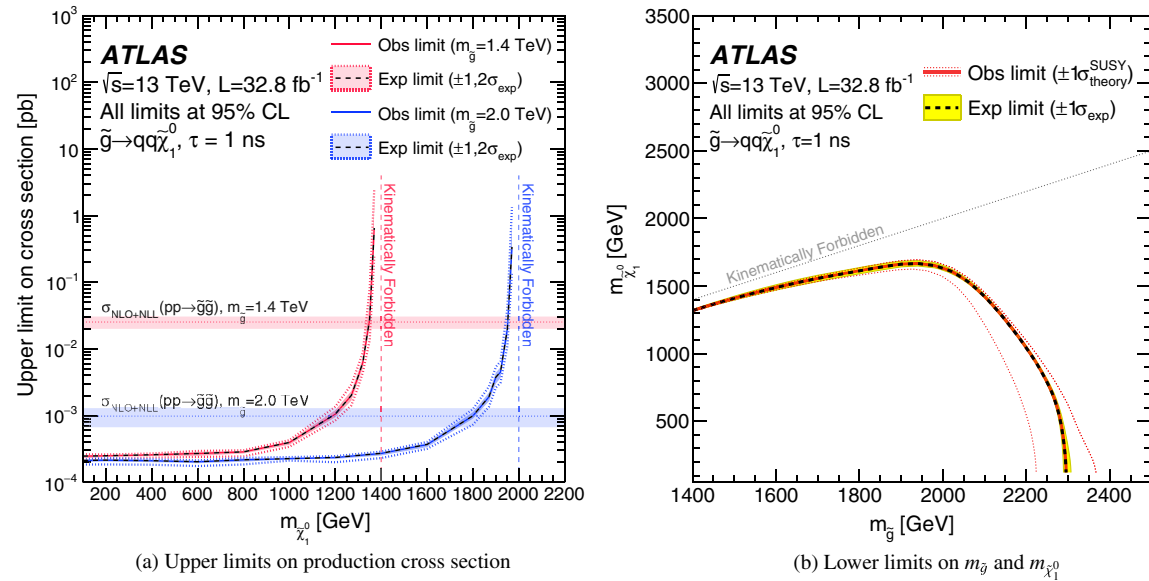


FIG. 10. Upper 95% C.L. limits on the signal cross section are shown in (a) for $m_{\tilde{g}} = 1400$ GeV and $m_{\tilde{g}} = 2000$ GeV as a function of $m_{\tilde{\chi}_1^0}$, for fixed $\tau = 1$ ns. Horizontal lines denote the $\tilde{g}\tilde{g}$ production cross section for the same values of $m_{\tilde{g}}$, shown with uncertainties $\sigma_{\text{theory}}^{\text{SUSY}}$ given by variations of the renormalization and factorization scale and PDF uncertainties. The 95% C.L. limit as a function of $m_{\tilde{g}}$ and $m_{\tilde{\chi}_1^0}$ is shown in (b) for fixed $\tau = 1$ ns. The nominal expected and observed limit contours coincide due to the signal region yield's high level of agreement with expectation.

shown as a function of $m_{\tilde{g}}$ and $m_{\tilde{\chi}_1^0}$ in Fig. 10. For $m_{\tilde{\chi}_1^0} = 100$ GeV, gluino masses are excluded below 2.29 TeV at $\tau = 1$ ns and below 2.37 TeV at around $\tau = 0.17$ ns.

VIII. CONCLUSIONS

A search for massive, long-lived particles with decays giving rise to displaced multitrack vertices is performed with 32.8 fb^{-1} of pp collisions at $\sqrt{s} = 13$ TeV collected

by the ATLAS experiment at the LHC. The search presented is sensitive to models predicting events with significant E_T^{miss} and at least one displaced vertex with five or more tracks and a visible invariant mass greater than 10 GeV. With an expected background of $0.02^{+0.02}_{-0.01}$ events, no events in the data sample were observed in the signal region. With results consistent with the background-only hypothesis, exclusion limits are derived for models predicting the existence of such particles, reaching roughly $m_{\tilde{g}} = 2000$ GeV to 2370 GeV for $m_{\tilde{\chi}_1^0} = 100$ GeV and gluino lifetimes between 0.02 and 10 ns. For a fixed gluino-neutralino mass difference of $\Delta m = 100$ GeV, exclusion limits reach roughly $m_{\tilde{g}} = 1550$ GeV to 1820 GeV for gluino lifetimes between 0.02 and 4 ns.

ACKNOWLEDGMENTS

We thank CERN for the very successful operation of the LHC, as well as the support staff from our institutions without whom ATLAS could not be operated efficiently. We acknowledge the support of ANPCyT, Argentina; YerPhI, Armenia; ARC, Australia; BMWFW and FWF, Austria; ANAS, Azerbaijan; SSTC, Belarus; CNPq and FAPESP, Brazil; NSERC, NRC, and CFI, Canada; CERN; CONICYT, Chile; CAS, MOST, and NSFC, China; COLCIENCIAS, Colombia; MSMT CR, MPO CR, and VSC CR, Czech Republic; DNRF and DNSRC, Denmark; IN2P3-CNRS, CEA-DRF/IRFU, France; SRNSFG, Georgia; BMBF, HGF, and MPG, Germany; GSRT, Greece; RGC, Hong Kong SAR, China; ISF, I-CORE, and Benoziyo Center, Israel; INFN, Italy; MEXT and JSPS,

Japan; CNRST, Morocco; NWO, Netherlands; RCN, Norway; MNiSW and NCN, Poland; FCT, Portugal; MNE/IFA, Romania; MES of Russia and NRC KI, Russian Federation; JINR; MESTD, Serbia; MSSR, Slovakia; ARRS and MIZŠ, Slovenia; DST/NRF, South Africa; MINECO, Spain; SRC and Wallenberg Foundation, Sweden; SERI, SNSF, and Cantons of Bern and Geneva, Switzerland; MOST, Taiwan; TAEK, Turkey; STFC, United Kingdom; DOE and NSF, USA. In addition, individual groups and members have received support from BCKDF, the Canada Council, CANARIE, CRC, Compute Canada, FQRNT, and the Ontario Innovation Trust, Canada; EPLANET, ERC, ERDF, FP7, Horizon 2020, and Marie Skłodowska-Curie Actions, European Union; Investissements d’Avenir Labex and Idex, ANR, Région Auvergne and Fondation Partager le Savoir, France; DFG and AvH Foundation, Germany; Herakleitos, Thales and Aristeia programs cofinanced by EU-ESF and the Greek NSRF; BSF, GIF, and Minerva, Israel; BRF, Norway; CERCA Programme Generalitat de Catalunya, Generalitat Valenciana, Spain; the Royal Society and Leverhulme Trust, United Kingdom. The crucial computing support from all WLCG partners is acknowledged gratefully, in particular from CERN, the ATLAS Tier-1 facilities at TRIUMF (Canada), NDGF (Denmark, Norway, Sweden), CC-IN2P3 (France), KIT/GridKA (Germany), INFN-CNAF (Italy), NL-T1 (Netherlands), PIC (Spain), ASGC (Taiwan), RAL (UK), and BNL (USA), the Tier-2 facilities worldwide, and large non-WLCG resource providers. Major contributors of computing resources are listed in Ref. [83].

-
- [1] G. Bertone, D. Hooper, and J. Silk, Particle dark matter: Evidence, candidates and constraints, *Phys. Rep.* **405**, 279 (2005).
 - [2] S. Weinberg, Implications of dynamical symmetry breaking, *Phys. Rev. D* **13**, 974 (1976).
 - [3] L. Susskind, Dynamics of spontaneous symmetry breaking in the Weinberg-Salam theory, *Phys. Rev. D* **20**, 2619 (1979).
 - [4] S. Dimopoulos, S. Raby, and F. Wilczek, Supersymmetry and the scale of unification, *Phys. Rev. D* **24**, 1681 (1981).
 - [5] M. J. Strassler and K. M. Zurek, Echoes of a hidden valley at hadron colliders, *Phys. Lett. B* **651**, 374 (2007).
 - [6] R. Barbier *et al.*, R -parity violating supersymmetry, *Phys. Rep.* **420**, 1 (2005).
 - [7] B. C. Allanach, M. A. Bernhardt, H. K. Dreiner, C. H. Kom, and P. Richardson, Mass spectrum in R -parity violating minimal supergravity and benchmark points, *Phys. Rev. D* **75**, 035002 (2007).
 - [8] N. Arkani-Hamed and S. Dimopoulos, Supersymmetric unification without low energy supersymmetry and signa-
 - tures for fine-tuning at the LHC, *J. High Energy Phys.* **06** (2005) 073.
 - [9] G. F. Giudice and A. Romanino, Split supersymmetry, *Nucl. Phys.* **B699**, 65 (2004); Erratum, *Nucl. Phys.* **B706**, 487 (2005).
 - [10] M. Fairbairn, A. C. Kraan, D. A. Milstead, T. Sjöstrand, P. Skands, and T. Sloan, Stable massive particles at colliders, *Phys. Rep.* **438**, 1 (2007).
 - [11] ATLAS Collaboration, Search for massive, long-lived particles using multitrack displaced vertices or displaced lepton pairs in pp collisions at $\sqrt{s} = 8$ TeV with the ATLAS detector, *Phys. Rev. D* **92**, 072004 (2015).
 - [12] ATLAS Collaboration, Search for displaced muonic lepton jets from light Higgs boson decay in proton-proton collisions at $\sqrt{s} = 7$ TeV with the ATLAS detector, *Phys. Lett. B* **721**, 32 (2013).
 - [13] ATLAS Collaboration, Search for non-pointing photons in the diphoton and E_T^{miss} final state in $\sqrt{s} = 7$ TeV proton-proton collisions using the ATLAS detector, *Phys. Rev. D* **88**, 012001 (2013).

- [14] ATLAS Collaboration, Search for non-pointing and delayed photons in the diphoton and missing transverse momentum final state in 8 TeV pp collisions at the LHC using the ATLAS detector, *Phys. Rev. D* **90**, 112005 (2014).
- [15] ATLAS Collaboration, Search for charginos nearly mass-degenerate with the lightest neutralino based on a disappearing-track signature in pp collisions at $\sqrt{s} = 8$ TeV with the ATLAS detector, *Phys. Rev. D* **88**, 112006 (2013).
- [16] ATLAS Collaboration, Search for pair-produced long-lived neutral particles decaying in the ATLAS hadronic calorimeter in pp collisions at $\sqrt{s} = 8$ TeV, *Phys. Lett. B* **743**, 15 (2015).
- [17] ATLAS Collaboration, Search for long-lived, weakly interacting particles that decay to displaced hadronic jets in proton-proton collisions at $\sqrt{s} = 8$ TeV with the ATLAS detector, *Phys. Rev. D* **92**, 012010 (2015).
- [18] ATLAS Collaboration, Search for displaced vertices arising from decays of new heavy particles in 7 TeV pp collisions at ATLAS, *Phys. Lett. B* **707**, 478 (2012).
- [19] ATLAS Collaboration, Search for long-lived, heavy particles in final states with a muon and multi-track displaced vertex in proton-proton collisions at $\sqrt{s} = 7$ TeV with the ATLAS detector, *Phys. Lett. B* **719**, 280 (2013).
- [20] ATLAS Collaboration, Search for heavy long-lived charged R -hadrons with the ATLAS detector in 3.2 fb^{-1} of proton-proton collision data at $\sqrt{s} = 13$ TeV, *Phys. Lett. B* **760**, 647 (2016).
- [21] ATLAS Collaboration, Search for metastable heavy charged particles with large ionization energy loss in pp collisions at $\sqrt{s} = 13$ TeV using the ATLAS experiment, *Phys. Rev. D* **93**, 112015 (2016).
- [22] CMS Collaboration, Search in leptonic channels for heavy resonances decaying to long-lived neutral particles, *J. High Energy Phys.* **02** (2013) 085.
- [23] CMS Collaboration, Search for Displaced Supersymmetry in Events with an Electron and a Muon with Large Impact parameters, *Phys. Rev. Lett.* **114**, 061801 (2015).
- [24] CMS Collaboration, Search for long-lived particles that decay into final states containing two electrons or two muons in proton-proton collisions at $\sqrt{s} = 8$ TeV, *Phys. Rev. D* **91**, 052012 (2015).
- [25] CMS Collaboration, Search for long-lived neutral particles decaying to quark-antiquark pairs in proton-proton collisions at $\sqrt{s} = 8$ TeV, *Phys. Rev. D* **91**, 012007 (2015).
- [26] CMS Collaboration, A search for pair production of new light bosons decaying into muons, *Phys. Lett. B* **752**, 146 (2016).
- [27] CMS Collaboration, Search for R -parity violating supersymmetry with displaced vertices in proton-proton collisions at $\sqrt(s) = 8$ TeV, *Phys. Rev. D* **95**, 012009 (2016).
- [28] CMS Collaboration, Search for long-lived charged particles in proton-proton collisions at $\sqrt{s} = 13$ TeV, *Phys. Rev. D* **94**, 112004 (2016).
- [29] CMS Collaboration, Search for long-lived particles in events with photons and missing energy in proton-proton collisions at $\sqrt{s} = 7$ TeV, *Phys. Lett. B* **722**, 273 (2013).
- [30] R. Aaij *et al.* (LHCb Collaboration), Search for long-lived particles decaying to jet pairs, *Eur. Phys. J. C* **75**, 152 (2015).
- [31] R. Aaij *et al.* (LHCb Collaboration), Search for Hidden-Sector Bosons in $B^0 \rightarrow K^{*0}\mu^+\mu^-$ Decays, *Phys. Rev. Lett.* **115**, 161802 (2015).
- [32] R. Aaij *et al.* (LHCb Collaboration), Search for massive long-lived particles decaying semileptonically in the LHCb detector, *Eur. Phys. J. C* **77**, 224 (2017).
- [33] R. Aaij *et al.* (LHCb Collaboration), Search for long-lived scalar particles in $B^+ \rightarrow K^+\chi(\mu^+\mu^-)$ decays, *Phys. Rev. D* **95**, 071101 (2017).
- [34] F. Abe *et al.* (CDF Collaboration), Search for long-lived parents of Z^0 bosons in $p\bar{p}$ collisions at $\sqrt{s} = 1.8$ TeV, *Phys. Rev. D* **58**, 051102 (1998).
- [35] V. M. Abazov *et al.* (D0 Collaboration), Search for Neutral, Long-Lived Particles Decaying into Two Muons in $p\bar{p}$ Collisions at $\sqrt{s} = 1.96$ TeV, *Phys. Rev. Lett.* **97**, 161802 (2006).
- [36] V. M. Abazov *et al.* (D0 Collaboration), Search for Resonant Pair Production of Long-Lived Particles Decaying to b anti- b in p anti- p Collisions at $\sqrt{s} = 1.96$ TeV, *Phys. Rev. Lett.* **103**, 071801 (2009).
- [37] J. P. Lees *et al.* (BABAR Collaboration), Search for Long-Lived Particles in e^+e^- Collisions, *Phys. Rev. Lett.* **114**, 171801 (2015).
- [38] D. Liventsev *et al.* (Belle Collaboration), Search for heavy neutrinos at Belle, *Phys. Rev. D* **87**, 071102 (2013).
- [39] A. Heister *et al.* (ALEPH Collaboration), Search for gauge mediated SUSY breaking topologies in e^+e^- collisions at center-of-mass energies up to 209-GeV, *Eur. Phys. J. C* **25**, 339 (2002).
- [40] ATLAS Collaboration, The ATLAS experiment at the CERN Large Hadron Collider, *J. Instrum.* **3**, S08003 (2008).
- [41] ATLAS Collaboration, ATLAS insertable B-layer technical design report, Report No. ATLAS-TDR-19, 2010, <https://cds.cern.ch/record/1291633>; ATLAS insertable B-layer technical design report addendum, Report No. ATLAS-TDR-19-ADD-1, 2012, <https://cds.cern.ch/record/1451888>.
- [42] ATLAS Collaboration, Performance of the ATLAS trigger system in 2015, *Eur. Phys. J. C* **77**, 317 (2017).
- [43] ATLAS Collaboration, Luminosity determination in pp collisions at $\sqrt{s} = 8$ TeV using the ATLAS detector at the LHC, *Eur. Phys. J. C* **76**, 653 (2016).
- [44] T. Sjöstrand, S. Mrenna, and P.Z. Skands, PYTHIA 6.4 physics and manual, *J. High Energy Phys.* **05** (2006) 026.
- [45] ATLAS Collaboration, Further ATLAS tunes of PYTHIA 6 and PYTHIA 8, Report No. ATL-PHYS-PUB-2011-014, <https://cds.cern.ch/record/1400677>.
- [46] J. Pumplin, D.R. Stump, J. Huston, H.-L. Lai, P. Nadolsky, and W.-K. Tung, New generation of parton distributions with uncertainties from global QCD analysis, *J. High Energy Phys.* **07** (2002) 012.
- [47] G.R. Farrar and P. Fayet, Phenomenology of the production, decay, and detection of new hadronic states associated with supersymmetry, *Phys. Lett.* **76B**, 575 (1978).
- [48] A.C. Kraan, Interactions of heavy stable hadronizing particles, *Eur. Phys. J. C* **37**, 91 (2004).
- [49] W. Beenakker, R. Hopker, M. Spira, and P. Zerwas, Squark and gluino production at hadron colliders, *Nucl. Phys.* **B492**, 51 (1997).
- [50] C. Borschensky, M. Krämer, A. Kulesza, M. Mangano, S. Padhi, T. Plehn, and X. Portell, Squark and gluino pro-

- duction cross sections in pp collisions at $\sqrt{s} = 13, 14, 33$ and 100 TeV, *Eur. Phys. J. C* **74**, 3174 (2014).
- [51] A. Kulesza and L. Motyka, Soft gluon resummation for the production of gluino-gluino and squark-antisquark pairs at the LHC, *Phys. Rev. D* **80**, 095004 (2009).
- [52] A. Kulesza and L. Motyka, Threshold resummation for squark-antisquark and gluino-pair production at the LHC, *Phys. Rev. Lett.* **102**, 111802 (2009).
- [53] P. M. Nadolsky, H.-L. Lai, Q.-H. Cao, J. Huston, J. Pumplin, D. Stump, W.-K. Tung, and C.-P. Yuan, Implications of CTEQ global analysis for collider observation, *Phys. Rev. D* **78**, 013004 (2008).
- [54] A. D. Martin, W. J. Stirling, R. S. Thorne, and G. Watt, Parton distributions for the LHC, *Eur. Phys. J. C* **63**, 189 (2009).
- [55] ATLAS Collaboration, The ATLAS simulation infrastructure, *Eur. Phys. J. C* **70**, 823 (2010).
- [56] S. Agostinelli *et al.*, GEANT4: A simulation toolkit, *Nucl. Instrum. Methods Phys. Res., Sect. A* **506**, 250 (2003).
- [57] R. Mackeprang and A. Rizzi, Interactions of coloured heavy stable particles in matter, *Eur. Phys. J. C* **50**, 353 (2007).
- [58] R. Mackeprang and D. Milstead, An updated description of heavy-hadron interactions in GEANT4, *Eur. Phys. J. C* **66**, 493 (2010).
- [59] J. Alwall, R. Frederix, S. Frixione, V. Hirschi, F. Maltoni, O. Mattelaer, H.-S. Shao, T. Stelzer, P. Torrielli, and M. Zaro, The automated computation of tree-level and next-to-leading order differential cross sections, and their matching to parton shower simulations, *J. High Energy Phys.* **07** (2014) 079.
- [60] ATLAS Collaboration, ATLAS Pythia 8 tunes to 7 TeV data, Report No. ATL-PHYS-PUB-2014-021, <https://cds.cern.ch/record/1966419>.
- [61] R. D. Ball *et al.*, Parton distributions with LHC data, *Nucl. Phys.* **B867**, 244 (2013).
- [62] T. Sjöstrand, S. Mrenna, and P. Z. Skands, A brief introduction to PYTHIA 8.1, *Comput. Phys. Commun.* **178**, 852 (2008).
- [63] ATLAS Collaboration, Summary of ATLAS Pythia 8 tunes, Report No. ATL-PHYS-PUB-2012-003, 2012, <https://cds.cern.ch/record/1474107>.
- [64] ATLAS Collaboration, Topological cell clustering in the ATLAS calorimeters and its performance in LHC Run 1, *Eur. Phys. J. C* **77**, 490 (2017).
- [65] M. Cacciari, G. P. Salam, and G. Soyez, The anti- k_t jet clustering algorithm, *J. High Energy Phys.* **04** (2008) 063.
- [66] M. Cacciari, G. P. Salam, and G. Soyez, FastJet user manual, *Eur. Phys. J. C* **72**, 1896 (2012).
- [67] ATLAS Collaboration, Single hadron response measurement and calorimeter jet energy scale uncertainty with the ATLAS detector at the LHC, *Eur. Phys. J. C* **73**, 2305 (2013).
- [68] ATLAS Collaboration, Jet energy measurement and its systematic uncertainty in proton-proton collisions at $\sqrt{s} = 7$ TeV with the ATLAS detector, *Eur. Phys. J. C* **75**, 17 (2015).
- [69] ATLAS Collaboration, Jet energy scale measurements and their systematic uncertainties in proton-proton collisions at $\sqrt{s} = 13$ TeV with the ATLAS detector, *Phys. Rev. D* **96**, 072002 (2017).
- [70] ATLAS Collaboration, Performance of missing transverse momentum reconstruction with the ATLAS detector in the first proton-proton collisions at $\sqrt{s} = 13$ TeV, Report No. ATL-PHYS-PUB-2015-027, <https://cds.cern.ch/record/2037904>.
- [71] ATLAS Collaboration, Performance of missing transverse momentum reconstruction in proton-proton collisions at $\sqrt{s} = 7$ TeV with ATLAS, *Eur. Phys. J. C* **72**, 1844 (2012).
- [72] ATLAS Collaboration, Performance of algorithms that reconstruct missing transverse momentum in $\sqrt{s} = 8$ TeV proton-proton collisions in the ATLAS detector, *Eur. Phys. J. C* **77**, 241 (2017).
- [73] ATLAS Collaboration, Track reconstruction performance of the ATLAS inner detector at $\sqrt{s} = 13$ TeV, Report No. ATL-PHYS-PUB-2015-018, <https://cds.cern.ch/record/2037683>.
- [74] ATLAS Collaboration, Performance of the reconstruction of large impact parameter tracks in the ATLAS inner detector, Report No. ATL-PHYS-PUB-2017-014, <https://cds.cern.ch/record/2275635>.
- [75] S. R. Das, On a new approach for finding all the modified cut-sets in an incompatibility graph, *IEEE Trans. Comput. C-22*, 187 (1973).
- [76] ATLAS Collaboration, A measurement of material in the ATLAS tracker using secondary hadronic interactions in 7 TeV pp collisions, *J. Instrum.* **11**, P11020 (2016).
- [77] ATLAS Collaboration, Study of the material of the ATLAS inner detector for Run 2 of the LHC, *J. Instrum.* **12**, P12009 (2017).
- [78] N. Nagata, H. Otono, and S. Shirai, Probing bino-wino coannihilation at the LHC, *J. High Energy Phys.* **10** (2015) 086.
- [79] N. Nagata, H. Otono, and S. Shirai, Probing bino-gluino coannihilation at the LHC, *Phys. Lett. B* **748**, 24 (2015).
- [80] N. Nagata, H. Otono, and S. Shirai, Cornering compressed gluino at the LHC, *J. High Energy Phys.* **03** (2017) 025.
- [81] A. L. Read, Presentation of search results: The CL_S technique, *J. Phys. G* **28**, 2693 (2002).
- [82] M. Baak, G. J. Besjes, D. Côté, A. Koutsman, J. Lorenz, and D. Short, HistFitter software framework for statistical data analysis, *Eur. Phys. J. C* **75**, 153 (2015).
- [83] ATLAS Collaboration, ATLAS computing acknowledgements, Report No. ATL-GEN-PUB-2016-002, <https://cds.cern.ch/record/2202407>.

- M. Aaboud,^{137d} G. Aad,⁸⁸ B. Abbott,¹¹⁵ O. Abdinov,^{12,a} B. Abeloos,¹¹⁹ S. H. Abidi,¹⁶¹ O. S. AbouZeid,¹³⁹ N. L. Abraham,¹⁵¹ H. Abramowicz,¹⁵⁵ H. Abreu,¹⁵⁴ R. Abreu,¹¹⁸ Y. Abulaiti,^{148a,148b} B. S. Acharya,^{167a,167b,b} S. Adachi,¹⁵⁷ L. Adamczyk,^{41a} J. Adelman,¹¹⁰ M. Adersberger,¹⁰² T. Adye,¹³³ A. A. Affolder,¹³⁹ T. Agatonovic-Jovin,¹⁴ C. Agheorghiesei,^{28c} J. A. Aguilar-Saavedra,^{128a,128f} S. P. Ahlen,²⁴ F. Ahmadov,^{68,c} G. Aielli,^{135a,135b} S. Akatsuka,⁷¹ H. Akerstedt,^{148a,148b} T. P. A. Åkesson,⁸⁴ E. Akilli,⁵² A. V. Akimov,⁹⁸ G. L. Alberghi,^{22a,22b} J. Albert,¹⁷² P. Albicocco,⁵⁰ M. J. Alconada Verzini,⁷⁴ S. C. Alderweireldt,¹⁰⁸ M. Aleksa,³² I. N. Aleksandrov,⁶⁸ C. Alexa,^{28b} G. Alexander,¹⁵⁵ T. Alexopoulos,¹⁰ M. Alhroob,¹¹⁵ B. Ali,¹³⁰ M. Aliev,^{76a,76b} G. Alimonti,^{94a} J. Alison,³³ S. P. Alkire,³⁸ B. M. M. Allbrooke,¹⁵¹ B. W. Allen,¹¹⁸ P. P. Allport,¹⁹ A. Aloisio,^{106a,106b} A. Alonso,³⁹ F. Alonso,⁷⁴ C. Alpigiani,¹⁴⁰ A. A. Alshehri,⁵⁶ M. I. Alstaty,⁸⁸ B. Alvarez Gonzalez,³² D. Álvarez Piqueras,¹⁷⁰ M. G. Alvaggi,^{106a,106b} B. T. Amadio,¹⁶ Y. Amaral Coutinho,^{26a} C. Amelung,²⁵ D. Amidei,⁹² S. P. Amor Dos Santos,^{128a,128c} A. Amorim,^{128a,128b} S. Amoroso,³² G. Amundsen,²⁵ C. Anastopoulos,¹⁴¹ L. S. Ancu,⁵² N. Andari,¹⁹ T. Andeen,¹¹ C. F. Anders,^{60b} J. K. Anders,⁷⁷ K. J. Anderson,³³ A. Andreazza,^{94a,94b} V. Andrei,^{60a} S. Angelidakis,⁹ I. Angelozzi,¹⁰⁹ A. Angerami,³⁸ A. V. Anisenkov,^{111,d} N. Anjos,¹³ A. Annovi,^{126a,126b} C. Antel,^{60a} M. Antonelli,⁵⁰ A. Antonov,^{100,a} D. J. Antrim,¹⁶⁶ F. Anulli,^{134a} M. Aoki,⁶⁹ L. Aperio Bella,³² G. Arabidze,⁹³ Y. Arai,⁶⁹ J. P. Araque,^{128a} V. Araujo Ferraz,^{26a} A. T. H. Arce,⁴⁸ R. E. Ardell,⁸⁰ F. A. Arduh,⁷⁴ J-F. Arguin,⁹⁷ S. Argyropoulos,⁶⁶ M. Arik,^{20a} A. J. Armbruster,³² L. J. Armitage,⁷⁹ O. Arnaez,¹⁶¹ H. Arnold,⁵¹ M. Arratia,³⁰ O. Arslan,²³ A. Artamonov,⁹⁹ G. Artoni,¹²² S. Artz,⁸⁶ S. Asai,¹⁵⁷ N. Asbah,⁴⁵ A. Ashkenazi,¹⁵⁵ L. Asquith,¹⁵¹ K. Assamagan,²⁷ R. Astalos,^{146a} M. Atkinson,¹⁶⁹ N. B. Atlay,¹⁴³ K. Augsten,¹³⁰ G. Avolio,³² B. Axen,¹⁶ M. K. Ayoub,¹¹⁹ G. Azuelos,^{97,e} A. E. Baas,^{60a} M. J. Baca,¹⁹ H. Bachacou,¹³⁸ K. Bachas,^{76a,76b} M. Backes,¹²² M. Backhaus,³² P. Bagnaia,^{134a,134b} M. Bahmani,⁴² H. Bahrasemani,¹⁴⁴ J. T. Baines,¹³³ M. Bajic,³⁹ O. K. Baker,¹⁷⁹ E. M. Baldin,^{111,d} P. Balek,¹⁷⁵ F. Balli,¹³⁸ W. K. Balunas,¹²⁴ E. Banas,⁴² A. Bandyopadhyay,²³ Sw. Banerjee,^{176,f} A. A. E. Bannoura,¹⁷⁸ L. Barak,³² E. L. Barberio,⁹¹ D. Barberis,^{53a,53b} M. Barbero,⁸⁸ T. Barillari,¹⁰³ M-S Barisits,³² J. T. Barkeloo,¹¹⁸ T. Barklow,¹⁴⁵ N. Barlow,³⁰ S. L. Barnes,^{36c} B. M. Barnett,¹³³ R. M. Barnett,¹⁶ Z. Barnovska-Blenessy,^{36a} A. Baroncelli,^{136a} G. Barone,²⁵ A. J. Barr,¹²² L. Barranco Navarro,¹⁷⁰ F. Barreiro,⁸⁵ J. Barreiro Guimarães da Costa,^{35a} R. Bartoldus,¹⁴⁵ A. E. Barton,⁷⁵ P. Bartos,^{146a} A. Basalaev,¹²⁵ A. Bassalat,^{119,g} R. L. Bates,⁵⁶ S. J. Batista,¹⁶¹ J. R. Batley,³⁰ M. Battaglia,¹³⁹ M. Bauce,^{134a,134b} F. Bauer,¹³⁸ H. S. Bawa,^{145,h} J. B. Beacham,¹¹³ M. D. Beattie,⁷⁵ T. Beau,⁸³ P. H. Beauchemin,¹⁶⁵ P. Bechtle,²³ H. P. Beck,^{18,i} H. C. Beck,⁵⁷ K. Becker,¹²² M. Becker,⁸⁶ M. Beckingham,¹⁷³ C. Becot,¹¹² A. J. Beddall,^{20e} A. Beddall,^{20b} V. A. Bednyakov,⁶⁸ M. Bedognetti,¹⁰⁹ C. P. Bee,¹⁵⁰ T. A. Beermann,³² M. Begalli,^{26a} M. Begel,²⁷ J. K. Behr,⁴⁵ A. S. Bell,⁸¹ G. Bella,¹⁵⁵ L. Bellagamba,^{22a} A. Bellerive,³¹ M. Bellomo,¹⁵⁴ K. Belotskiy,¹⁰⁰ O. Beltramello,³² N. L. Belyaev,¹⁰⁰ O. Benary,^{155,a} D. Benchekroun,^{137a} M. Bender,¹⁰² K. Bendtz,^{148a,148b} N. Benekos,¹⁰ Y. Benhammou,¹⁵⁵ E. Benhar Noccioli,¹⁷⁹ J. Benitez,⁶⁶ D. P. Benjamin,⁴⁸ M. Benoit,⁵² J. R. Bensinger,²⁵ S. Bentvelsen,¹⁰⁹ L. Beresford,¹²² M. Beretta,⁵⁰ D. Berge,¹⁰⁹ E. Bergeaas Kuutmann,¹⁶⁸ N. Berger,⁵ J. Beringer,¹⁶ S. Berlendis,⁵⁸ N. R. Bernard,⁸⁹ G. Bernardi,⁸³ C. Bernius,¹⁴⁵ F. U. Bernlochner,²³ T. Berry,⁸⁰ P. Berta,¹³¹ C. Bertella,^{35a} G. Bertoli,^{148a,148b} F. Bertolucci,^{126a,126b} I. A. Bertram,⁷⁵ C. Bertsche,⁴⁵ D. Bertsche,¹¹⁵ G. J. Besjes,³⁹ O. Bessidskaia Bylund,^{148a,148b} M. Bessner,⁴⁵ N. Besson,¹³⁸ C. Betancourt,⁵¹ A. Bethani,⁸⁷ S. Bethke,¹⁰³ A. J. Bevan,⁷⁹ J. Beyer,¹⁰³ R. M. Bianchi,¹²⁷ O. Biebel,¹⁰² D. Biedermann,¹⁷ R. Bielski,⁸⁷ K. Bierwagen,⁸⁶ N. V. Biesuz,^{126a,126b} M. Biglietti,^{136a} T. R. V. Billoud,⁹⁷ H. Bilokon,⁵⁰ M. Bindi,⁵⁷ A. Bingul,^{20b} C. Bini,^{134a,134b} S. Biondi,^{22a,22b} T. Bisanz,⁵⁷ C. Bittrich,⁴⁷ D. M. Bjergaard,⁴⁸ C. W. Black,¹⁵² J. E. Black,¹⁴⁵ K. M. Black,²⁴ R. E. Blair,⁶ T. Blazek,^{146a} I. Bloch,⁴⁵ C. Blocker,²⁵ A. Blue,⁵⁶ W. Blum,^{86,a} U. Blumenschein,⁷⁹ S. Blunier,^{34a} G. J. Bobbink,¹⁰⁹ V. S. Bobrovnikov,^{111,d} S. S. Bocchetta,⁸⁴ A. Bocci,⁴⁸ C. Bock,¹⁰² M. Boehler,⁵¹ D. Boerner,¹⁷⁸ D. Bogavac,¹⁰² A. G. Bogdanchikov,¹¹¹ C. Bohm,^{148a} V. Boisvert,⁸⁰ P. Bokan,^{168,j} T. Bold,^{41a} A. S. Boldyrev,¹⁰¹ A. E. Bolz,^{60b} M. Bomben,⁸³ M. Bona,⁷⁹ M. Boonekamp,¹³⁸ A. Borisov,¹³² G. Borissov,⁷⁵ J. Bortfeldt,³² D. Bortolotto,¹²² V. Bortolotto,^{62a} D. Boscherini,^{22a} M. Bosman,¹³ J. D. Bossio Sola,²⁹ J. Boudreau,¹²⁷ J. Bouffard,² E. V. Bouhova-Thacker,⁷⁵ D. Boumediene,³⁷ C. Bourdarios,¹¹⁹ S. K. Boutle,⁵⁶ A. Boveia,¹¹³ J. Boyd,³² I. R. Boyko,⁶⁸ J. Bracinik,¹⁹ A. Brandt,⁸ G. Brandt,⁵⁷ O. Brandt,^{60a} U. Bratzler,¹⁵⁸ B. Brau,⁸⁹ J. E. Brau,¹¹⁸ W. D. Breaden Madden,⁵⁶ K. Brendlinger,⁴⁵ A. J. Brennan,⁹¹ L. Brenner,¹⁰⁹ R. Brenner,¹⁶⁸ S. Bressler,¹⁷⁵ D. L. Briglin,¹⁹ T. M. Bristow,⁴⁹ D. Britton,⁵⁶ D. Britzger,⁴⁵ F. M. Brochu,³⁰ I. Brock,²³ R. Brock,⁹³ G. Brooijmans,³⁸ T. Brooks,⁸⁰ W. K. Brooks,^{34b} J. Brosamer,¹⁶ E. Brost,¹¹⁰ J. H. Broughton,¹⁹ P. A. Bruckman de Renstrom,⁴² D. Bruncko,^{146b} A. Bruni,^{22a} G. Bruni,^{22a} L. S. Bruni,¹⁰⁹ BH Brunt,³⁰ M. Bruschi,^{22a} N. Bruscino,²³ P. Bryant,³³ L. Bryngemark,⁴⁵ T. Buanes,¹⁵ Q. Buat,¹⁴⁴ P. Buchholz,¹⁴³ A. G. Buckley,⁵⁶ I. A. Budagov,⁶⁸ F. Buehrer,⁵¹ M. K. Bugge,¹²¹ O. Bulekov,¹⁰⁰ D. Bullock,⁸ T. J. Burch,¹¹⁰ S. Burdin,⁷⁷ C. D. Burgard,⁵¹ A. M. Burger,⁵ B. Burghgrave,¹¹⁰ K. Burka,⁴² S. Burke,¹³³ I. Burmeister,⁴⁶ J. T. P. Burr,¹²² E. Busato,³⁷ D. Büscher,

- V. Büscher,⁸⁶ P. Bussey,⁵⁶ J. M. Butler,²⁴ C. M. Buttar,⁵⁶ J. M. Butterworth,⁸¹ P. Butti,³² W. Buttlinger,²⁷ A. Buzatu,^{35c}
 A. R. Buzykaev,^{111,d} S. Cabrera Urbán,¹⁷⁰ D. Caforio,¹³⁰ V. M. Cairo,^{40a,40b} O. Cakir,^{4a} N. Calace,⁵² P. Calafiura,¹⁶
 A. Calandri,⁸⁸ G. Calderini,⁸³ P. Calfayan,⁶⁴ G. Callea,^{40a,40b} L. P. Caloba,^{26a} S. Calvente Lopez,⁸⁵ D. Calvet,³⁷ S. Calvet,³⁷
 T. P. Calvet,⁸⁸ R. Camacho Toro,³³ S. Camarda,³² P. Camarri,^{135a,135b} D. Cameron,¹²¹ R. Caminal Armadans,¹⁶⁹
 C. Camincher,⁵⁸ S. Campana,³² M. Campanelli,⁸¹ A. Camplani,^{94a,94b} A. Campoverde,¹⁴³ V. Canale,^{106a,106b} M. Cano Bret,^{36c}
 J. Cantero,¹¹⁶ T. Cao,¹⁵⁵ M. D. M. Capeans Garrido,³² I. Caprini,^{28b} M. Caprini,^{28b} M. Capua,^{40a,40b} R. M. Carbone,³⁸
 R. Cardarelli,^{135a} F. Cardillo,⁵¹ I. Carli,¹³¹ T. Carli,³² G. Carlino,^{106a} B. T. Carlson,¹²⁷ L. Carminati,^{94a,94b}
 R. M. D. Carney,^{148a,148b} S. Caron,¹⁰⁸ E. Carquin,^{34b} S. Carrá,^{94a,94b} G. D. Carrillo-Montoya,³² J. Carvalho,^{128a,128c}
 D. Casadei,¹⁹ M. P. Casado,^{13,k} M. Casolino,¹³ D. W. Casper,¹⁶⁶ R. Castelijn,¹⁰⁹ V. Castillo Gimenez,¹⁷⁰ N. F. Castro,^{128a,l}
 A. Catinaccio,³² J. R. Catmore,¹²¹ A. Cattai,³² J. Caudron,²³ V. Cavaliere,¹⁶⁹ E. Cavallaro,¹³ D. Cavalli,^{94a}
 M. Cavalli-Sforza,¹³ V. Cavasinni,^{126a,126b} E. Celebi,^{20d} F. Ceradini,^{136a,136b} L. Cerdá Alberich,¹⁷⁰ A. S. Cerqueira,^{26b}
 A. Cerri,¹⁵¹ L. Cerrito,^{135a,135b} F. Cerutti,¹⁶ A. Cervelli,¹⁸ S. A. Cetin,^{20d} A. Chafaq,^{137a} D. Chakraborty,¹¹⁰ S. K. Chan,⁵⁹
 W. S. Chan,¹⁰⁹ Y. L. Chan,^{62a} P. Chang,¹⁶⁹ J. D. Chapman,³⁰ D. G. Charlton,¹⁹ C. C. Chau,³¹ C. A. Chavez Barajas,¹⁵¹
 S. Che,¹¹³ S. Cheatham,^{167a,167c} A. Chegwidden,⁹³ S. Chekanov,⁶ S. V. Chekulaev,^{163a} G. A. Chelkov,^{68,m}
 M. A. Chelstowska,³² C. Chen,⁶⁷ H. Chen,²⁷ J. Chen,^{36a} S. Chen,^{35b} S. Chen,¹⁵⁷ X. Chen,^{35c,n} Y. Chen,⁷⁰ H. C. Cheng,⁹²
 H. J. Cheng,^{35a,35d} A. Cheplakov,⁶⁸ E. Cheremushkina,¹³² R. Cherkaoui El Moursli,^{137e} E. Cheu,⁷ K. Cheung,⁶³
 L. Chevalier,¹³⁸ V. Chiarella,⁵⁰ G. Chiarelli,^{126a,126b} G. Chiodini,^{76a} A. S. Chisholm,³² A. Chitan,^{28b} Y. H. Chiu,¹⁷²
 M. V. Chizhov,⁶⁸ K. Choi,⁶⁴ A. R. Chomont,³⁷ S. Chouridou,¹⁵⁶ Y. S. Chow,^{62a} V. Christodou lou,⁸¹ M. C. Chu,^{62a}
 J. Chudoba,¹²⁹ A. J. Chuinard,⁹⁰ J. J. Chwastowski,⁴² L. Chytka,¹¹⁷ A. K. Ciftci,^{4a} D. Cinca,⁴⁶ V. Cindro,⁷⁸ I. A. Cioara,²³
 C. Ciocca,^{22a,22b} A. Ciocio,¹⁶ F. Cirotto,^{106a,106b} Z. H. Citron,¹⁷⁵ M. Citterio,^{94a} M. Ciubancan,^{28b} A. Clark,⁵² B. L. Clark,⁵⁹
 M. R. Clark,³⁸ P. J. Clark,⁴⁹ R. N. Clarke,¹⁶ C. Clement,^{148a,148b} Y. Coadou,⁸⁸ M. Cobal,^{167a,167c} A. Coccaro,⁵² J. Cochran,⁶⁷
 L. Colasurdo,¹⁰⁸ B. Cole,³⁸ A. P. Colijn,¹⁰⁹ J. Collot,⁵⁸ T. Colombo,¹⁶⁶ P. Conde Muño,^{128a,128b} E. Coniavitis,⁵¹
 S. H. Connell,^{147b} I. A. Connelly,⁸⁷ S. Constantinescu,^{28b} G. Conti,³² F. Conventi,^{106a,o} M. Cooke,¹⁶ A. M. Cooper-Sarkar,¹²²
 F. Cormier,¹⁷¹ K. J. R. Cormier,¹⁶¹ M. Corradi,^{134a,134b} F. Corriveau,^{90,p} A. Cortes-Gonzalez,³² G. Cortiana,¹⁰³ G. Costa,^{94a}
 M. J. Costa,¹⁷⁰ D. Costanzo,¹⁴¹ G. Cottin,³⁰ G. Cowan,⁸⁰ B. E. Cox,⁸⁷ K. Cranmer,¹¹² S. J. Crawley,⁵⁶ R. A. Creager,¹²⁴
 G. Cree,³¹ S. Crépé-Renaudin,⁵⁸ F. Crescioli,⁸³ W. A. Cribbs,^{148a,148b} M. Cristinziani,²³ V. Croft,¹⁰⁸ G. Crosetti,^{40a,40b}
 A. Cueto,⁸⁵ T. Cuhadar Donszelmann,¹⁴¹ A. R. Cukierman,¹⁴⁵ J. Cummings,¹⁷⁹ M. Curatolo,⁵⁰ J. Cúth,⁸⁶ S. Czekiera,⁴²
 P. Czodrowski,³² G. D'amen,^{22a,22b} S. D'Auria,⁵⁶ L. D'eramo,⁸³ M. D'Onofrio,⁷⁷ M. J. Da Cunha Sargedas De Sousa,^{128a,128b}
 C. Da Via,⁸⁷ W. Dabrowski,^{41a} T. Dado,^{146a} T. Dai,⁹² O. Dale,¹⁵ F. Dallaire,⁹⁷ C. Dallapiccola,⁸⁹ M. Dam,³⁹ J. R. Dandoy,¹²⁴
 M. F. Daneri,²⁹ N. P. Dang,¹⁷⁶ A. C. Daniells,¹⁹ N. S. Dann,⁸⁷ M. Danninger,¹⁷¹ M. Dano Hoffmann,¹³⁸ V. Dao,¹⁵⁰
 G. Darbo,^{53a} S. Darmora,⁸ J. Dassoulas,³ A. Dattagupta,¹¹⁸ T. Daubney,⁴⁵ W. Davey,²³ C. David,⁴⁵ T. Davidek,¹³¹
 D. R. Davis,⁴⁸ P. Davison,⁸¹ E. Dawe,⁹¹ I. Dawson,¹⁴¹ K. De,⁸ R. de Asmundis,^{106a} A. De Benedetti,¹¹⁵ S. De Castro,^{22a,22b}
 S. De Cecco,⁸³ N. De Groot,¹⁰⁸ P. de Jong,¹⁰⁹ H. De la Torre,⁹³ F. De Lorenzi,⁶⁷ A. De Maria,⁵⁷ D. De Pedis,^{134a}
 A. De Salvo,^{134a} U. De Sanctis,^{135a,135b} A. De Santo,¹⁵¹ K. De Vasconcelos Corga,⁸⁸ J. B. De Vivie De Regie,¹¹⁹
 W. J. Dearnaley,⁷⁵ R. Debbe,²⁷ C. Debenedetti,¹³⁹ D. V. Dedovich,⁶⁸ N. Dehghanian,³ I. Deigaard,¹⁰⁹ M. Del Gaudio,^{40a,40b}
 J. Del Peso,⁸⁵ D. Delgove,¹¹⁹ F. Deliot,¹³⁸ C. M. Delitzsch,⁷ A. Dell'Acqua,³² L. Dell'Asta,²⁴ M. Dell'Orso,^{126a,126b}
 M. Della Pietra,^{106a,106b} D. della Volpe,⁵² M. Delmastro,⁵ C. Delporte,¹¹⁹ P. A. Delsart,⁵⁸ D. A. DeMarco,¹⁶¹ S. Demers,¹⁷⁹
 M. Demichev,⁶⁸ A. Demilly,⁸³ S. P. Denisov,¹³² D. Denysiuk,¹³⁸ D. Derendarz,⁴² J. E. Derkaoui,^{137d} F. Derue,⁸³ P. Dervan,⁷⁷
 K. Desch,²³ C. Deterre,⁴⁵ K. Dette,⁴⁶ M. R. Devesa,²⁹ P. O. Deviveiros,³² A. Dewhurst,¹³³ S. Dhaliwal,²⁵ F. A. Di Bello,⁵²
 A. Di Ciacio,^{135a,135b} L. Di Ciacio,⁵ W. K. Di Clemente,¹²⁴ C. Di Donato,^{106a,106b} A. Di Girolamo,³² B. Di Girolamo,³²
 B. Di Micco,^{136a,136b} R. Di Nardo,³² K. F. Di Petrillo,⁵⁹ A. Di Simone,⁵¹ R. Di Sipio,¹⁶¹ D. Di Valentino,³¹ C. Diaconu,⁸⁸
 M. Diamond,¹⁶¹ F. A. Dias,³⁹ M. A. Diaz,^{34a} E. B. Diehl,⁹² J. Dietrich,¹⁷ S. Díez Cornell,⁴⁵ A. Dimitrijevska,¹⁴
 J. Dingfelder,²³ P. Dita,^{28b} S. Dita,^{28b} F. Dittus,³² F. Djama,⁸⁸ T. Djobava,^{54b} J. I. Djupsland,^{60a} M. A. B. do Vale,^{26c}
 D. Dobos,³² M. Dobre,^{28b} C. Doglioni,⁸⁴ J. Dolejsi,¹³¹ Z. Dolezal,¹³¹ M. Donadelli,^{26d} S. Donati,^{126a,126b} P. Dondero,^{123a,123b}
 J. Donini,³⁷ J. Dopke,¹³³ A. Doria,^{106a} M. T. Dova,⁷⁴ A. T. Doyle,⁵⁶ E. Drechsler,⁵⁷ M. Dris,¹⁰ Y. Du,^{36b}
 J. Duarte-Campderros,¹⁵⁵ A. Dubreuil,⁵² E. Duchovni,¹⁷⁵ G. Duckeck,¹⁰² A. Ducourthial,⁸³ O. A. Ducu,^{97,q} D. Duda,¹⁰⁹
 A. Dudarev,³² A. Chr. Dudder,⁸⁶ E. M. Duffield,¹⁶ L. Duflot,¹¹⁹ M. Dührssen,³² M. Dumancic,¹⁷⁵ A. E. Dumitriu,^{28b}
 A. K. Duncan,⁵⁶ M. Dunford,^{60a} H. Duran Yildiz,^{4a} M. Düren,⁵⁵ A. Durglishvili,^{54b} D. Duschinger,⁴⁷ B. Dutta,⁴⁵
 D. Duvnjak,¹ M. Dyndal,⁴⁵ B. S. Dziedzic,⁴² C. Eckardt,⁴⁵ K. M. Ecker,¹⁰³ R. C. Edgar,⁹² T. Eifert,³² G. Eigen,¹⁵

- K. Einsweiler,¹⁶ T. Ekelof,¹⁶⁸ M. El Kacimi,^{137c} R. El Kosseifi,⁸⁸ V. Ellajosyula,⁸⁸ M. Ellert,¹⁶⁸ S. Elles,⁵ F. Ellinghaus,¹⁷⁸
A. A. Elliot,¹⁷² N. Ellis,³² J. Elmsheuser,²⁷ M. Elsing,³² D. Emeliyanov,¹³³ Y. Enari,¹⁵⁷ O. C. Endner,⁸⁶ J. S. Ennis,¹⁷³
J. Erdmann,⁴⁶ A. Ereditato,¹⁸ M. Ernst,²⁷ S. Errede,¹⁶⁹ M. Escalier,¹¹⁹ C. Escobar,¹⁷⁰ B. Esposito,⁵⁰ O. Estrada Pastor,¹⁷⁰
A. I. Etienne,¹³⁸ E. Etzion,¹⁵⁵ H. Evans,⁶⁴ A. Ezhilov,¹²⁵ M. Ezzi,^{137e} F. Fabbri,^{22a,22b} L. Fabbri,^{22a,22b} V. Fabiani,¹⁰⁸
G. Facini,⁸¹ R. M. Fakhrutdinov,¹³² S. Falciano,^{134a} R. J. Falla,⁸¹ J. Faltova,³² Y. Fang,^{35a} M. Fanti,^{94a,94b} A. Farbin,⁸
A. Farilla,^{136a} C. Farina,¹²⁷ E. M. Farina,^{123a,123b} T. Farooque,⁹³ S. Farrell,¹⁶ S. M. Farrington,¹⁷³ P. Farthouat,³² F. Fassi,^{137e}
P. Fassnacht,³² D. Fassouliotis,⁹ M. Faucci Giannelli,⁸⁰ A. Favareto,^{53a,53b} W. J. Fawcett,¹²² L. Fayard,¹¹⁹ O. L. Fedin,^{125,r}
W. Fedorko,¹⁷¹ S. Feigl,¹²¹ L. Feligioni,⁸⁸ C. Feng,^{36b} E. J. Feng,³² H. Feng,⁹² M. J. Fenton,⁵⁶ A. B. Fenyuk,¹³²
L. Feremenga,⁸ P. Fernandez Martinez,¹⁷⁰ S. Fernandez Perez,¹³ J. Ferrando,⁴⁵ A. Ferrari,¹⁶⁸ P. Ferrari,¹⁰⁹ R. Ferrari,^{123a}
D. E. Ferreira de Lima,^{60b} A. Ferrer,¹⁷⁰ D. Ferrere,⁵² C. Ferretti,⁹² F. Fiedler,⁸⁶ A. Filipčič,⁷⁸ M. Filipuzzi,⁴⁵ F. Filthaut,¹⁰⁸
M. Fincke-Keeler,¹⁷² K. D. Finelli,¹⁵² M. C. N. Fiolhais,^{128a,128c,s} L. Fiorini,¹⁷⁰ A. Fischer,² C. Fischer,¹³ J. Fischer,¹⁷⁸
W. C. Fisher,⁹³ N. Flaschel,⁴⁵ I. Fleck,¹⁴³ P. Fleischmann,⁹² R. R. M. Fletcher,¹²⁴ T. Flick,¹⁷⁸ B. M. Flierl,¹⁰²
L. R. Flores Castillo,^{62a} M. J. Flowerdew,¹⁰³ G. T. Forcolin,⁸⁷ A. Formica,¹³⁸ F. A. Förster,¹³ A. Forti,⁸⁷ A. G. Foster,¹⁹
D. Fournier,¹¹⁹ H. Fox,⁷⁵ S. Fracchia,¹⁴¹ P. Francavilla,⁸³ M. Franchini,^{60a} S. Franchino,^{60a} D. Francis,³² L. Franconi,¹²¹
M. Franklin,⁵⁹ M. Frate,¹⁶⁶ M. Fraternali,^{123a,123b} D. Freeborn,⁸¹ S. M. Fressard-Batraneanu,³² B. Freund,⁹⁷ D. Froidevaux,³²
J. A. Frost,¹²² C. Fukunaga,¹⁵⁸ T. Fusayasu,¹⁰⁴ J. Fuster,¹⁷⁰ C. Gabaldon,⁵⁸ O. Gabizon,¹⁵⁴ A. Gabrielli,^{22a,22b} A. Gabrielli,¹⁶
G. P. Gach,^{41a} S. Gadatsch,³² S. Gadomski,⁸⁰ G. Gagliardi,^{53a,53b} L. G. Gagnon,⁹⁷ C. Galea,¹⁰⁸ B. Galhardo,^{128a,128c}
E. J. Gallas,¹²² B. J. Gallop,¹³³ P. Gallus,¹³⁰ G. Galster,³⁹ K. K. Gan,¹¹³ S. Ganguly,³⁷ Y. Gao,⁷⁷ Y. S. Gao,^{145,h}
F. M. Garay Walls,⁴⁹ C. García,¹⁷⁰ J. E. García Navarro,¹⁷⁰ J. A. García Pascual,^{35a} M. Garcia-Sciveres,¹⁶ R. W. Gardner,³³
N. Garelli,¹⁴⁵ V. Garonne,¹²¹ A. Gascon Bravo,⁴⁵ K. Gasnikova,⁴⁵ C. Gatti,⁵⁰ A. Gaudiello,^{53a,53b} G. Gaudio,^{123a}
I. L. Gavrilenco,⁹⁸ C. Gay,¹⁷¹ G. Gaycken,²³ E. N. Gazis,¹⁰ C. N. P. Gee,¹³³ J. Geisen,⁵⁷ M. Geisen,⁸⁶ M. P. Geisler,^{60a}
K. Gellerstedt,^{148a,148b} C. Gemme,^{53a} M. H. Genest,⁵⁸ C. Geng,⁹² S. Gentile,^{134a,134b} C. Gentsos,¹⁵⁶ S. George,⁸⁰
D. Gerbaudo,¹³ A. Gershon,¹⁵⁵ G. Geßner,⁴⁶ S. Ghasemi,¹⁴³ M. Ghneimat,²³ B. Giacobbe,^{22a} S. Giagu,^{134a,134b}
N. Giangiacomi,^{22a,22b} P. Giannetti,^{126a,126b} S. M. Gibson,⁸⁰ M. Gignac,¹⁷¹ M. Gilchriese,¹⁶ D. Gillberg,³¹ G. Gilles,¹⁷⁸
D. M. Gingrich,^{3,e} N. Giokaris,^{9,a} M. P. Giordani,^{167a,167c} F. M. Giorgi,^{22a} P. F. Giraud,¹³⁸ P. Giromini,⁵⁹
G. Giugliarelli,^{167a,167c} D. Giugni,^{94a} F. Giuli,¹²² C. Giuliani,¹⁰³ M. Giulini,^{60b} B. K. Gjelsten,¹²¹ S. Gkaitatzis,¹⁵⁶ I. Gkialas,^{9,t}
E. L. Gkougkousis,¹³⁹ P. Gkountoumis,¹⁰ L. K. Gladilin,¹⁰¹ C. Glasman,⁸⁵ J. Glatzer,¹³ P. C. F. Glaysher,⁴⁵ A. Glazov,⁴⁵
M. Goblirsch-Kolb,²⁵ J. Godlewski,⁴² S. Goldfarb,⁹¹ T. Golling,⁵² D. Golubkov,¹³² A. Gomes,^{128a,128b,128d} R. Gonçalo,^{128a}
R. Goncalves Gama,^{26a} J. Goncalves Pinto Firmino Da Costa,¹³⁸ G. Gonella,⁵¹ L. Gonella,¹⁹ A. Gongadze,⁶⁸
S. González de la Hoz,¹⁷⁰ S. Gonzalez-Sevilla,⁵² L. Goossens,³² P. A. Gorbounov,⁹⁹ H. A. Gordon,²⁷ I. Gorelov,¹⁰⁷
B. Gorini,³² E. Gorini,^{76a,76b} A. Gorišek,⁷⁸ A. T. Goshaw,⁴⁸ C. Gössling,⁴⁶ M. I. Gostkin,⁶⁸ C. A. Gottardo,²³ C. R. Goudet,¹¹⁹
D. Goujdami,^{137c} A. G. Goussiou,¹⁴⁰ N. Govender,^{147b,u} E. Gozani,¹⁵⁴ L. Gruber,⁵⁷ I. Grabowska-Bold,^{41a} P. O. J. Gradin,¹⁶⁸
J. Gramling,¹⁶⁶ E. Gramstad,¹²¹ S. Grancagnolo,¹⁷ V. Gratchev,¹²⁵ P. M. Gravila,^{28f} C. Gray,⁵⁶ H. M. Gray,¹⁶
Z. D. Greenwood,^{82,v} C. Grefe,²³ K. Gregersen,⁸¹ I. M. Gregor,⁴⁵ P. Grenier,¹⁴⁵ K. Grevtsov,⁵ J. Griffiths,⁸ A. A. Grillo,¹³⁹
K. Grimm,⁷⁵ S. Grinstein,^{13,w} Ph. Gris,³⁷ J.-F. Grivaz,¹¹⁹ S. Groh,⁸⁶ E. Gross,¹⁷⁵ J. Grosse-Knetter,⁵⁷ G. C. Grossi,⁸²
Z. J. Grout,⁸¹ A. Grummer,¹⁰⁷ L. Guan,⁹² W. Guan,¹⁷⁶ J. Guenther,⁶⁵ F. Guescini,^{163a} D. Guest,¹⁶⁶ O. Gueta,¹⁵⁵ B. Gui,¹¹³
E. Guido,^{53a,53b} T. Guillemin,⁵ S. Guindon,² U. Gul,⁵⁶ C. Gumpert,³² J. Guo,^{36c} W. Guo,⁹² Y. Guo,^{36a,x} R. Gupta,⁴³
S. Gupta,¹²² G. Gustavino,¹¹⁵ P. Gutierrez,¹¹⁵ N. G. Gutierrez Ortiz,⁸¹ C. Gutschow,⁸¹ C. Guyot,¹³⁸ M. P. Guzik,^{41a}
C. Gwenlan,¹²² C. B. Gwilliam,⁷⁷ A. Haas,¹¹² C. Haber,¹⁶ H. K. Hadavand,⁸ N. Haddad,^{137e} A. Hadef,⁸⁸ S. Hageböck,²³
M. Hagihara,¹⁶⁴ H. Hakobyan,^{180,a} M. Haleem,⁴⁵ J. Haley,¹¹⁶ G. Halladjian,⁹³ G. D. Hallewell,⁸⁸ K. Hamacher,¹⁷⁸
P. Hamal,¹¹⁷ K. Hamano,¹⁷² A. Hamilton,^{147a} G. N. Hamity,¹⁴¹ P. G. Hamnett,⁴⁵ L. Han,^{36a} S. Han,^{35a,35d} K. Hanagaki,^{69,y}
K. Hanawa,¹⁵⁷ M. Hance,¹³⁹ B. Haney,¹²⁴ P. Hanke,^{60a} J. B. Hansen,³⁹ J. D. Hansen,³⁹ M. C. Hansen,²³ P. H. Hansen,³⁹
K. Hara,¹⁶⁴ A. S. Hard,¹⁷⁶ T. Harenberg,¹⁷⁸ F. Hariri,¹¹⁹ S. Harkusha,⁹⁵ R. D. Harrington,⁴⁹ P. F. Harrison,¹⁷³
N. M. Hartmann,¹⁰² M. Hasegawa,⁷⁰ Y. Hasegawa,¹⁴² A. Hasib,⁴⁹ S. Hassani,¹³⁸ S. Haug,¹⁸ R. Hauser,⁹³ L. Hauswald,⁴⁷
L. B. Havener,³⁸ M. Havranek,¹³⁰ C. M. Hawkes,¹⁹ R. J. Hawkings,³² D. Hayakawa,¹⁵⁹ D. Hayden,⁹³ C. P. Hays,¹²²
J. M. Hays,⁷⁹ H. S. Hayward,⁷⁷ S. J. Haywood,¹³³ S. J. Head,¹⁹ T. Heck,⁸⁶ V. Hedberg,⁸⁴ L. Heelan,⁸ S. Heer,²³
K. K. Heidegger,⁵¹ S. Heim,⁴⁵ T. Heim,¹⁶ B. Heinemann,^{45,z} J. J. Heinrich,¹⁰² L. Heinrich,¹¹² C. Heinz,⁵⁵ J. Hejbal,¹²⁹
L. Helary,³² A. Held,¹⁷¹ S. Hellman,^{148a,148b} C. Helsens,³² R. C. W. Henderson,⁷⁵ Y. Heng,¹⁷⁶ S. Henkelmann,¹⁷¹
A. M. Henriques Correia,³² S. Henrot-Versille,¹¹⁹ G. H. Herbert,¹⁷ H. Herde,²⁵ V. Herget,¹⁷⁷ Y. Hernández Jiménez,^{147c}

- H. Herr,⁸⁶ G. Herten,⁵¹ R. Hertenberger,¹⁰² L. Hervas,³² T. C. Herwig,¹²⁴ G. G. Hesketh,⁸¹ N. P. Hessey,^{163a} J. W. Hetherly,⁴³ S. Higashino,⁶⁹ E. Higón-Rodriguez,¹⁷⁰ K. Hildebrand,³³ E. Hill,¹⁷² J. C. Hill,³⁰ K. H. Hiller,⁴⁵ S. J. Hillier,¹⁹ M. Hils,⁴⁷ I. Hinchliffe,¹⁶ M. Hirose,⁵¹ D. Hirschbuehl,¹⁷⁸ B. Hiti,⁷⁸ O. Hladík,¹²⁹ X. Hoad,⁴⁹ J. Hobbs,¹⁵⁰ N. Hod,^{163a} M. C. Hodgkinson,¹⁴¹ P. Hodgson,¹⁴¹ A. Hoecker,³² M. R. Hoeferkamp,¹⁰⁷ F. Hoenig,¹⁰² D. Hohn,²³ T. R. Holmes,³³ M. Homann,⁴⁶ S. Honda,¹⁶⁴ T. Honda,⁶⁹ T. M. Hong,¹²⁷ B. H. Hooberman,¹⁶⁹ W. H. Hopkins,¹¹⁸ Y. Horii,¹⁰⁵ A. J. Horton,¹⁴⁴ J.-Y. Hostachy,⁵⁸ S. Hou,¹⁵³ A. Hoummada,^{137a} J. Howarth,⁸⁷ J. Hoya,⁷⁴ M. Hrabovsky,¹¹⁷ J. Hrdinka,³² I. Hristova,¹⁷ J. Hrivnac,¹¹⁹ T. Hrynová,⁵ A. Hrynevich,⁹⁶ P. J. Hsu,⁶³ S.-C. Hsu,¹⁴⁰ Q. Hu,^{36a} S. Hu,^{36c} Y. Huang,^{35a} Z. Hubacek,¹³⁰ F. Hubaut,⁸⁸ F. Huegging,²³ T. B. Huffman,¹²² E. W. Hughes,³⁸ G. Hughes,⁷⁵ M. Huhtinen,³² P. Huo,¹⁵⁰ N. Huseynov,^{68,c} J. Huston,⁹³ J. Huth,⁵⁹ G. Iacobucci,⁵² G. Iakovidis,²⁷ I. Ibragimov,¹⁴³ L. Iconomidou-Fayard,¹¹⁹ Z. Idrissi,^{137e} P. Iengo,³² O. Igonkina,^{109,aa} T. Iizawa,¹⁷⁴ Y. Ikegami,⁶⁹ M. Ikeno,⁶⁹ Y. Ilchenko,^{11,bb} D. Iliadis,¹⁵⁶ N. Ilic,¹⁴⁵ G. Introzzi,^{123a,123b} P. Ioannou,^{9,a} M. Iodice,^{136a} K. Iordanidou,³⁸ V. Ippolito,⁵⁹ M. F. Isacson,¹⁶⁸ N. Ishijima,¹²⁰ M. Ishino,¹⁵⁷ M. Ishitsuka,¹⁵⁹ C. Issever,¹²² S. Istin,^{20a} F. Ito,¹⁶⁴ J. M. Iturbe Ponce,^{62a} R. Iuppa,^{162a,162b} H. Iwasaki,⁶⁹ J. M. Izen,⁴⁴ V. Izzo,^{106a} S. Jabbar,³ P. Jackson,¹ R. M. Jacobs,²³ V. Jain,² K. B. Jakobi,⁸⁶ K. Jakobs,⁵¹ S. Jakobsen,⁶⁵ T. Jakoubek,¹²⁹ D. O. Jamin,¹¹⁶ D. K. Jana,⁸² R. Jansky,⁵² J. Janssen,²³ M. Janus,⁵⁷ P. A. Janus,^{41a} G. Jarlskog,⁸⁴ N. Javadov,^{68,c} T. Javůrek,⁵¹ M. Javurkova,⁵¹ F. Jeanneau,¹³⁸ L. Jeanty,¹⁶ J. Jejelava,^{54a,cc} A. Jelinskas,¹⁷³ P. Jenni,^{51,dd} C. Jeske,¹⁷³ S. Jézéquel,⁵ H. Ji,¹⁷⁶ J. Jia,¹⁵⁰ H. Jiang,⁶⁷ Y. Jiang,^{36a} Z. Jiang,¹⁴⁵ S. Jiggins,⁸¹ J. Jimenez Pena,¹⁷⁰ S. Jin,^{35a} A. Jinaru,^{28b} O. Jinnouchi,¹⁵⁹ H. Jivan,^{147c} P. Johansson,¹⁴¹ K. A. Johns,⁷ C. A. Johnson,⁶⁴ W. J. Johnson,¹⁴⁰ K. Jon-And,^{148a,148b} R. W. L. Jones,⁷⁵ S. D. Jones,¹⁵¹ S. Jones,⁷ T. J. Jones,⁷⁷ J. Jongmanns,^{60a} P. M. Jorge,^{128a,128b} J. Jovicevic,^{163a} X. Ju,¹⁷⁶ A. Juste Rozas,^{13,w} M. K. Köhler,¹⁷⁵ A. Kaczmarska,⁴² M. Kado,¹¹⁹ H. Kagan,¹¹³ M. Kagan,¹⁴⁵ S. J. Kahn,⁸⁸ T. Kaji,¹⁷⁴ E. Kajomovitz,⁴⁸ C. W. Kalderon,⁸⁴ A. Kaluza,⁸⁶ S. Kama,⁴³ A. Kamenshchikov,¹³² N. Kanaya,¹⁵⁷ L. Kanjir,⁷⁸ V. A. Kantserov,¹⁰⁰ J. Kanzaki,⁶⁹ B. Kaplan,¹¹² L. S. Kaplan,¹⁷⁶ D. Kar,^{147c} K. Karakostas,¹⁰ N. Karastathis,¹⁰ M. J. Kareem,⁵⁷ E. Karentzos,¹⁰ S. N. Karpov,⁶⁸ Z. M. Karpova,⁶⁸ K. Karthik,¹¹² V. Kartvelishvili,⁷⁵ A. N. Karyukhin,¹³² K. Kasahara,¹⁶⁴ L. Kashif,¹⁷⁶ R. D. Kass,¹¹³ A. Kastanas,¹⁴⁹ Y. Kataoka,¹⁵⁷ C. Kato,¹⁵⁷ A. Katre,⁵² J. Katzy,⁴⁵ K. Kawade,⁷⁰ K. Kawagoe,⁷³ T. Kawamoto,¹⁵⁷ G. Kawamura,⁵⁷ E. F. Kay,⁷⁷ V. F. Kazanin,^{111,d} R. Keeler,¹⁷² R. Kehoe,⁴³ J. S. Keller,³¹ E. Kellermann,⁸⁴ J. J. Kempster,⁸⁰ J. Kendrick,¹⁹ H. Keoshkerian,¹⁶¹ O. Kepka,¹²⁹ B. P. Kerševan,⁷⁸ S. Kersten,¹⁷⁸ R. A. Keyes,⁹⁰ M. Khader,¹⁶⁹ F. Khalil-zada,¹² A. Khanov,¹¹⁶ A. G. Kharlamov,^{111,d} T. Kharlamova,^{111,d} A. Khodinov,¹⁶⁰ T. J. Khoo,⁵² V. Khovanskiy,^{99,a} E. Khramov,⁶⁸ J. Khubua,^{54b,ee} S. Kido,⁷⁰ C. R. Kilby,⁸⁰ H. Y. Kim,⁸ S. H. Kim,¹⁶⁴ Y. K. Kim,³³ N. Kimura,¹⁵⁶ O. M. Kind,¹⁷ B. T. King,⁷⁷ D. Kirchmeier,⁴⁷ J. Kirk,¹³³ A. E. Kiryunin,¹⁰³ T. Kishimoto,¹⁵⁷ D. Kisielewska,^{41a} V. Kitali,⁴⁵ K. Kiuchi,¹⁶⁴ O. Kivernyk,⁵ E. Kladiva,^{146b} T. Klapdor-Kleingrothaus,⁵¹ M. H. Klein,⁹² M. Klein,⁷⁷ U. Klein,⁷⁷ K. Kleinknecht,⁸⁶ P. Klimek,¹¹⁰ A. Klimentov,²⁷ R. Klingenberg,⁴⁶ T. Klingl,²³ T. Klioutchnikova,³² E.-E. Kluge,^{60a} P. Kluit,¹⁰⁹ S. Kluth,¹⁰³ E. Knerner,⁶⁵ E. B. F. G. Knoops,⁸⁸ A. Knue,¹⁰³ A. Kobayashi,¹⁵⁷ D. Kobayashi,¹⁵⁹ T. Kobayashi,¹⁵⁷ M. Kobel,⁴⁷ M. Kocian,¹⁴⁵ P. Kodys,¹³¹ T. Koffas,³¹ E. Koffeman,¹⁰⁹ N. M. Köhler,¹⁰³ T. Koi,¹⁴⁵ M. Kolb,^{60b} I. Koletsou,⁵ A. A. Komar,^{98,a} Y. Komori,¹⁵⁷ T. Kondo,⁶⁹ N. Kondrashova,^{36c} K. Köneke,⁵¹ A. C. König,¹⁰⁸ T. Kono,^{69,ff} R. Konoplich,^{112,gg} N. Konstantinidis,⁸¹ R. Kopeliansky,⁶⁴ S. Koperny,^{41a} A. K. Kopp,⁵¹ K. Korcyl,⁴² K. Kordas,¹⁵⁶ A. Korn,⁸¹ A. A. Korol,^{111,d} I. Korolkov,¹³ E. V. Korolkova,¹⁴¹ O. Kortner,¹⁰³ S. Kortner,¹⁰³ T. Kosek,¹³¹ V. V. Kostyukhin,²³ A. Kotwal,⁴⁸ A. Koulouris,¹⁰ A. Kourkoumeli-Charalampidi,^{123a,123b} C. Kourkoumelis,⁹ E. Kourlitis,¹⁴¹ V. Kouskoura,²⁷ A. B. Kowalewska,⁴² R. Kowalewski,¹⁷² T. Z. Kowalski,^{41a} C. Kozakai,¹⁵⁷ W. Kozanecki,¹³⁸ A. S. Kozhin,¹³² V. A. Kramarenko,¹⁰¹ G. Kramberger,⁷⁸ D. Krasnopevtsev,¹⁰⁰ M. W. Krasny,⁸³ A. Krasznahorkay,³² D. Krauss,¹⁰³ J. A. Kremer,^{41a} J. Kretzschmar,⁷⁷ K. Kreutzfeldt,⁵⁵ P. Krieger,¹⁶¹ K. Krizka,³³ K. Kroeninger,⁴⁶ H. Kroha,¹⁰³ J. Kroll,¹²⁹ J. Kroll,¹²⁴ J. Kroseberg,²³ J. Krstic,¹⁴ U. Kruchonak,⁶⁸ H. Krüger,²³ N. Krumnack,⁶⁷ M. C. Kruse,⁴⁸ T. Kubota,⁹¹ H. Kucuk,⁸¹ S. Kuday,^{4b} J. T. Kuechler,¹⁷⁸ S. Kuehn,³² A. Kugel,^{60a} F. Kuger,¹⁷⁷ T. Kuhl,⁴⁵ V. Kukhtin,⁶⁸ R. Kukla,⁸⁸ Y. Kulchitsky,⁹⁵ S. Kuleshov,^{34b} Y. P. Kulinich,¹⁶⁹ M. Kuna,^{134a,134b} T. Kunigo,⁷¹ A. Kupco,¹²⁹ T. Kupfer,⁴⁶ O. Kuprash,¹⁵⁵ H. Kurashige,⁷⁰ L. L. Kurchaninov,^{163a} Y. A. Kurochkin,⁹⁵ M. G. Kurth,^{35a,35d} V. Kus,¹²⁹ E. S. Kuwertz,¹⁷² M. Kuze,¹⁵⁹ J. Kvita,¹¹⁷ T. Kwan,¹⁷² D. Kyriazopoulos,¹⁴¹ A. La Rosa,¹⁰³ J. L. La Rosa Navarro,^{26d} L. La Rotonda,^{40a,40b} F. La Ruffa,^{40a,40b} C. Lacasta,¹⁷⁰ F. Lacava,^{134a,134b} J. Lacey,⁴⁵ H. Lacker,¹⁷ D. Lacour,⁸³ E. Ladygin,⁶⁸ R. Lafaye,⁵ B. Laforge,⁸³ T. Lagouri,¹⁷⁹ S. Lai,⁵⁷ S. Lammers,⁶⁴ W. Lampl,⁷ E. Lançon,²⁷ U. Landgraf,⁵¹ M. P. J. Landon,⁷⁹ M. C. Lanfermann,⁵² V. S. Lang,^{60a} J. C. Lange,¹³ R. J. Langenberg,³² A. J. Lankford,¹⁶⁶ F. Lanni,²⁷ K. Lantzsch,²³ A. Lanza,^{123a} A. Lapertosa,^{53a,53b} S. Laplace,⁸³ J. F. Laporte,¹³⁸ T. Lari,^{94a} F. Lasagni Manghi,^{22a,22b} M. Lassnig,³² P. Laurelli,⁵⁰ W. Lavrijisen,¹⁶ A. T. Law,¹³⁹ P. Laycock,⁷⁷ T. Lazovich,⁵⁹ M. Lazzaroni,^{94a,94b} B. Le,⁹¹ O. Le Dortz,⁸³

- E. Le Guiriec,⁸⁸ E. P. Le Quilleuc,¹³⁸ M. LeBlanc,¹⁷² T. LeCompte,⁶ F. Ledroit-Guillon,⁵⁸ C. A. Lee,²⁷ G. R. Lee,^{133,hh}
 S. C. Lee,¹⁵³ L. Lee,⁵⁹ B. Lefebvre,⁹⁰ G. Lefebvre,⁸³ M. Lefebvre,¹⁷² F. Legger,¹⁰² C. Leggett,¹⁶ G. Lehmann Miotto,³²
 X. Lei,⁷ W. A. Leight,⁴⁵ M. A. L. Leite,^{26d} R. Leitner,¹³¹ D. Lellouch,¹⁷⁵ B. Lemmer,⁵⁷ K. J. C. Leney,⁸¹ T. Lenz,²³
 B. Lenzi,³² R. Leone,⁷ S. Leone,^{126a,126b} C. Leonidopoulos,⁴⁹ G. Lerner,¹⁵¹ C. Leroy,⁹⁷ A. A. J. Lesage,¹³⁸ C. G. Lester,³⁰
 M. Levchenko,¹²⁵ J. Levêque,⁵ D. Levin,⁹² L. J. Levinson,¹⁷⁵ M. Levy,¹⁹ D. Lewis,⁷⁹ B. Li,^{36a,x} Changqiao Li,^{36a} H. Li,¹⁵⁰
 L. Li,^{36c} Q. Li,^{35a,35d} S. Li,⁴⁸ X. Li,^{36c} Y. Li,¹⁴³ Z. Liang,^{35a} B. Liberti,^{135a} A. Liblong,¹⁶¹ K. Lie,^{62c} J. Liebal,²³ W. Liebig,¹⁵
 A. Limosani,¹⁵² S. C. Lin,¹⁸² T. H. Lin,⁸⁶ R. A. Linck,⁶⁴ B. E. Lindquist,¹⁵⁰ A. E. Lionti,⁵² E. Lipeles,¹²⁴ A. Lipniacka,¹⁵
 M. Lisovyi,^{60b} T. M. Liss,^{169,ii} A. Lister,¹⁷¹ A. M. Litke,¹³⁹ B. Liu,^{153,ij} H. Liu,⁹² H. Liu,²⁷ J. K. K. Liu,¹²² J. Liu,^{36b}
 J. B. Liu,^{36a} K. Liu,⁸⁸ L. Liu,¹⁶⁹ M. Liu,^{36a} Y. L. Liu,^{36a} Y. Liu,^{36a} M. Livan,^{123a,123b} A. Lleres,⁵⁸ J. Llorente Merino,^{35a}
 S. L. Lloyd,⁷⁹ C. Y. Lo,^{62b} F. Lo Sterzo,¹⁵³ E. M. Lobodzinska,⁴⁵ P. Loch,⁷ F. K. Loebinger,⁸⁷ A. Loesle,⁵¹ K. M. Loew,²⁵
 A. Loginov,^{179,a} T. Lohse,¹⁷ K. Lohwasser,¹⁴¹ M. Lokajicek,¹²⁹ B. A. Long,²⁴ J. D. Long,¹⁶⁹ R. E. Long,⁷⁵ L. Longo,^{76a,76b}
 K. A.Looper,¹¹³ J. A. Lopez,^{34b} D. Lopez Mateos,⁵⁹ I. Lopez Paz,¹³ A. Lopez Solis,⁸³ J. Lorenz,¹⁰² N. Lorenzo Martinez,⁵
 M. Losada,²¹ P. J. Lösel,¹⁰² X. Lou,^{35a} A. Lounis,¹¹⁹ J. Love,⁶ P. A. Love,⁷⁵ H. Lu,^{62a} N. Lu,⁹² Y. J. Lu,⁶³ H. J. Lubatti,¹⁴⁰
 C. Luci,^{134a,134b} A. Lucotte,⁵⁸ C. Luedtke,⁵¹ F. Luehring,⁶⁴ W. Lukas,⁶⁵ L. Luminari,^{134a} O. Lundberg,^{148a,148b}
 B. Lund-Jensen,¹⁴⁹ M. S. Lutz,⁸⁹ P. M. Luzi,⁸³ D. Lynn,²⁷ R. Lysak,¹²⁹ E. Lytken,⁸⁴ F. Lyu,^{35a} V. Lyubushkin,⁶⁸ H. Ma,²⁷
 L. L. Ma,^{36b} Y. Ma,^{36b} G. Maccarrone,⁵⁰ A. Macchiolo,¹⁰³ C. M. Macdonald,¹⁴¹ B. Maček,⁷⁸ J. Machado Miguens,^{124,128b}
 D. Madaffari,¹⁷⁰ R. Madar,³⁷ W. F. Mader,⁴⁷ A. Madsen,⁴⁵ J. Maeda,⁷⁰ S. Maeland,¹⁵ T. Maeno,²⁷ A. S. Maevskiy,¹⁰¹
 V. Magerl,⁵¹ J. Mahlstedt,¹⁰⁹ C. Maiani,¹¹⁹ C. Maidantchik,^{26a} A. A. Maier,¹⁰³ T. Maier,¹⁰² A. Maio,^{128a,128b,128d}
 O. Majersky,^{146a} S. Majewski,¹¹⁸ Y. Makida,⁶⁹ N. Makovec,¹¹⁹ B. Malaescu,⁸³ Pa. Malecki,⁴² V. P. Maleev,¹²⁵ F. Malek,⁵⁸
 U. Mallik,⁶⁶ D. Malon,⁶ C. Malone,³⁰ S. Maltezos,¹⁰ S. Malyukov,³² J. Mamuzic,¹⁷⁰ G. Mancini,⁵⁰ I. Mandić,⁷⁸
 J. Maneira,^{128a,128b} L. Manhaes de Andrade Filho,^{26b} J. Manjarres Ramos,⁴⁷ K. H. Mankinen,⁸⁴ A. Mann,¹⁰² A. Manousos,³²
 B. Mansoulie,¹³⁸ J. D. Mansour,^{35a} R. Mantifel,⁹⁰ M. Mantoani,⁵⁷ S. Manzoni,^{94a,94b} L. Mapelli,³² G. Marceca,²⁹ L. March,⁵²
 L. Marchese,¹²² G. Marchiori,⁸³ M. Marcisovsky,¹²⁹ M. Marjanovic,³⁷ D. E. Marley,⁹² F. Marroquim,^{26a} S. P. Marsden,⁸⁷
 Z. Marshall,¹⁶ M. U. F Martensson,¹⁶⁸ S. Marti-Garcia,¹⁷⁰ C. B. Martin,¹¹³ T. A. Martin,¹⁷³ V. J. Martin,⁴⁹
 B. Martin dit Latour,¹⁵ M. Martinez,^{13,w} V. I. Martinez Outschoorn,¹⁶⁹ S. Martin-Haugh,¹³³ V. S. Martouiu,^{28b}
 A. C. Martyniuk,⁸¹ A. Marzin,³² L. Masetti,⁸⁶ T. Mashimo,¹⁵⁷ R. Mashinistov,⁹⁸ J. Masik,⁸⁷ A. L. Maslenikov,^{111,d}
 L. Massa,^{135a,135b} P. Mastrandrea,⁵ A. Mastroberardino,^{40a,40b} T. Masubuchi,¹⁵⁷ P. Mättig,¹⁷⁸ J. Maurer,^{28b} S. J. Maxfield,⁷⁷
 D. A. Maximov,^{111,d} R. Mazini,¹⁵³ I. Maznas,¹⁵⁶ S. M. Mazza,^{94a,94b} N. C. Mc Fadden,¹⁰⁷ G. Mc Goldrick,¹⁶¹ S. P. Mc Kee,⁹²
 A. McCarn,⁹² R. L. McCarthy,¹⁵⁰ T. G. McCarthy,¹⁰³ L. I. McClymont,⁸¹ E. F. McDonald,⁹¹ J. A. McFayden,⁸¹
 G. Mchedlidze,⁵⁷ S. J. McMahon,¹³³ P. C. McNamara,⁹¹ R. A. McPherson,^{172,p} S. Meehan,¹⁴⁰ T. J. Megy,⁵¹ S. Mehlhase,¹⁰²
 A. Mehta,⁷⁷ T. Meideck,⁵⁸ K. Meier,^{60a} B. Meirose,⁴⁴ D. Melini,^{170,kk} B. R. Mellado Garcia,^{147c} J. D. Mellenthin,⁵⁷
 M. Melo,^{146a} F. Meloni,¹⁸ A. Melzer,²³ S. B. Menary,⁸⁷ L. Meng,⁷⁷ X. T. Meng,⁹² A. Mengarelli,^{22a,22b} S. Menke,¹⁰³
 E. Meoni,^{40a,40b} S. Mergelmeyer,¹⁷ P. Mermod,⁵² L. Merola,^{106a,106b} C. Meroni,^{94a} F. S. Merritt,³³ A. Messina,^{134a,134b}
 J. Metcalfe,⁶ A. S. Mete,¹⁶⁶ C. Meyer,¹²⁴ J.-P. Meyer,¹³⁸ J. Meyer,¹⁰⁹ H. Meyer Zu Theenhausen,^{60a} F. Miano,¹⁵¹
 R. P. Middleton,¹³³ S. Miglioranzi,^{53a,53b} L. Mijović,⁴⁹ G. Mikenberg,¹⁷⁵ M. Mikestikova,¹²⁹ M. Mikuž,⁷⁸ M. Milesi,⁹¹
 A. Milic,¹⁶¹ D. W. Miller,³³ C. Mills,⁴⁹ A. Milov,¹⁷⁵ D. A. Milstead,^{148a,148b} A. A. Minaenko,¹³² Y. Minami,¹⁵⁷
 I. A. Minashvili,^{54b} A. I. Mincer,¹¹² B. Mindur,^{41a} M. Mineev,⁶⁸ Y. Minegishi,¹⁵⁷ Y. Ming,¹⁷⁶ L. M. Mir,¹³ K. P. Mistry,¹²⁴
 T. Mitani,¹⁷⁴ J. Mitrevski,¹⁰² V. A. Mitsou,¹⁷⁰ A. Miucci,¹⁸ P. S. Miyagawa,¹⁴¹ A. Mizukami,⁶⁹ J. U. Mjörnmark,⁸⁴
 T. Mkrtchyan,¹⁸⁰ M. Mlynarikova,¹³¹ T. Moa,^{148a,148b} K. Mochizuki,⁹⁷ P. Mogg,⁵¹ S. Mohapatra,³⁸ S. Molander,^{148a,148b}
 R. Moles-Valls,²³ R. Monden,⁷¹ M. C. Mondragon,⁹³ K. Mönig,⁴⁵ J. Monk,³⁹ E. Monnier,⁸⁸ A. Montalbano,¹⁵⁰
 J. Montejano Berlingen,³² F. Monticelli,⁷⁴ S. Monzani,^{94a,94b} R. W. Moore,³ N. Morange,¹¹⁹ D. Moreno,²¹ M. Moreno Llácer,³²
 P. Morettini,^{53a} S. Morgenstern,³² D. Mori,¹⁴⁴ T. Mori,¹⁵⁷ M. Morii,⁵⁹ M. Morinaga,¹⁵⁷ V. Morisbak,¹²¹ A. K. Morley,³²
 G. Mornacchi,³² J. D. Morris,⁷⁹ L. Morvaj,¹⁵⁰ P. Moschovakos,¹⁰ M. Mosidze,^{54b} H. J. Moss,¹⁴¹ J. Moss,^{145,II}
 K. Motohashi,¹⁵⁹ R. Mount,¹⁴⁵ E. Mountricha,²⁷ E. J. W. Moyse,⁸⁹ S. Muanza,⁸⁸ F. Mueller,¹⁰³ J. Mueller,¹²⁷
 R. S. P. Mueller,¹⁰² D. Muenstermann,⁷⁵ P. Mullen,⁵⁶ G. A. Mullier,¹⁸ F. J. Munoz Sanchez,⁸⁷ W. J. Murray,^{173,133}
 H. Musheghyan,³² M. Muškinja,⁷⁸ A. G. Myagkov,^{132,mm} M. Myska,¹³⁰ B. P. Nachman,¹⁶ O. Nackenhorst,⁵² K. Nagai,¹²²
 R. Nagai,^{69,ff} K. Nagano,⁶⁹ Y. Nagasaka,⁶¹ K. Nagata,¹⁶⁴ M. Nagel,⁵¹ E. Nagy,⁸⁸ A. M. Nairz,³² Y. Nakahama,¹⁰⁵
 K. Nakamura,⁶⁹ T. Nakamura,¹⁵⁷ I. Nakano,¹¹⁴ R. F. Narango Garcia,⁴⁵ R. Narayan,¹¹ D. I. Narrias Villar,^{60a} I. Naryshkin,¹²⁵
 T. Naumann,⁴⁵ G. Navarro,²¹ R. Nayyar,⁷ H. A. Neal,⁹² P. Yu. Nechaeva,⁹⁸ T. J. Neep,¹³⁸ A. Negri,^{123a,123b} M. Negrini,^{22a}

- S. Nektarijevic,¹⁰⁸ C. Nellist,¹¹⁹ A. Nelson,¹⁶⁶ M. E. Nelson,¹²² S. Nemecek,¹²⁹ P. Nemethy,¹¹² M. Nessi,^{32,nn}
 M. S. Neubauer,¹⁶⁹ M. Neumann,¹⁷⁸ P. R. Newman,¹⁹ T. Y. Ng,^{62c} T. Nguyen Manh,⁹⁷ R. B. Nickerson,¹²² R. Nicolaidou,¹³⁸
 J. Nielsen,¹³⁹ V. Nikolaenko,^{132,mm} I. Nikolic-Audit,⁸³ K. Nikolopoulos,¹⁹ J. K. Nilsen,¹²¹ P. Nilsson,²⁷ Y. Ninomiya,¹⁵⁷
 A. Nisati,^{134a} N. Nishu,^{35c} R. Nisius,¹⁰³ I. Nitsche,⁴⁶ T. Nitta,¹⁷⁴ T. Nobe,¹⁵⁷ Y. Noguchi,⁷¹ M. Nomachi,¹²⁰ I. Nomidis,³¹
 M. A. Nomura,²⁷ T. Nooney,⁷⁹ M. Nordberg,³² N. Norjoharuddeen,¹²² O. Novgorodova,⁴⁷ M. Nozaki,⁶⁹ L. Nozka,¹¹⁷
 K. Ntekas,¹⁶⁶ E. Nurse,⁸¹ F. Nuti,⁹¹ K. O'connor,²⁵ D. C. O'Neil,¹⁴⁴ A. A. O'Rourke,⁴⁵ V. O'Shea,⁵⁶ F. G. Oakham,^{31,e}
 H. Oberlack,¹⁰³ T. Obermann,²³ J. Ocariz,⁸³ A. Ochi,⁷⁰ I. Ochoa,³⁸ J. P. Ochoa-Ricoux,^{34a} S. Oda,⁷³ S. Odaka,⁶⁹ A. Oh,⁸⁷
 S. H. Oh,⁴⁸ C. C. Ohm,¹⁶ H. Ohman,¹⁶⁸ H. Oide,^{53a,53b} H. Okawa,¹⁶⁴ Y. Okumura,¹⁵⁷ T. Okuyama,⁶⁹ A. Olariu,^{28b}
 L. F. Oleiro Seabra,^{128a} S. A. Olivares Pino,^{34a} D. Oliveira Damazio,²⁷ A. Olszewski,⁴² J. Olszowska,⁴² A. Onofre,^{128a,128e}
 K. Onogi,¹⁰⁵ P. U. E. Onyisi,^{11,bb} H. Oppen,¹²¹ M. J. Oreglia,³³ Y. Oren,¹⁵⁵ D. Orestano,^{136a,136b} N. Orlando,^{62b} R. S. Orr,¹⁶¹
 B. Osculati,^{53a,53b,a} R. Ospanov,^{36a} G. Otero y Garzon,²⁹ H. Otono,⁷³ M. Ouchrif,^{137d} F. Ould-Saada,¹²¹ A. Ouraou,¹³⁸
 K. P. Oussoren,¹⁰⁹ Q. Ouyang,^{35a} M. Owen,⁵⁶ R. E. Owen,¹⁹ V. E. Ozcan,^{20a} N. Ozturk,⁸ K. Pachal,¹⁴⁴ A. Pacheco Pages,¹³
 L. Pacheco Rodriguez,¹³⁸ C. Padilla Aranda,¹³ S. Pagan Griso,¹⁶ M. Paganini,¹⁷⁹ F. Paige,²⁷ G. Palacino,⁶⁴ S. Palazzo,^{40a,40b}
 S. Palestini,³² M. Palka,^{41b} D. Pallin,³⁷ E. St. Panagiotopoulou,¹⁰ I. Panagoulias,¹⁰ C. E. Pandini,^{126a,126b}
 J. G. Panduro Vazquez,⁸⁰ P. Pani,³² S. Panitkin,²⁷ D. Pantea,^{28b} L. Paolozzi,⁵² Th. D. Papadopoulou,¹⁰ K. Papageorgiou,^{9,t}
 A. Paramonov,⁶ D. Paredes Hernandez,¹⁷⁹ A. J. Parker,⁷⁵ M. A. Parker,³⁰ K. A. Parker,⁴⁵ F. Parodi,^{53a,53b} J. A. Parsons,³⁸
 U. Parzefall,⁵¹ V. R. Pascuzzi,¹⁶¹ J. M. Pasner,¹³⁹ E. Pasqualucci,^{134a} S. Passaggio,^{53a} Fr. Pastore,⁸⁰ S. Pataraia,⁸⁶ J. R. Pater,⁸⁷
 T. Pauly,³² B. Pearson,¹⁰³ S. Pedraza Lopez,¹⁷⁰ R. Pedro,^{128a,128b} S. V. Peleganchuk,^{111,d} O. Penc,¹²⁹ C. Peng,^{35a,35d}
 H. Peng,^{36a} J. Penwell,⁶⁴ B. S. Peralva,^{26b} M. M. Perego,¹³⁸ D. V. Perepelitsa,²⁷ F. Peri,¹⁷ L. Perini,^{94a,94b} H. Pernegger,³²
 S. Perrella,^{106a,106b} R. Peschke,⁴⁵ V. D. Pesekhonov,^{68,a} K. Peters,⁴⁵ R. F. Y. Peters,⁸⁷ B. A. Petersen,³² T. C. Petersen,³⁹
 E. Petit,⁵⁸ A. Petridis,¹ C. Petridou,¹⁵⁶ P. Petroff,¹¹⁹ E. Petrolo,^{134a} M. Petrov,¹²² F. Petrucci,^{136a,136b} N. E. Pettersson,⁸⁹
 A. Peyaud,¹³⁸ R. Pezoa,^{34b} F. H. Phillips,⁹³ P. W. Phillips,¹³³ G. Piacquadio,¹⁵⁰ E. Pianori,¹⁷³ A. Picazio,⁸⁹ E. Piccaro,⁷⁹
 M. A. Pickering,¹²² R. Piegaia,²⁹ J. E. Pilcher,³³ A. D. Pilkington,⁸⁷ A. W. J. Pin,⁸⁷ M. Pinamonti,^{135a,135b} J. L. Pinfold,³
 H. Pirumov,⁴⁵ M. Pitt,¹⁷⁵ L. Plazak,^{146a} M.-A. Pleier,²⁷ V. Plotnikova,⁶⁸ D. Pluth,⁶⁷ P. Podberezko,¹¹¹
 R. Poettgen,⁸⁴ R. Poggi,^{123a,123b} L. Poggiali,¹¹⁹ D. Pohl,²³ G. Polesello,^{123a} A. Poley,⁴⁵ A. Policicchio,^{40a,40b} R. Polifka,³²
 A. Polini,^{22a} C. S. Pollard,⁵⁶ V. Polychronakos,²⁷ K. Pommès,³² D. Ponomarenko,¹⁰⁰ L. Pontecorvo,^{134a} G. A. Popeneciu,^{28d}
 S. Pospisil,¹³⁰ K. Potamianos,¹⁶ I. N. Potrap,⁶⁸ C. J. Potter,³⁰ T. Poulsen,⁸⁴ J. Poveda,³² M. E. Pozo Astigarraga,³²
 P. Pralavorio,⁸⁸ A. Pranko,¹⁶ S. Prell,⁶⁷ D. Price,⁸⁷ M. Primavera,^{76a} S. Prince,⁹⁰ N. Proklova,¹⁰⁰ K. Prokofiev,^{62c}
 F. Prokoshin,^{34b} S. Protopopescu,²⁷ J. Proudfoot,⁶ M. Przybycien,^{41a} A. Puri,¹⁶⁹ P. Puzo,¹¹⁹ J. Qian,⁹² G. Qin,⁵⁶ Y. Qin,⁸⁷
 A. Quadt,⁵⁷ M. Queitsch-Maitland,⁴⁵ D. Quilty,⁵⁶ S. Raddum,¹²¹ V. Radeka,²⁷ V. Radescu,¹²² S. K. Radhakrishnan,¹⁵⁰
 P. Radloff,¹¹⁸ P. Rados,⁹¹ F. Ragusa,^{94a,94b} G. Rahal,¹⁸¹ J. A. Raine,⁸⁷ S. Rajagopalan,²⁷ C. Rangel-Smith,¹⁶⁸ T. Rashid,¹¹⁹
 S. Raspopov,⁵ M. G. Ratti,^{94a,94b} D. M. Rauch,⁴⁵ F. Rauscher,¹⁰² S. Rave,⁸⁶ I. Ravinovich,¹⁷⁵ J. H. Rawling,⁸⁷
 M. Raymond,³² A. L. Read,¹²¹ N. P. Readoff,⁵⁸ M. Reale,^{76a,76b} D. M. Rebuzzi,^{123a,123b} A. Redelbach,¹⁷⁷ G. Redlinger,²⁷
 R. Reece,¹³⁹ R. G. Reed,^{147c} K. Reeves,⁴⁴ L. Rehnisch,¹⁷ J. Reichert,¹²⁴ A. Reiss,⁸⁶ C. Rembser,³² H. Ren,^{35a,35d}
 M. Rescigno,^{134a} S. Resconi,^{94a} E. D. Resseguei,¹²⁴ S. Rettie,¹⁷¹ E. Reynolds,¹⁹ O. L. Rezanova,^{111,d} P. Reznicek,¹³¹
 R. Rezvani,⁹⁷ R. Richter,¹⁰³ S. Richter,⁸¹ E. Richter-Was,^{41b} O. Ricken,²³ M. Ridel,⁸³ P. Rieck,¹⁰³ C. J. Riegel,¹⁷⁸ J. Rieger,⁵⁷
 O. Rifki,¹¹⁵ M. Rijssenbeek,¹⁵⁰ A. Rimoldi,^{123a,123b} M. Rimoldi,¹⁸ L. Rinaldi,^{22a} G. Ripellino,¹⁴⁹ B. Ristić,³² E. Ritsch,³²
 I. Riu,¹³ F. Rizatdinova,¹¹⁶ E. Rizvi,⁷⁹ C. Rizzi,¹³ R. T. Roberts,⁸⁷ S. H. Robertson,^{90,p} A. Robichaud-Veronneau,⁹⁰
 D. Robinson,³⁰ J. E. M. Robinson,⁴⁵ A. Robson,⁵⁶ E. Rocco,⁸⁶ C. Roda,^{126a,126b} Y. Rodina,^{88,oo} S. Rodriguez Bosca,¹⁷⁰
 A. Rodriguez Perez,¹³ D. Rodriguez Rodriguez,¹⁷⁰ S. Roe,³² C. S. Rogan,⁵⁹ O. Røhne,¹²¹ J. Roloff,⁵⁹ A. Romaniouk,¹⁰⁰
 M. Romano,^{22a,22b} S. M. Romano Saez,³⁷ E. Romero Adam,¹⁷⁰ N. Rompotis,⁷⁷ M. Ronzani,⁵¹ L. Roos,⁸³ S. Rosati,^{134a}
 K. Rosbach,⁵¹ P. Rose,¹³⁹ N.-A. Rosien,⁵⁷ E. Rossi,^{106a,106b} L. P. Rossi,^{53a} J. H. N. Rosten,³⁰ R. Rosten,¹⁴⁰ M. Rotaru,^{28b}
 J. Rothberg,¹⁴⁰ D. Rousseau,¹¹⁹ A. Rozanov,⁸⁸ Y. Rozen,¹⁵⁴ X. Ruan,^{147c} F. Rubbo,¹⁴⁵ F. Rühr,⁵¹ A. Ruiz-Martinez,³¹
 Z. Rurikova,⁵¹ N. A. Rusakovich,⁶⁸ H. L. Russell,⁹⁰ J. P. Rutherford,⁷ N. Ruthmann,³² Y. F. Ryabov,¹²⁵ M. Rybar,¹⁶⁹
 G. Rybkin,¹¹⁹ S. Ryu,⁶ A. Ryzhov,¹³² G. F. Rzehorz,⁵⁷ A. F. Saavedra,¹⁵² G. Sabato,¹⁰⁹ S. Sacerdoti,²⁹
 H. F.-W. Sadrozinski,¹³⁹ R. Sadykov,⁶⁸ F. Safai Tehrani,^{134a} P. Saha,¹¹⁰ M. Sahinsoy,^{60a} M. Saimpert,⁴⁵ M. Saito,¹⁵⁷
 T. Saito,¹⁵⁷ H. Sakamoto,¹⁵⁷ Y. Sakurai,¹⁷⁴ G. Salamanna,^{136a,136b} J. E. Salazar Loyola,^{34b} D. Salek,¹⁰⁹
 P. H. Sales De Bruin,¹⁶⁸ D. Salihagic,¹⁰³ A. Salnikov,¹⁴⁵ J. Salt,¹⁷⁰ D. Salvatore,^{40a,40b} F. Salvatore,¹⁵¹ A. Salvucci,^{62a,62b,62c}
 A. Salzburger,³² D. Sammel,⁵¹ D. Sampsonidis,¹⁵⁶ D. Sampsonidou,¹⁵⁶ J. Sánchez,¹⁷⁰ V. Sanchez Martinez,¹⁷⁰

- A. Sanchez Pineda,^{167a,167c} H. Sandaker,¹²¹ R. L. Sandbach,⁷⁹ C. O. Sander,⁴⁵ M. Sandhoff,¹⁷⁸ C. Sandoval,²¹
 D. P. C. Sankey,¹³³ M. Sannino,^{53a,53b} Y. Sano,¹⁰⁵ A. Sansoni,⁵⁰ C. Santoni,³⁷ H. Santos,^{128a} I. Santoyo Castillo,¹⁵¹
 A. Sapronov,⁶⁸ J. G. Saraiva,^{128a,128d} B. Sarrazin,²³ O. Sasaki,⁶⁹ K. Sato,¹⁶⁴ E. Sauvan,⁵ G. Savage,⁸⁰ P. Savard,^{161e}
 N. Savic,¹⁰³ C. Sawyer,¹³³ L. Sawyer,^{82,v} J. Saxon,³³ C. Sbarra,^{22a} A. Sbrizzi,^{22a,22b} T. Scanlon,⁸¹ D. A. Scannicchio,¹⁶⁶
 M. Scarcella,¹⁵² J. Schaarschmidt,¹⁴⁰ P. Schacht,¹⁰³ B. M. Schachtner,¹⁰² D. Schaefer,³² L. Schaefer,¹²⁴ R. Schaefer,⁴⁵
 J. Schaeffer,⁸⁶ S. Schaepe,²³ S. Schaetzl,^{60b} U. Schäfer,⁸⁶ A. C. Schaffer,¹¹⁹ D. Schaile,¹⁰² R. D. Schamberger,¹⁵⁰
 V. A. Schegelsky,¹²⁵ D. Scheirich,¹³¹ M. Schernau,¹⁶⁶ C. Schiavi,^{53a,53b} S. Schier,¹³⁹ L. K. Schildgen,²³ C. Schillo,⁵¹
 M. Schioppa,^{40a,40b} S. Schlenker,³² K. R. Schmidt-Sommerfeld,¹⁰³ K. Schmieden,³² C. Schmitt,⁸⁶ S. Schmitt,⁴⁵ S. Schmitz,⁸⁶
 U. Schnoor,⁵¹ L. Schoeffel,¹³⁸ A. Schoening,^{60b} B. D. Schoenrock,⁹³ E. Schopf,²³ M. Schott,⁸⁶ J. F. P. Schouwenberg,¹⁰⁸
 J. Schovancova,³² S. Schramm,⁵² N. Schuh,⁸⁶ A. Schulte,⁸⁶ M. J. Schultens,²³ H.-C. Schultz-Coulon,^{60a} H. Schulz,¹⁷
 M. Schumacher,⁵¹ B. A. Schumm,¹³⁹ Ph. Schune,¹³⁸ A. Schwartzman,¹⁴⁵ T. A. Schwarz,⁹² H. Schweiger,⁸⁷
 Ph. Schwemling,¹³⁸ R. Schwienhorst,⁹³ J. Schwindling,¹³⁸ A. Sciandra,²³ G. Sciolla,²⁵ M. Scornajenghi,^{40a,40b}
 F. Scuri,^{126a,126b} F. Scutti,⁹¹ J. Searcy,⁹² P. Seema,²³ S. C. Seidel,¹⁰⁷ A. Seiden,¹³⁹ J. M. Seixas,^{26a} G. Sekhniadze,^{106a}
 K. Sekhon,⁹² S. J. Sekula,⁴³ N. Semprini-Cesari,^{22a,22b} S. Senkin,³⁷ C. Serfon,¹²¹ L. Serin,¹¹⁹ L. Serkin,^{167a,167b}
 M. Sessa,^{136a,136b} R. Seuster,¹⁷² H. Severini,¹¹⁵ T. Sfiligoi,⁷⁸ F. Sforza,³² A. Sfyrla,⁵² E. Shabalina,⁵⁷ N. W. Shaikh,^{148a,148b}
 L. Y. Shan,^{35a} R. Shang,¹⁶⁹ J. T. Shank,²⁴ M. Shapiro,¹⁶ P. B. Shatalov,⁹⁹ K. Shaw,^{167a,167b} S. M. Shaw,⁸⁷
 A. Shcherbakova,^{148a,148b} C. Y. Shehu,¹⁵¹ Y. Shen,¹¹⁵ N. Sherafati,³¹ P. Sherwood,⁸¹ L. Shi,^{153,pp} S. Shimizu,⁷⁰
 C. O. Shimmin,¹⁷⁹ M. Shimojima,¹⁰⁴ I. P. J. Shipsey,¹²² S. Shirabe,⁷³ M. Shiyakova,^{68,qq} J. Shlomi,¹⁷⁵ A. Shmeleva,⁹⁸
 D. Shoaleh Saadi,⁹⁷ M. J. Shochet,³³ S. Shojaii,^{94a} D. R. Shope,¹¹⁵ S. Shrestha,¹¹³ E. Shulga,¹⁰⁰ M. A. Shupe,⁷ P. Sicho,¹²⁹
 A. M. Sickles,¹⁶⁹ P. E. Sidebo,¹⁴⁹ E. Sideras Haddad,^{147c} O. Sidiropoulou,¹⁷⁷ A. Sidoti,^{22a,22b} F. Siegert,⁴⁷ Dj. Sijacki,¹⁴
 J. Silva,^{128a,128d} S. B. Silverstein,^{148a} V. Simak,¹³⁰ L. Simic,¹⁴ S. Simion,¹¹⁹ E. Simioni,⁸⁶ B. Simmons,⁸¹ M. Simon,⁸⁶
 P. Sinervo,¹⁶¹ N. B. Sinev,¹¹⁸ M. Sioli,^{22a,22b} G. Siragusa,¹⁷⁷ I. Siral,⁹² S. Yu. Sivoklokov,¹⁰¹ J. Sjölin,^{148a,148b} M. B. Skinner,⁷⁵
 P. Skubic,¹¹⁵ M. Slater,¹⁹ T. Slavicek,¹³⁰ M. Slawinska,⁴² K. Sliwa,¹⁶⁵ R. Slovak,¹³¹ V. Smakhtin,¹⁷⁵ B. H. Smart,⁵
 J. Smiesko,^{146a} N. Smirnov,¹⁰⁰ S. Yu. Smirnov,¹⁰⁰ Y. Smirnov,¹⁰⁰ L. N. Smirnova,^{101,rr} O. Smirnova,⁸⁴ J. W. Smith,⁵⁷
 M. N. K. Smith,³⁸ R. W. Smith,³⁸ M. Smizanska,⁷⁵ K. Smolek,¹³⁰ A. A. Snesarev,⁹⁸ I. M. Snyder,¹¹⁸ S. Snyder,²⁷
 R. Sobie,^{172,pp} F. Socher,⁴⁷ A. Soffer,¹⁵⁵ A. Søgaard,⁴⁹ D. A. Soh,¹⁵³ G. Sokhrannyi,⁷⁸ C. A. Solans Sanchez,³² M. Solar,¹³⁰
 E. Yu. Soldatov,¹⁰⁰ U. Soldevila,¹⁷⁰ A. A. Solodkov,¹³² A. Soloshenko,⁶⁸ O. V. Solovyanov,¹³² V. Solovyev,¹²⁵ P. Sommer,⁵¹
 H. Son,¹⁶⁵ A. Sopczak,¹³⁰ D. Sosa,^{60b} C. L. Sotiropoulou,^{126a,126b} R. Soualah,^{167a,167c} A. M. Soukharev,^{111,d} D. South,⁴⁵
 B. C. Sowden,⁸⁰ S. Spagnolo,^{76a,76b} M. Spalla,^{126a,126b} M. Spangenberg,¹⁷³ F. Spanò,⁸⁰ D. Sperlich,¹⁷ F. Spettel,¹⁰³
 T. M. Spieker,^{60a} R. Spighi,^{22a} G. Spigo,³² L. A. Spiller,⁹¹ M. Spousta,¹³¹ R. D. St. Denis,^{56,a} A. Stabile,^{94a} R. Stamen,^{60a}
 S. Stamm,¹⁷ E. Stanecka,⁴² R. W. Stanek,⁶ C. Stanescu,^{136a} M. M. Stanitzki,⁴⁵ B. S. Stapf,¹⁰⁹ S. Stapnes,¹²¹
 E. A. Starchenko,¹³² G. H. Stark,³³ J. Stark,⁵⁸ S. H Stark,³⁹ P. Staroba,¹²⁹ P. Starovoitov,^{60a} S. Stärz,³² R. Staszewski,⁴²
 P. Steinberg,²⁷ B. Stelzer,¹⁴⁴ H. J. Stelzer,³² O. Stelzer-Chilton,^{163a} H. Stenzel,⁵⁵ G. A. Stewart,⁵⁶ M. C. Stockton,¹¹⁸
 M. Stoebe,⁹⁰ G. Stoica,^{28b} P. Stolte,⁵⁷ S. Stonjek,¹⁰³ A. R. Stradling,⁸ A. Straessner,⁴⁷ M. E. Stramaglia,¹⁸ J. Strandberg,¹⁴⁹
 S. Strandberg,^{148a,148b} M. Strauss,¹¹⁵ P. Strizenec,^{146b} R. Ströhmer,¹⁷⁷ D. M. Strom,¹¹⁸ R. Stroynowski,⁴³ A. Strubig,⁴⁹
 S. A. Stucci,²⁷ B. Stugu,¹⁵ N. A. Styles,⁴⁵ D. Su,¹⁴⁵ J. Su,¹²⁷ S. Suchek,^{60a} Y. Sugaya,¹²⁰ M. Suk,¹³⁰ V. V. Sulin,⁹⁸
 DMS Sultan,^{162a,162b} S. Sultansoy,^{4c} T. Sumida,⁷¹ S. Sun,⁵⁹ X. Sun,³ K. Suruliz,¹⁵¹ C. J. E. Suster,¹⁵² M. R. Sutton,¹⁵¹
 S. Suzuki,⁶⁹ M. Svatos,¹²⁹ M. Swiatlowski,³³ S. P. Swift,² I. Sykora,^{146a} T. Sykora,¹³¹ D. Ta,⁵¹ K. Tackmann,⁴⁵ J. Taenzer,¹⁵⁵
 A. Taffard,¹⁶⁶ R. Tafirout,^{163a} E. Tahirovic,⁷⁹ N. Taiblum,¹⁵⁵ H. Takai,²⁷ R. Takashima,⁷² E. H. Takasugi,¹⁰³ T. Takeshita,¹⁴²
 Y. Takubo,⁶⁹ M. Talby,⁸⁸ A. A. Talyshев,^{111,d} J. Tanaka,¹⁵⁷ M. Tanaka,¹⁵⁹ R. Tanaka,¹¹⁹ S. Tanaka,⁶⁹ R. Tanioka,⁷⁰
 B. B. Tannenwald,¹¹³ S. Tapia Araya,^{34b} S. Tapprogge,⁸⁶ S. Tarem,¹⁵⁴ G. F. Tartarelli,^{94a} P. Tas,¹³¹ M. Tasevsky,¹²⁹
 T. Tashiro,⁷¹ E. Tassi,^{40a,40b} A. Tavares Delgado,^{128a,128b} Y. Tayalati,^{137e} A. C. Taylor,¹⁰⁷ G. N. Taylor,⁹¹ P. T. E. Taylor,⁹¹
 W. Taylor,^{163b} P. Teixeira-Dias,⁸⁰ D. Temple,¹⁴⁴ H. Ten Kate,³² P. K. Teng,¹⁵³ J. J. Teoh,¹²⁰ F. Tepel,¹⁷⁸ S. Terada,⁶⁹
 K. Terashi,¹⁵⁷ J. Terron,⁸⁵ S. Terzo,¹³ M. Testa,⁵⁰ R. J. Teuscher,^{161,pp} T. Theveneaux-Pelzer,⁸⁸ F. Thiele,³⁹ J. P. Thomas,¹⁹
 J. Thomas-Wilsker,⁸⁰ P. D. Thompson,¹⁹ A. S. Thompson,⁵⁶ L. A. Thomsen,¹⁷⁹ E. Thomson,¹²⁴ M. J. Tibbetts,¹⁶
 R. E. Ticse Torres,⁸⁸ V. O. Tikhomirov,^{98,ss} Yu. A. Tikhonov,^{111,d} S. Timoshenko,¹⁰⁰ P. Tipton,¹⁷⁹ S. Tisserant,⁸⁸
 K. Todome,¹⁵⁹ S. Todorova-Nova,⁵ S. Todt,⁴⁷ J. Tojo,⁷³ S. Tokár,^{146a} K. Tokushuku,⁶⁹ E. Tolley,¹¹³ L. Tomlinson,⁸⁷
 M. Tomoto,¹⁰⁵ L. Tompkins,^{145,tt} K. Toms,¹⁰⁷ B. Tong,⁵⁹ P. Tornambe,⁵¹ E. Torrence,¹¹⁸ H. Torres,¹⁴⁴ E. Torró Pastor,¹⁴⁰
 J. Toth,^{88,uu} F. Touchard,⁸⁸ D. R. Tovey,¹⁴¹ C. J. Treado,¹¹² T. Trefzger,¹⁷⁷ F. Tresoldi,¹⁵¹ A. Tricoli,²⁷ I. M. Trigger,^{163a}

- S. Trincaz-Duvold,⁸³ M. F. Tripiana,¹³ W. Trischuk,¹⁶¹ B. Trocmé,⁵⁸ A. Trofymov,⁴⁵ C. Troncon,^{94a}
 M. Trottier-McDonald,¹⁶ M. Trovatelli,¹⁷² L. Truong,^{147b} M. Trzebinski,⁴² A. Trzupek,⁴² K. W. Tsang,^{62a} J. C.-L. Tseng,¹²²
 P. V. Tsiareshka,⁹⁵ G. Tsipolitis,¹⁰ N. Tsirintanis,⁹ S. Tsiskaridze,¹³ V. Tsiskaridze,⁵¹ E. G. Tskhadadze,^{54a} K. M. Tsui,^{62a}
 I. I. Tsukerman,⁹⁹ V. Tsulaia,¹⁶ S. Tsuno,⁶⁹ D. Tsybychev,¹⁵⁰ Y. Tu,^{62b} A. Tudorache,^{28b} V. Tudorache,^{28b} T. T. Tulbure,^{28a}
 A. N. Tuna,⁵⁹ S. A. Tupputi,^{22a,22b} S. Turchikhin,⁶⁸ D. Turgeman,¹⁷⁵ I. Turk Cakir,^{4b,vv} R. Turra,^{94a} P. M. Tuts,³⁸
 G. Uccielli,^{22a,22b} I. Ueda,⁶⁹ M. Ughetto,^{148a,148b} F. Ukegawa,¹⁶⁴ G. Unal,³² A. Undrus,²⁷ G. Unel,¹⁶⁶ F. C. Ungaro,⁹¹
 Y. Unno,⁶⁹ C. Unverdorben,¹⁰² J. Urban,^{146b} P. Urquijo,⁹¹ P. Urrejola,⁸⁶ G. Usai,⁸ J. Usui,⁶⁹ L. Vacavant,⁸⁸ V. Vacek,¹³⁰
 B. Vachon,⁹⁰ K. O. H. Vadla,¹²¹ A. Vaidya,⁸¹ C. Valderanis,¹⁰² E. Valdes Santurio,^{148a,148b} M. Valente,⁵² S. Valentini,^{22a,22b}
 A. Valero,¹⁷⁰ L. Valéry,¹³ S. Valkar,¹³¹ A. Vallier,⁵ J. A. Valls Ferrer,¹⁷⁰ W. Van Den Wollenberg,¹⁰⁹ H. van der Graaf,¹⁰⁹
 P. van Gemmeren,⁶ J. Van Nieuwkoop,¹⁴⁴ I. van Vulpen,¹⁰⁹ M. C. van Woerden,¹⁰⁹ M. Vanadia,^{135a,135b} W. Vandelli,³²
 A. Vaniachine,¹⁶⁰ P. Vankov,¹⁰⁹ G. Vardanyan,¹⁸⁰ R. Vari,^{134a} E. W. Varnes,⁷ C. Varni,^{53a,53b} T. Varol,⁴³ D. Varouchas,¹¹⁹
 A. Vartapetian,⁸ K. E. Varvell,¹⁵² J. G. Vasquez,¹⁷⁹ G. A. Vasquez,^{34b} F. Vazeille,³⁷ T. Vazquez Schroeder,⁹⁰ J. Veatch,⁵⁷
 V. Veeraraghavan,⁷ L. M. Veloce,¹⁶¹ F. Veloso,^{128a,128c} S. Veneziano,^{134a} A. Ventura,^{76a,76b} M. Venturi,¹⁷² N. Venturi,³²
 A. Venturini,²⁵ V. Vercesi,^{123a} M. Verducci,^{136a,136b} W. Verkerke,¹⁰⁹ A. T. Vermeulen,¹⁰⁹ J. C. Vermeulen,¹⁰⁹
 M. C. Vetterli,^{144,e} N. Viaux Maira,^{34b} O. Viazlo,⁸⁴ I. Vichou,^{169,a} T. Vickey,¹⁴¹ O. E. Vickey Boeriu,¹⁴¹
 G. H. A. Viehhauser,¹²² S. Viel,¹⁶ L. Vigani,¹²² M. Villa,^{22a,22b} M. Villaplana Perez,^{94a,94b} E. Vilucchi,⁵⁰ M. G. Vincter,³¹
 V. B. Vinogradov,⁶⁸ A. Vishwakarma,⁴⁵ C. Vittori,^{22a,22b} I. Vivarelli,¹⁵¹ S. Vlachos,¹⁰ M. Vogel,¹⁷⁸ P. Vokac,¹³⁰
 G. Volpi,^{126a,126b} H. von der Schmitt,¹⁰³ E. von Toerne,²³ V. Vorobel,¹³¹ K. Vorobev,¹⁰⁰ M. Vos,¹⁷⁰ R. Voss,³²
 J. H. Vossebeld,⁷⁷ N. Vranjes,¹⁴ M. Vranjes Milosavljevic,¹⁴ V. Vrba,¹³⁰ M. Vreeswijk,¹⁰⁹ R. Vuillermet,³² I. Vukotic,³³
 P. Wagner,²³ W. Wagner,¹⁷⁸ J. Wagner-Kuhr,¹⁰² H. Wahlberg,⁷⁴ S. Wahrmund,⁴⁷ J. Wakabayashi,¹⁰⁵ J. Walder,⁷⁵
 R. Walker,¹⁰² W. Walkowiak,¹⁴³ V. Wallangen,^{148a,148b} C. Wang,^{35b} C. Wang,^{36b,ww} F. Wang,¹⁷⁶ H. Wang,¹⁶ H. Wang,³
 J. Wang,⁴⁵ J. Wang,¹⁵² Q. Wang,¹¹⁵ R. Wang,⁶ S. M. Wang,¹⁵³ T. Wang,³⁸ W. Wang,^{153,xx} W. Wang,^{36a,yv} Z. Wang,^{36c}
 C. Wanotayaroj,¹¹⁸ A. Warburton,⁹⁰ C. P. Ward,³⁰ D. R. Wardrobe,⁸¹ A. Washbrook,⁴⁹ P. M. Watkins,¹⁹ A. T. Watson,¹⁹
 M. F. Watson,¹⁹ G. Watts,¹⁴⁰ S. Watts,⁸⁷ B. M. Waugh,⁸¹ A. F. Webb,¹¹ S. Webb,⁸⁶ M. S. Weber,¹⁸ S. W. Weber,¹⁷⁷
 S. A. Weber,³¹ J. S. Webster,⁶ A. R. Weidberg,¹²² B. Weinert,⁶⁴ J. Weingarten,⁵⁷ M. Weirich,⁸⁶ C. Weiser,⁵¹ H. Weits,¹⁰⁹
 P. S. Wells,³² T. Wenaus,²⁷ T. Wengler,³² S. Wenig,³² N. Wermes,²³ M. D. Werner,⁶⁷ P. Werner,³² M. Wessels,^{60a}
 T. D. Weston,¹⁸ K. Whalen,¹¹⁸ N. L. Whallon,¹⁴⁰ A. M. Wharton,⁷⁵ A. S. White,⁹² A. White,⁸ M. J. White,¹ R. White,^{34b}
 D. Whiteson,¹⁶⁶ B. W. Whitmore,⁷⁵ F. J. Wickens,¹³³ W. Wiedenmann,¹⁷⁶ M. Wielers,¹³³ C. Wiglesworth,³⁹
 L. A. M. Wiik-Fuchs,⁵¹ A. Wildauer,¹⁰³ F. Wilk,⁸⁷ H. G. Wilkens,³² H. H. Williams,¹²⁴ S. Williams,¹⁰⁹ C. Willis,⁹³
 S. Willocq,⁸⁹ J. A. Wilson,¹⁹ I. Wingerter-Seez,⁵ E. Winkels,¹⁵¹ F. Winklmeier,¹¹⁸ O. J. Winston,¹⁵¹ B. T. Winter,²³
 M. Wittgen,¹⁴⁵ M. Wobisch,^{82,v} T. M. H. Wolf,¹⁰⁹ R. Wolff,⁸⁸ M. W. Wolter,⁴² H. Wolters,^{128a,128c} V. W. S. Wong,¹⁷¹
 S. D. Worm,¹⁹ B. K. Wosiek,⁴² J. Wotschack,³² K. W. Wozniak,⁴² M. Wu,³³ S. L. Wu,¹⁷⁶ X. Wu,⁵² Y. Wu,⁹² T. R. Wyatt,⁸⁷
 B. M. Wynne,⁴⁹ S. Xella,³⁹ Z. Xi,⁹² L. Xia,^{35c} D. Xu,^{35a} L. Xu,²⁷ T. Xu,¹³⁸ B. Yabsley,¹⁵² S. Yacoob,^{147a} D. Yamaguchi,¹⁵⁹
 Y. Yamaguchi,¹²⁰ A. Yamamoto,⁶⁹ S. Yamamoto,¹⁵⁷ T. Yamanaka,¹⁵⁷ M. Yamatani,¹⁵⁷ K. Yamauchi,¹⁰⁵ Y. Yamazaki,⁷⁰
 Z. Yan,²⁴ H. Yang,^{36c} H. Yang,¹⁶ Y. Yang,¹⁵³ Z. Yang,¹⁵ W.-M. Yao,¹⁶ Y. C. Yap,⁸³ Y. Yasu,⁶⁹ E. Yatsenko,⁵
 K. H. Yau Wong,²³ J. Ye,⁴³ S. Ye,²⁷ I. Yeletskikh,⁶⁸ E. Yigitbasi,²⁴ E. Yildirim,⁸⁶ K. Yorita,¹⁷⁴ K. Yoshihara,¹²⁴ C. Young,¹⁴⁵
 C. J. S. Young,³² J. Yu,⁸ J. Yu,⁶⁷ S. P. Y. Yuen,²³ I. Yusuff,^{30,zz} B. Zabinski,⁴² G. Zacharis,¹⁰ R. Zaidan,¹³ A. M. Zaitsev,^{132,mm}
 N. Zakharchuk,⁴⁵ J. Zalieckas,¹⁵ A. Zaman,¹⁵⁰ S. Zambito,⁵⁹ D. Zanzi,⁹¹ C. Zeitnitz,¹⁷⁸ G. Zemaityte,¹²² A. Zemla,^{41a}
 J. C. Zeng,¹⁶⁹ Q. Zeng,¹⁴⁵ O. Zenin,¹³² T. Ženiš,^{146a} D. Zerwas,¹¹⁹ D. Zhang,⁹² F. Zhang,¹⁷⁶ G. Zhang,^{36a,yy} H. Zhang,^{35b}
 J. Zhang,⁶ L. Zhang,⁵¹ L. Zhang,^{36a} M. Zhang,¹⁶⁹ P. Zhang,^{35b} R. Zhang,²³ R. Zhang,^{36a,ww} X. Zhang,^{36b} Y. Zhang,^{35a,35d}
 Z. Zhang,¹¹⁹ X. Zhao,⁴³ Y. Zhao,^{36b,aaa} Z. Zhao,^{36a} A. Zhemchugov,⁶⁸ B. Zhou,⁹² C. Zhou,¹⁷⁶ L. Zhou,⁴³ M. Zhou,^{35a,35d}
 M. Zhou,¹⁵⁰ N. Zhou,^{35c} C. G. Zhu,^{36b} H. Zhu,^{35a} J. Zhu,⁹² Y. Zhu,^{36a} X. Zhuang,^{35a} K. Zhukov,⁹⁸ A. Zibell,¹⁷⁷
 D. Ziemińska,⁶⁴ N. I. Zimine,⁶⁸ C. Zimmermann,⁸⁶ S. Zimmermann,⁵¹ Z. Zinonos,¹⁰³ M. Zinser,⁸⁶ M. Ziolkowski,¹⁴³
 L. Živković,¹⁴ G. Zobernig,¹⁷⁶ A. Zoccoli,^{22a,22b} R. Zou,³³ M. zur Nedden,¹⁷ and L. Zwalski³²

(ATLAS Collaboration)

¹Department of Physics, University of Adelaide, Adelaide, Australia²Physics Department, SUNY Albany, Albany, New York, USA³Department of Physics, University of Alberta, Edmonton, Alberta, Canada

- ^{4a}Department of Physics, Ankara University, Ankara, Turkey
^{4b}Istanbul Aydin University, Istanbul, Turkey
- ^{4c}Division of Physics, TOBB University of Economics and Technology, Ankara, Turkey
- ⁵LAPP, CNRS/IN2P3 and Université Savoie Mont Blanc, Annecy-le-Vieux, France
- ⁶High Energy Physics Division, Argonne National Laboratory, Argonne, Illinois, USA
⁷Department of Physics, University of Arizona, Tucson, Arizona, USA
- ⁸Department of Physics, The University of Texas at Arlington, Arlington, Texas, USA
- ⁹Physics Department, National and Kapodistrian University of Athens, Athens, Greece
- ¹⁰Physics Department, National Technical University of Athens, Zografou, Greece
- ¹¹Department of Physics, The University of Texas at Austin, Austin, Texas, USA
¹²Institute of Physics, Azerbaijan Academy of Sciences, Baku, Azerbaijan
- ¹³Institut de Física d'Altes Energies (IFAE), The Barcelona Institute of Science and Technology, Barcelona, Spain
¹⁴Institute of Physics, University of Belgrade, Belgrade, Serbia
- ¹⁵Department for Physics and Technology, University of Bergen, Bergen, Norway
- ¹⁶Physics Division, Lawrence Berkeley National Laboratory and University of California, Berkeley, California, USA
¹⁷Department of Physics, Humboldt University, Berlin, Germany
- ¹⁸Albert Einstein Center for Fundamental Physics and Laboratory for High Energy Physics, University of Bern, Bern, Switzerland
- ¹⁹School of Physics and Astronomy, University of Birmingham, Birmingham, United Kingdom
^{20a}Department of Physics, Bogazici University, Istanbul, Turkey
^{20b}Department of Physics Engineering, Gaziantep University, Gaziantep, Turkey
- ^{20d}Istanbul Bilgi University, Faculty of Engineering and Natural Sciences, Istanbul, Turkey
- ^{20e}Bahcesehir University, Faculty of Engineering and Natural Sciences, Istanbul, Turkey
²¹Centro de Investigaciones, Universidad Antonio Narino, Bogota, Colombia
^{22a}INFN Sezione di Bologna, Italy
- ^{22b}Dipartimento di Fisica e Astronomia, Università di Bologna, Bologna, Italy
²³Physikalisches Institut, University of Bonn, Bonn, Germany
- ²⁴Department of Physics, Boston University, Boston, Massachusetts, USA
²⁵Department of Physics, Brandeis University, Waltham, Massachusetts, USA
- ^{26a}Universidade Federal do Rio De Janeiro COPPE/EE/IF, Rio de Janeiro, Brazil
^{26b}Electrical Circuits Department, Federal University of Juiz de Fora (UFJF), Juiz de Fora, Brazil
^{26c}Federal University of Sao Joao del Rei (UFSJ), Sao Joao del Rei, Brazil
^{26d}Instituto de Fisica, Universidade de Sao Paulo, Sao Paulo, Brazil
- ²⁷Physics Department, Brookhaven National Laboratory, Upton, New York, USA
^{28a}Transilvania University of Brasov, Brasov, Romania
- ^{28b}Horia Hulubei National Institute of Physics and Nuclear Engineering, Bucharest, Romania
^{28c}Department of Physics, Alexandru Ioan Cuza University of Iasi, Iasi, Romania
- ^{28d}National Institute for Research and Development of Isotopic and Molecular Technologies, Physics Department, Cluj Napoca, Romania
^{28e}University Politehnica Bucharest, Bucharest, Romania
^{28f}West University in Timisoara, Timisoara, Romania
- ²⁹Departamento de Física, Universidad de Buenos Aires, Buenos Aires, Argentina
³⁰Cavendish Laboratory, University of Cambridge, Cambridge, United Kingdom
³¹Department of Physics, Carleton University, Ottawa, Ontario, Canada
³²CERN, Geneva, Switzerland
³³Enrico Fermi Institute, University of Chicago, Chicago, Illinois, USA
^{34a}Departamento de Física, Pontifícia Universidad Católica de Chile, Santiago, Chile
^{34b}Departamento de Física, Universidad Técnica Federico Santa María, Valparaíso, Chile
^{35a}Institute of High Energy Physics, Chinese Academy of Sciences, Beijing, China
^{35b}Department of Physics, Nanjing University, Jiangsu, China
^{35c}Physics Department, Tsinghua University, Beijing 100084, China
^{35d}University of Chinese Academy of Science (UCAS), Beijing, China
^{36a}Department of Modern Physics and State Key Laboratory of Particle Detection and Electronics, University of Science and Technology of China, Anhui, China
^{36b}School of Physics, Shandong University, Shandong, China
^{36c}Department of Physics and Astronomy, Key Laboratory for Particle Physics, Astrophysics and Cosmology, Ministry of Education; Shanghai Key Laboratory for Particle Physics and Cosmology, Shanghai Jiao Tong University, Shanghai(also at PKU-CHEP), China

- ³⁷*Université Clermont Auvergne, CNRS/IN2P3, LPC, Clermont-Ferrand, France*
³⁸*Nevis Laboratory, Columbia University, Irvington, New York, USA*
³⁹*Niels Bohr Institute, University of Copenhagen, Kobenhavn, Denmark*
^{40a}*INFN Gruppo Collegato di Cosenza, Laboratori Nazionali di Frascati, Italy*
^{40b}*Dipartimento di Fisica, Università della Calabria, Rende, Italy*
^{41a}*AGH University of Science and Technology, Faculty of Physics and Applied Computer Science, Krakow, Poland*
^{41b}*Marian Smoluchowski Institute of Physics, Jagiellonian University, Krakow, Poland*
⁴²*Institute of Nuclear Physics Polish Academy of Sciences, Krakow, Poland*
⁴³*Physics Department, Southern Methodist University, Dallas, Texas, USA*
⁴⁴*Physics Department, University of Texas at Dallas, Richardson, Texas, USA*
⁴⁵*DESY, Hamburg and Zeuthen, Germany*
⁴⁶*Lehrstuhl für Experimentelle Physik IV, Technische Universität Dortmund, Dortmund, Germany*
⁴⁷*Institut für Kern- und Teilchenphysik, Technische Universität Dresden, Dresden, Germany*
⁴⁸*Department of Physics, Duke University, Durham, North Carolina, USA*
⁴⁹*SUPA—School of Physics and Astronomy, University of Edinburgh, Edinburgh, United Kingdom*
⁵⁰*INFN e Laboratori Nazionali di Frascati, Frascati, Italy*
⁵¹*Fakultät für Mathematik und Physik, Albert-Ludwigs-Universität, Freiburg, Germany*
⁵²*Departement de Physique Nucléaire et Corpusculaire, Université de Genève, Geneva, Switzerland*
^{53a}*INFN Sezione di Genova, Italy*
^{53b}*Dipartimento di Fisica, Università di Genova, Genova, Italy*
^{54a}*E. Andronikashvili Institute of Physics, Iv. Javakhishvili Tbilisi State University, Tbilisi, Georgia*
^{54b}*High Energy Physics Institute, Tbilisi State University, Tbilisi, Georgia*
⁵⁵*II Physikalisches Institut, Justus-Liebig-Universität Giessen, Giessen, Germany*
⁵⁶*SUPA—School of Physics and Astronomy, University of Glasgow, Glasgow, United Kingdom*
⁵⁷*II Physikalisches Institut, Georg-August-Universität, Göttingen, Germany*
⁵⁸*Laboratoire de Physique Subatomique et de Cosmologie, Université Grenoble-Alpes, CNRS/IN2P3, Grenoble, France*
⁵⁹*Laboratory for Particle Physics and Cosmology, Harvard University, Cambridge, Massachusetts, USA*
^{60a}*Kirchhoff-Institut für Physik, Ruprecht-Karls-Universität Heidelberg, Heidelberg, Germany*
^{60b}*Physikalisches Institut, Ruprecht-Karls-Universität Heidelberg, Heidelberg, Germany*
⁶¹*Faculty of Applied Information Science, Hiroshima Institute of Technology, Hiroshima, Japan*
^{62a}*Department of Physics, The Chinese University of Hong Kong, Shatin, N.T., Hong Kong, China*
^{62b}*Department of Physics, The University of Hong Kong, Hong Kong, China*
^{62c}*Department of Physics and Institute for Advanced Study, The Hong Kong University of Science and Technology, Clear Water Bay, Kowloon, Hong Kong, China*
⁶³*Department of Physics, National Tsing Hua University, Taiwan, Taiwan*
⁶⁴*Department of Physics, Indiana University, Bloomington, Indiana, USA*
⁶⁵*Institut für Astro- und Teilchenphysik, Leopold-Franzens-Universität, Innsbruck, Austria*
⁶⁶*University of Iowa, Iowa City, Iowa, USA*
⁶⁷*Department of Physics and Astronomy, Iowa State University, Ames, Iowa, USA*
⁶⁸*Joint Institute for Nuclear Research, JINR Dubna, Dubna, Russia*
⁶⁹*KEK, High Energy Accelerator Research Organization, Tsukuba, Japan*
⁷⁰*Graduate School of Science, Kobe University, Kobe, Japan*
⁷¹*Faculty of Science, Kyoto University, Kyoto, Japan*
⁷²*Kyoto University of Education, Kyoto, Japan*
⁷³*Research Center for Advanced Particle Physics and Department of Physics, Kyushu University, Fukuoka, Japan*
⁷⁴*Instituto de Física La Plata, Universidad Nacional de La Plata and CONICET, La Plata, Argentina*
⁷⁵*Physics Department, Lancaster University, Lancaster, United Kingdom*
^{76a}*INFN Sezione di Lecce, Italy*
^{76b}*Dipartimento di Matematica e Fisica, Università del Salento, Lecce, Italy*
⁷⁷*Oliver Lodge Laboratory, University of Liverpool, Liverpool, United Kingdom*
⁷⁸*Department of Experimental Particle Physics, Jožef Stefan Institute and Department of Physics, University of Ljubljana, Ljubljana, Slovenia*
⁷⁹*School of Physics and Astronomy, Queen Mary University of London, London, United Kingdom*
⁸⁰*Department of Physics, Royal Holloway University of London, Surrey, United Kingdom*
⁸¹*Department of Physics and Astronomy, University College London, London, United Kingdom*
⁸²*Louisiana Tech University, Ruston, Louisiana, USA*

- ⁸³*Laboratoire de Physique Nucléaire et de Hautes Energies, UPMC and Université Paris-Diderot and CNRS/IN2P3, Paris, France*
- ⁸⁴*Fysiska institutionen, Lunds universitet, Lund, Sweden*
- ⁸⁵*Departamento de Fisica Teorica C-15, Universidad Autonoma de Madrid, Madrid, Spain*
- ⁸⁶*Institut für Physik, Universität Mainz, Mainz, Germany*
- ⁸⁷*School of Physics and Astronomy, University of Manchester, Manchester, United Kingdom*
- ⁸⁸*CPPM, Aix-Marseille Université and CNRS/IN2P3, Marseille, France*
- ⁸⁹*Department of Physics, University of Massachusetts, Amherst, Massachusetts, USA*
- ⁹⁰*Department of Physics, McGill University, Montreal, Quebec, Canada*
- ⁹¹*School of Physics, University of Melbourne, Victoria, Australia*
- ⁹²*Department of Physics, The University of Michigan, Ann Arbor, Michigan, USA*
- ⁹³*Department of Physics and Astronomy, Michigan State University, East Lansing, Michigan, USA*
- ^{94a}*INFN Sezione di Milano, Italy*
- ^{94b}*Dipartimento di Fisica, Università di Milano, Milano, Italy*
- ⁹⁵*B.I. Stepanov Institute of Physics, National Academy of Sciences of Belarus, Minsk, Republic of Belarus*
- ⁹⁶*Research Institute for Nuclear Problems of Byelorussian State University, Minsk, Republic of Belarus*
- ⁹⁷*Group of Particle Physics, University of Montreal, Montreal, Quebec, Canada*
- ⁹⁸*P.N. Lebedev Physical Institute of the Russian Academy of Sciences, Moscow, Russia*
- ⁹⁹*Institute for Theoretical and Experimental Physics (ITEP), Moscow, Russia*
- ¹⁰⁰*National Research Nuclear University MEPhI, Moscow, Russia*
- ¹⁰¹*D.V. Skobeltsyn Institute of Nuclear Physics, M.V. Lomonosov Moscow State University, Moscow, Russia*
- ¹⁰²*Fakultät für Physik, Ludwig-Maximilians-Universität München, München, Germany*
- ¹⁰³*Max-Planck-Institut für Physik (Werner-Heisenberg-Institut), München, Germany*
- ¹⁰⁴*Nagasaki Institute of Applied Science, Nagasaki, Japan*
- ¹⁰⁵*Graduate School of Science and Kobayashi-Maskawa Institute, Nagoya University, Nagoya, Japan*
- ^{106a}*INFN Sezione di Napoli, Italy*
- ^{106b}*Dipartimento di Fisica, Università di Napoli, Napoli, Italy*
- ¹⁰⁷*Department of Physics and Astronomy, University of New Mexico, Albuquerque, New Mexico, USA*
- ¹⁰⁸*Institute for Mathematics, Astrophysics and Particle Physics, Radboud University Nijmegen/Nikhef, Nijmegen, Netherlands*
- ¹⁰⁹*Nikhef National Institute for Subatomic Physics and University of Amsterdam, Amsterdam, Netherlands*
- ¹¹⁰*Department of Physics, Northern Illinois University, DeKalb, Illinois, USA*
- ¹¹¹*Budker Institute of Nuclear Physics, SB RAS, Novosibirsk, Russia*
- ¹¹²*Department of Physics, New York University, New York, New York, USA*
- ¹¹³*Ohio State University, Columbus, Ohio, USA*
- ¹¹⁴*Faculty of Science, Okayama University, Okayama, Japan*
- ¹¹⁵*Homer L. Dodge Department of Physics and Astronomy, University of Oklahoma, Norman, Oklahoma, USA*
- ¹¹⁶*Department of Physics, Oklahoma State University, Stillwater, Oklahoma, USA*
- ¹¹⁷*Palacký University, RCPMT, Olomouc, Czech Republic*
- ¹¹⁸*Center for High Energy Physics, University of Oregon, Eugene, Oregon, USA*
- ¹¹⁹*LAL, Univ. Paris-Sud, CNRS/IN2P3, Université Paris-Saclay, Orsay, France*
- ¹²⁰*Graduate School of Science, Osaka University, Osaka, Japan*
- ¹²¹*Department of Physics, University of Oslo, Oslo, Norway*
- ¹²²*Department of Physics, Oxford University, Oxford, United Kingdom*
- ^{123a}*INFN Sezione di Pavia, Italy*
- ^{123b}*Dipartimento di Fisica, Università di Pavia, Pavia, Italy*
- ¹²⁴*Department of Physics, University of Pennsylvania, Philadelphia, Pennsylvania, USA*
- ¹²⁵*National Research Centre “Kurchatov Institute” B.P. Konstantinov Petersburg Nuclear Physics Institute, St. Petersburg, Russia*
- ^{126a}*INFN Sezione di Pisa, Italy*
- ^{126b}*Dipartimento di Fisica E. Fermi, Università di Pisa, Pisa, Italy*
- ¹²⁷*Department of Physics and Astronomy, University of Pittsburgh, Pittsburgh, Pennsylvania, USA*
- ^{128a}*Laboratório de Instrumentação e Física Experimental de Partículas—LIP, Lisboa, Portugal*
- ^{128b}*Faculdade de Ciências, Universidade de Lisboa, Lisboa, Portugal*
- ^{128c}*Department of Physics, University of Coimbra, Coimbra, Portugal*
- ^{128d}*Centro de Física Nuclear da Universidade de Lisboa, Lisboa, Portugal*
- ^{128e}*Departamento de Física, Universidade do Minho, Braga, Portugal*
- ^{128f}*Departamento de Física Teórica y del Cosmos, Universidad de Granada, Granada, Spain*

^{128g}*Dep Fisica and CEFITEC of Faculdade de Ciencias e Tecnologia, Universidade Nova de Lisboa, Caparica, Portugal*

¹²⁹*Institute of Physics, Academy of Sciences of the Czech Republic, Praha, Czech Republic*

¹³⁰*Czech Technical University in Prague, Praha, Czech Republic*

¹³¹*Charles University, Faculty of Mathematics and Physics, Prague, Czech Republic*

¹³²*State Research Center Institute for High Energy Physics (Protvino), NRC KI, Russia*

¹³³*Particle Physics Department, Rutherford Appleton Laboratory, Didcot, United Kingdom*

^{134a}*INFN Sezione di Roma, Italy*

^{134b}*Dipartimento di Fisica, Sapienza Università di Roma, Roma, Italy*

^{135a}*INFN Sezione di Roma Tor Vergata, Italy*

^{135b}*Dipartimento di Fisica, Università di Roma Tor Vergata, Roma, Italy*

^{136a}*INFN Sezione di Roma Tre, Italy*

^{136b}*Dipartimento di Matematica e Fisica, Università Roma Tre, Roma, Italy*

^{137a}*Faculté des Sciences Ain Chock, Réseau Universitaire de Physique des Hautes Energies—Université Hassan II, Casablanca, Morocco*

^{137b}*Centre National de l'Energie des Sciences Techniques Nucléaires, Rabat, Morocco*

^{137c}*Faculté des Sciences Semlalia, Université Cadi Ayyad, LPHEA-Marrakech, Morocco*

^{137d}*Faculté des Sciences, Université Mohamed Premier and LPTPM, Oujda, Morocco*

^{137e}*Faculté des sciences, Université Mohammed V, Rabat, Morocco*

¹³⁸*DSM/IRFU (Institut de Recherches sur les Lois Fondamentales de l'Univers), CEA Saclay (Commissariat à l'Energie Atomique et aux Energies Alternatives), Gif-sur-Yvette, France*

¹³⁹*Santa Cruz Institute for Particle Physics, University of California Santa Cruz, Santa Cruz, California, USA*

¹⁴⁰*Department of Physics, University of Washington, Seattle, Washington, USA*

¹⁴¹*Department of Physics and Astronomy, University of Sheffield, Sheffield, United Kingdom*

¹⁴²*Department of Physics, Shinshu University, Nagano, Japan*

¹⁴³*Department Physik, Universität Siegen, Siegen, Germany*

¹⁴⁴*Department of Physics, Simon Fraser University, Burnaby, British Columbia, Canada*

¹⁴⁵*SLAC National Accelerator Laboratory, Stanford, California, USA*

^{146a}*Faculty of Mathematics, Physics & Informatics, Comenius University, Bratislava, Slovak Republic*

^{146b}*Department of Subnuclear Physics, Institute of Experimental Physics of the Slovak Academy of Sciences, Košice, Slovak Republic*

^{147a}*Department of Physics, University of Cape Town, Cape Town, South Africa*

^{147b}*Department of Physics, University of Johannesburg, Johannesburg, South Africa*

^{147c}*School of Physics, University of the Witwatersrand, Johannesburg, South Africa*

^{148a}*Department of Physics, Stockholm University, Sweden*

^{148b}*The Oskar Klein Centre, Stockholm, Sweden*

¹⁴⁹*Physics Department, Royal Institute of Technology, Stockholm, Sweden*

¹⁵⁰*Departments of Physics & Astronomy and Chemistry, Stony Brook University, Stony Brook, New York, USA*

¹⁵¹*Department of Physics and Astronomy, University of Sussex, Brighton, United Kingdom*

¹⁵²*School of Physics, University of Sydney, Sydney, Australia*

¹⁵³*Institute of Physics, Academia Sinica, Taipei, Taiwan*

¹⁵⁴*Department of Physics, Technion: Israel Institute of Technology, Haifa, Israel*

¹⁵⁵*Raymond and Beverly Sackler School of Physics and Astronomy, Tel Aviv University, Tel Aviv, Israel*

¹⁵⁶*Department of Physics, Aristotle University of Thessaloniki, Thessaloniki, Greece*

¹⁵⁷*International Center for Elementary Particle Physics and Department of Physics, The University of Tokyo, Tokyo, Japan*

¹⁵⁸*Graduate School of Science and Technology, Tokyo Metropolitan University, Tokyo, Japan*

¹⁵⁹*Department of Physics, Tokyo Institute of Technology, Tokyo, Japan*

¹⁶⁰*Tomsk State University, Tomsk, Russia*

¹⁶¹*Department of Physics, University of Toronto, Toronto, Ontario, Canada*

^{162a}*INFN-TIFPA, Italy*

^{162b}*University of Trento, Trento, Italy*

^{163a}*TRIUMF, Vancouver, British Columbia, Canada*

^{163b}*Department of Physics and Astronomy, York University, Toronto, Ontario, Canada*

¹⁶⁴*Faculty of Pure and Applied Sciences, and Center for Integrated Research in Fundamental Science and Engineering, University of Tsukuba, Tsukuba, Japan*

¹⁶⁵*Department of Physics and Astronomy, Tufts University, Medford, Massachusetts, USA*

¹⁶⁶*Department of Physics and Astronomy, University of California Irvine, Irvine, California, USA*

^{167a}*INFN Gruppo Collegato di Udine, Sezione di Trieste, Udine, Italy*
^{167b}*ICTP, Trieste, Italy*

^{167c}*Dipartimento di Chimica, Fisica e Ambiente, Università di Udine, Udine, Italy*

¹⁶⁸*Department of Physics and Astronomy, University of Uppsala, Uppsala, Sweden*

¹⁶⁹*Department of Physics, University of Illinois, Urbana, Illinois, USA*

¹⁷⁰*Instituto de Física Corpuscular (IFIC), Centro Mixto Universidad de Valencia—CSIC, Spain*

¹⁷¹*Department of Physics, University of British Columbia, Vancouver, British Columbia, Canada*

¹⁷²*Department of Physics and Astronomy, University of Victoria, Victoria, British Columbia, Canada*

¹⁷³*Department of Physics, University of Warwick, Coventry, United Kingdom*

¹⁷⁴*Waseda University, Tokyo, Japan*

¹⁷⁵*Department of Particle Physics, The Weizmann Institute of Science, Rehovot, Israel*

¹⁷⁶*Department of Physics, University of Wisconsin, Madison, Wisconsin, USA*

¹⁷⁷*Fakultät für Physik und Astronomie, Julius-Maximilians-Universität, Würzburg, Germany*

¹⁷⁸*Fakultät für Mathematik und Naturwissenschaften, Fachgruppe Physik,*

Bergische Universität Wuppertal, Wuppertal, Germany

¹⁷⁹*Department of Physics, Yale University, New Haven, Connecticut, USA*

¹⁸⁰*Yerevan Physics Institute, Yerevan, Armenia*

¹⁸¹*Centre de Calcul de l’Institut National de Physique Nucléaire et de Physique des Particules (IN2P3), Villeurbanne, France*

¹⁸²*Academia Sinica Grid Computing, Institute of Physics, Academia Sinica, Taipei, Taiwan*

^aDeceased.

^bAlso at Department of Physics, King’s College London, London, United Kingdom.

^cAlso at Institute of Physics, Azerbaijan Academy of Sciences, Baku, Azerbaijan.

^dAlso at Novosibirsk State University, Novosibirsk, Russia.

^eAlso at TRIUMF, Vancouver BC, Canada.

^fAlso at Department of Physics & Astronomy, University of Louisville, Louisville, KY, USA.

^gAlso at Physics Department, An-Najah National University, Nablus, Palestine.

^hAlso at Department of Physics, California State University, Fresno California, USA.

ⁱAlso at Department of Physics, University of Fribourg, Fribourg, Switzerland.

^jAlso at II Physikalisches Institut, Georg-August-Universität, Göttingen, Germany.

^kAlso at Departament de Fisica de la Universitat Autònoma de Barcelona, Barcelona, Spain.

^lAlso at Departamento de Fisica e Astronomia, Faculdade de Ciencias, Universidade do Porto, Portugal.

^mAlso at Tomsk State University, Tomsk, and Moscow Institute of Physics and Technology State University, Dolgoprudny, Russia.

ⁿAlso at The Collaborative Innovation Center of Quantum Matter (CICQM), Beijing, China.

^oAlso at Universita di Napoli Parthenope, Napoli, Italy.

^pAlso at Institute of Particle Physics (IPP), Canada.

^qAlso at Horia Hulubei National Institute of Physics and Nuclear Engineering, Bucharest, Romania.

^rAlso at Department of Physics, St. Petersburg State Polytechnical University, St. Petersburg, Russia.

^sAlso at Borough of Manhattan Community College, City University of New York, New York City, USA.

^tAlso at Department of Financial and Management Engineering, University of the Aegean, Chios, Greece.

^uAlso at Centre for High Performance Computing, CSIR Campus, Rosebank, Cape Town, South Africa.

^vAlso at Louisiana Tech University, Ruston LA, USA.

^wAlso at Institutio Catalana de Recerca i Estudis Avancats, ICREA, Barcelona, Spain.

^xAlso at Department of Physics, The University of Michigan, Ann Arbor MI, USA.

^yAlso at Graduate School of Science, Osaka University, Osaka, Japan.

^zAlso at Fakultät für Mathematik und Physik, Albert-Ludwigs-Universität, Freiburg, Germany.

^{aa}Also at Institute for Mathematics, Astrophysics and Particle Physics, Radboud University Nijmegen/Nikhef, Nijmegen, Netherlands.

^{bb}Also at Department of Physics, The University of Texas at Austin, Austin Texas, USA.

^{cc}Also at Institute of Theoretical Physics, Ilia State University, Tbilisi, Georgia.

^{dd}Also at CERN, Geneva, Switzerland.

^{ee}Also at Georgian Technical University (GTU), Tbilisi, Georgia.

^{ff}Also at Ochadai Academic Production, Ochanomizu University, Tokyo, Japan.

^{gg}Also at Manhattan College, New York New York, USA.

^{hh}Also at Departamento de Física, Pontificia Universidad Católica de Chile, Santiago, Chile.

ⁱⁱAlso at The City College of New York, New York New York, USA.

^{jj}Also at School of Physics, Shandong University, Shandong, China.

^{kk}Also at Departamento de Física Teórica y del Cosmos, Universidad de Granada, Granada, Spain.

^{ll}Also at Department of Physics, California State University, Sacramento California, USA.

- ^{mm} Also at Moscow Institute of Physics and Technology State University, Dolgoprudny, Russia.
ⁿⁿ Also at Departement de Physique Nucleaire et Corpusculaire, Université de Genève, Geneva, Switzerland.
^{oo} Also at Institut de Física d'Altes Energies (IFAE), The Barcelona Institute of Science and Technology, Barcelona, Spain.
^{pp} Also at School of Physics, Sun Yat-sen University, Guangzhou, China.
^{qq} Also at Institute for Nuclear Research and Nuclear Energy (INRNE) of the Bulgarian Academy of Sciences, Sofia, Bulgaria.
^{rr} Also at Faculty of Physics, M.V.Lomonosov Moscow State University, Moscow, Russia.
^{ss} Also at National Research Nuclear University MEPhI, Moscow, Russia.
^{tt} Also at Department of Physics, Stanford University, Stanford California, USA.
^{uu} Also at Institute for Particle and Nuclear Physics, Wigner Research Centre for Physics, Budapest, Hungary.
^{vv} Also at Giresun University, Faculty of Engineering, Turkey.
^{ww} Also at CPPM, Aix-Marseille Université and CNRS/IN2P3, Marseille, France.
^{xx} Also at Department of Physics, Nanjing University, Jiangsu, China.
^{yy} Also at Institute of Physics, Academia Sinica, Taipei, Taiwan.
^{zz} Also at University of Malaya, Department of Physics, Kuala Lumpur, Malaysia.
^{aaa} Also at LAL, Univ. Paris-Sud, CNRS/IN2P3, Université Paris-Saclay, Orsay, France.